I hereby certify that this correspondence is being filed via EFS-Web with the United States Patent and Trademark Office

on 14 Sept. 2009

TOWNSEND and TOWNSEND and CREW LLP

By: Malvida Adagit

PATENT
Attorney Docket No. 02307O-067720US
Client Ref. No. 96-215-3

IN THE UNITED STATES PATENT AND TRADEMARK OFFICE

In re application of:	Confirmation No. 5513
LALEH SHAYESTEH et al.	Examiner: Sheela Huff
Application No.: 08/905,508	Technology Center/Art Unit: 1643
Filed: August 4, 1997	APPELLANTS' BRIEF UNDER 37 CFR §41.37
For: GENETIC ALTERATIONS ASSOCIATED WITH CANCER	

Mail Stop Appeal Brief
Commissioner for Patents
P.O. Box 1450
Alexandria, VA 22313-1450

Commissioner:

Further to the Notice of Appeal filed February 12, 2009 for the above-referenced application, Appellants submit this Brief on Appeal. Also submitted with this brief is authorization to pay the fee as set forth in 37 C.F.R. §41.20(b)(2) and a petition with fee authorization for a five-month extension of time.

TABLE OF CONTENTS

1. REAL PARTY IN INTEREST

The Regents of the University of California and The Board of Regents, The University of Texas System are the assignees of the above-referenced patent application and therefore the real parties in interest.

2. RELATED APPEALS AND INTERFERENCES

none

3. STATUS OF CLAIMS

Claim 1-36 and 40 are cancelled.

No claims are allowed.

No claims are objected to.

Claims 37-39 are rejected.

Claims 37-39 are being appealed.

4. STATUS OF AMENDMENTS

No claim amendments were made subsequent to the Final Office Action mailed November 7, 2008.

5. SUMMARY OF CLAIMED SUBJECT MATTER

Independent claim 37 relates to a method of inhibiting the pathological proliferation of ovarian cancer cells in a patient, the method comprising: detecting the presence of an amplification of *PIK3CA* in ovarian cancer cells from the patient; and administering a therapeutically effective dose of an inhibitor of PI3 kinase to the patient, wherein the inhibitor inhibits PI3 kinase enzymatic activity. Support can be found, *e.g.,* at page 14, lines 18-26; page 24, lines 7-13; and page 33, lines 1-3.

6. GROUNDS OF REJECTION TO BE REVIEWED ON APPEAL

A. The rejection of claims 37 and 38 under 35 U.S.C. § 103 as being unpatentable over Bonjouklian *et al.*, U.S. Patent No. 5,378,725 ("Bonjouklian") in view of Arnold *et al.*, *Genes, Chromosomes, and Cancer* 16:46-54, 1996 ("Arnold") and Volinia *et al.*, *Genomics* 24:472-477, 1994 ("Volinia"); and further in view of (in the alternative) Xiao *et al.*, *International Journal of Oncology* 6:405-411, 1995 ("Xiao") or Skorski *et al.*, *Blood* 86:726-736, 1995 ("Skorski") is to be reviewed on appeal.

B. The rejection of claim 39 under 35 U.S.C. § 103 as being unpatentable over Bonjouklian in view of Arnold and Volinia; and further in view of (in the alternative) Xiao or Skorski as applied to claims 37 and 38; and further in view of Powis *et al., International Journal of Pharmacology* 33:17-26, 1995 ("Powis") is to be reviewed on appeal.

C. The rejection of claim 39 under 35 U.S.C. § 103 as being unpatentable over Bonjouklian in view of Arnold and Volinia; and further in view of (in the alternative) Xiao or Skorski as applied to claims 37 and 38; and further in view of June *et al.*, U.S. Patent No. 6,632,789 ("June") is to be reviewed on appeal.

D. The rejection of claim 39 under 35 U.S.C. § 103 as being unpatentable over Bonjouklian in view of Arnold and Volinia; and further in view of (in the alternative) Xiao or Skorski as applied to claims 37 and 38; and further in view of Lavin *et al., Experientia* 52:979-994, 1996 ("Lavin") is to be reviewed on appeal.

7. ARGUMENT

A. Rejection of claims 37 and 38 under 35 U.S.C. § 103 over Bonjouklian, Arnold, Volinia, and Xiao or Skorski

The rejection

The Examiner characterizes Bonjouklian as teaching a method of treating a PI3 kinase-dependent condition, such as abnormal cell growth found in a neoplasm such as ovarian cancer, by administering a non-peptidic inhibitor of phosphotidylinositol-3 (PI3) kinase (wortmannin). See, *e.g.*, page 3, Office Action dated May 10, 2007. The rejection further states that it was known in the art that chromosome region 3q26 that comprises *PIK3CA* was

commonly amplified in ovarian tumors (Arnold); and that the catalytic p110 subunit of PI3 kinase was localized to chromosome 3q26.3 (Volinia). The rejection additionally cites Xiao and Skorski as teaching that wortmannin suppresses growth of gastric cancer cell lines (Xiao) and selectively inhibits the proliferation of leukemic cells (Skorski). The Examiner alleges that in view of these references, it would have been *prima facie* obvious to use the PI3 kinase inhibitor wortmannin to treat any ovarian cancer, including ovarian cancer comprising cells that had regions of chromosome 3q26 amplified.

The Examiner urges that the ordinary artisan would have been motivated to include ovarian tumors that are characterized by the amplification *PIK3CA* in the method of Bonjouklian because it was known in the art that *PIK3CA* was found at 3q26.3. The Examiner additionally contends that one of skill would have had a reasonable expectation of success that wortmannin would be an effective inhibitor of ovarian tumor cells having amplification of *PIK3CA* because wortmannin inhibited growth of gastric cancer cell lines and leukemia cells that had elevated PI3 kinase activity and therefore, according to the Examiner's reasoning, are PI3-kinase dependent neoplasms (page 5, Final Office Action mailed May 10, 2007). The Examiner further alleges that it was known in the art that gene amplification is associated with over-expression (see, May 10, 2007 Office Action, page 12). The Examiner has suggested that an amplification of a large chromosomal region such as 3q26-qter would lead to over-expression of the genes contained within that region and accordingly, that cells having an amplification at 3q26 would also exhibit increased PIK3CA expression and therefore, according to the Examiner, qualify as "PI3 kinase-dependent" neoplasms (see, page 7 of the May 10, 2007 Office Action). However, this position is inconsistent with the facts.

The rejection fails to establish a proper case of *prima facie* obviousness

The current claims are based, in part, on the discovery that amplification of the particular subregion at 3q26.3, including *PIK3CA*, is of diagnostic significance for cancer and further, that amplification of *PIK3CA* is in fact associated with increased PIK3CA expression and ovarian cancer cell proliferation. Appellants have thus determined that cancer cells that contain an amplification of *PIK3CA* are therapeutic targets for PIK3CA kinase inhibitors.

The issue here is whether based on the prior art, one of skill would have been motivated to detect the presence of an amplification of the *PIK3CA* gene in ovarian cancer cells from an ovarian cancer patient and administer a therapeutically effective dose of a PI3 kinase inhibitor to that patient. Further, the issue is whether it was predictable, based on the cited art, that the *PIK3CA* gene is a focal point of amplification in ovarian cancer and that administration of a PI3 kinase inhibitor to a patient having ovarian cancer cells harboring a *PIK3CA* amplification would be effective therapeutically.

The cited art does not teach or suggest that PIK3CA amplification is important in tumorigenesis.

First, although Bonjouklian describes treating a PI3 kinase-dependent condition with wortmannin, Bonjouklian does not provide any insight as to what a PI3 kinase-dependent condition is or how PI3-kinase-dependent conditions, including PI3 kinase-dependent neoplasms, are identified.

Volinia describes *PIK3CA* as being localized to 3q26.3; however, notes only that this area is re-arranged in myeloid dysplasia (Volinia, p. 476, first column). Arnold states that amplification of 3q26-qter observed in ovarian cancer suggests that the regions may contain one or more genes important for tumor initiation and/or progression, but states that no candidate oncogenes are known in this region (Arnold, page 49, last paragraph of column 2). Arnold makes no mention of *PIK3CA*. It is additionally noted that Volinia's disclosure that *PIK3CA* is present at 3q26.3 predates Arnold's work. Arnold therefore provides evidence that one of the skill in the art prior to Appellants' invention would not have reasonably expected that *PIK3CA* is an important focal point of amplification in ovarian cancer. Additional evidence is provided in the Gray I and Gray II Declarations, discussed below.

Next, as summarized above, the Examiner contends that a PI3 kinase-dependent neoplasm over-expresses PI 3 kinase (citing Xiao and Skorski in support) and further, that one of skill would expect that neoplasms in which 3q26 and/or 3q26-qter are amplified would also have elevations in PI3 kinase activity and as such, would be PI3 kinase-dependent neoplasms. No credible evidence is provided, however, supporting the position that one of skill would expect

that ovarian cancer cells that have amplification of *PIK3CA* would necessarily over-express the protein. If Examiner's supposition were true (amplification will predictably lead to over-expression), every gene contained in a chromosomal region that is amplified in cancer would be expected to be over-expressed.

During prosecution Appellants submitted two Declarations under 37 C.F.R. § 1.132 by Joe W. Gray, Ph.D to further support the unobviousness of the claims at issue. The first declaration was filed January 8, 2007 ("the Gray I Declaration"). The second declaration was filed June 13, 2008 ("the Gray II Declaration").

In brief, in the Gray I Declaration, Dr. Gray explains that the fact that the broad region of 3q26-qter was known to be amplified in ovarian cancer does not lead one of skill in the art to conclude that amplification of *PIK3CA*, which is one of numerous genes located in this broad region, results in overexpression of PIK3CA and is therefore indicative of a role for PI3 kinase in oncogenesis in ovarian cancer cells that contain the amplified region. Dr. Gray first points out that the comparative genomic hybridization (CGH) study as performed by Arnold using metaphase chromosomes does not provide sufficient resolution to determine that the chromosomal subregion containing the *PIK3CA* locus is a focal point of amplification (Gray I Declaration, section 6). Dr. Gray further explains that even though a gene may be present in an amplified chromosomal region, that fact alone does not lead one of skill to conclude that a particular gene is overexpressed. Dr. Gray notes that many genes are present in chromosomal region 3q26-qter, providing a printout from the genome browser of the University of California, Santa Cruz in support (Gray I, section 7). Dr. Gray points out that there is no evidence that all or even most of the products of these many genes are overexpressed in ovarian tumors.

The Gray II Declaration was submitted to provide further details.

Gray II Declaration

In the Gray II Declaration, Dr. Gray provides additional evidence that amplification does not necessarily correlate with overexpression. As an example, Dr. Gray provides a publication by Chin *et al.* (2006) *Cancer Cell.* 10:529-4 ("Chin", Exhibit A of the Declaration). Chin evaluated breast cancer and the correlation of amplification of four different

chromosomal regions with overexpression of gene product. As Dr. Gray explains, Chin demonstrates that, in reality, although chromosomal amplification are common in cancer, increased expression of genes within these amplicons happens only in a minority of cases (Gray II Declaration, section 6).

Dr. Gray further describes work performed in his laboratory in which 68 genes from the 3q26 regions of amplification were analyzed. Of these, only 30 had expression levels that were associated with copy number (Gray II Declaration, section 7).

In section 10 of the Gray II Declaration, Dr. Gray further explains that regardless of the number of genes in the amplified region, prior to Appellants' invention, one of skill could not conclude that amplification would lead to overexpression of *PIK3CA* and activation of phosphoinositide 3-kinase because transcriptional upregulation of a gene frequently does not lead to increased protein expression, and expression of one subunit of a signaling complex would not necessarily lead to increased activity of the complex. The inventors demonstrated that in fact, amplification and overexpression of *PIK3CA* is associated with increased PI3-kinase activity and that treatment with the PI3-kinase inhibitor decreases proliferation and increases apoptosis.

In section 11, Dr. Gray points out that despite the fact that it is known that 3q26 is amplified, the identification of a potential role of other genes in this region in ovarian cancer warranted publication in high-rank journals. This provides additional evidence that those in the art do not consider the simple presence of a gene in an amplified region to predict utility as a therapeutic target.

The Gray II Declaration provides additional details regarding the large number of genes present in the region described by Arnold. Dr. Gray provides a printout of information from the Ensembl genome browser that provides more detailed information as to the number of genes that have been identified in this chromosomal region. The region identified by Arnold as amplified in ovarian cancer, 3q26-3qter, in fact contains a large number of genes, as does the subregion of 3q26, as noted in the Gray I Declaration. There are more than 50 genes in the region. Even assuming that 30-50 genes would be considered "reasonable" in terms of evaluating overexpression and correlation with cancer and gene amplification (which Appellants

do not concede), Arnold teaches that the amplification area is 3q26-3qter and further, teaches that it is this whole region that is of interest. For example, Arnold points to a gene encoding a zinc finger, BCL6, that is located in the amplified area that may be of interest as a potential oncogene. BCL6 is located at 3q27.3 (see, e.g., the printout from the Ensemble genome browser). Thus, the prior art teaches that a very large region, 3q26-3qter, is amplified and does not narrow the region of interest. The Gray II Declaration establishes that there are hundreds of genes contained in 3q26-3qter.

Thus, Gray II not only provides evidence that amplification does not correlate with overexpression, but also shows that there are many, many genes in the amplified region identified by Arnold. In light of the facts, the genes present in 3q26-3qter, including the genes present at 3q26 in particular, could not be characterized as "predictable solutions" to the problem of identifying cancer cells that are targets for PIK3CA kinase inhibitor therapy.

In the Final Office Action mailed November 7, 2008, the Examiner concedes that the Gray II Declaration is relevant to the arguments that gene amplification does not necessarily lead to expression. However, the Examiner contends that the argument is not persuasive because in Bonjouklian, the PI3-kinase inhibitor is inhibiting the PI3 kinase enzyme. Therefore, according to the Examiner, absent objective evidence to the contrary, it is expected that since the inhibitor is inhibiting the protein, the protein must be expressed. Appellants respectfully disagree with the Examiner's reasoning. Bonjouklian provides no teaching or suggestion as to what would constitute a PI3 kinase-dependent condition that could be effectively treated with wortmannin.

Appellants acknowledge that the PI3 kinase protein is in fact expressed in many cell types, as it is involved in various growth factor signaling processes (see, *e.g.*, Powis, page 19). As noted above, however, the issue to be addressed here is whether based on the prior art, one of skill would have been motivated to detect the presence of an amplification of *PIK3CA* in ovarian cancer cells from an ovarian cancer patient and administer a therapeutically effective dose of a PI3 kinase inhibitor to that patient; and whether there was a reasonable expectation of success that there would be a therapeutic benefit to ovarian cancers having amplified *PIK3CA*.

Legal standards

The Supreme Court in *KSR International Co. v. Teleflex Inc.*, 127 S. Ct. 1727, 82 USPQ2d 1385, 1395-97 (2007) identified several rationales to support a conclusion of obviousness. The key to supporting any rejection under 35 U.S.C. §103 is the clear articulation of the reason(s) why the claimed invention would have been obvious. The Office Action of May 10, 2007 cites *KSR International Co. v Telefex Inc.* as broadening the standard of obviousness as it relates to "obvious to try". Specifically, the Examiner quotes the Supreme Court as stating that "when there is a design need or market pressure to solve a problem and there are a finite number of identified, predictable solutions a person or ordinary skill has good reason to pursue the known options within his or her technical grasp. If this leads to the anticipated success, it is likely the product not of innovation but of ordinary skill and common sense." The Examiner contends that there are a finite number of genes at 3q26 and that therefore, this standard is applicable here.

The Examiner additionally cites *Pfizer Inc v. Apotex Inc*, 480 F.3d1348, 82 USPQ2d 1321 (Fed. Cir. 2007) (see, the May 10, 2007 Office Action) as allegedly supporting the Examiner's position that the claims are obvious. However, the facts here are not analogous to those in *Apotex*, nor do they fall under the "obvious to try" circumstances mentioned by the Supreme Court.

In *Apotex*, there were about 50 salts to be tested. These salts were known to be useful in making pharmaceutical formulations. The Federal Circuit concluded that Pfizer would have had a reasonable expectation of success for various reasons including the following: Pfizer conceded in prior litigation that the type of salt had no effect on the therapeutic effect of the active ingredient, amiodipine, and was practically interchangeable; and numerous other publications clearly directed the skilled artisan to a pharmaceutically-acceptable acid-addition salt made from benzene sulphonate, including the besylate acid addition-salt for another dihydropyridine pharmaceutical compound (*Apotex*, 82 USPQ2d 1321, 1334).

Such a reasonable expectation of success is not present here. There are many, many genes present in 3q26-qter, even in the subregion 3q26 as explained in the Gray I and Gray II Declarations. Unlike *Apotex*, where all of the 50 salts were acknowledged to be useful in

making a pharmaceutical formulation, there is no evidence that any of these particular genes would be expected to likely be overexpressed and play a role in ovarian cancer. As Dr. Gray noted in the Gray I Declaration, it was simply not possible to determine the focal point of amplification in the studies described by Arnold. Volinia's observation that *PIK3CA* is localized to 3q26.3 provides no indication that it would be expected to play a role in ovarian cancer in which 3q26-3qter is amplified. The studies of Xiao and Skorski that look at PIK3CA activity in gastric cancer cell lines and leukemia cells do not provide any insights into ovarian cancer. Bonjouklian does not explain just what a "PI3 kinase-dependent" neoplasm is, nor does the reference provide any insight into why an ovarian cancer cell having amplified 3q26-3qter would be expected to be such a "PI3 kinase-dependent" neoplasm.

The evidence provided by Appellants further demonstrate that it is unpredictable whether any particular gene, even if it is amplified, would play a role in cancer, given the complexity of the disease, and thereby serve as a therapeutic target. Thus, in the present case, there is no finite number of identified predictable solutions that would be obvious to try.

Accordingly, under the standard of obviousness articulated by the Supreme Court in *KSR International Co. V. Telefex Inc.* 82 USPQ2d 1385 (S. Ct. 2007), the claims are patentable.

B. Rejection of claim 39 under 35 U.S.C. § 103 over Bonjouklian in view of Arnold and Volinia and further in view of (in the alternative) Xiao or Skorski; and further, in view of Powis

The rejection of claim 39 as allegedly unpatentable over Bonjouklian, Arnold, Volinia, and Xiao or Skorski as applied to claims 37 and 38 above, and further in view of Powis is also being appealed. Powis is characterized by the Examiner as describing that LY294002 is a selective PI 3 kinase inhibitor (May 10, 2007 Office Action, page 8). The Examiner contends that claim 39 is obvious, as one of skill would have been motivated to use LY294002 in the methods of the invention, because it was known to be an effective inhibitor of PI3 kinase. However, the cited primary references (Bonjouklian, Arnold, Volinia, and Xiao or Skorski) fail to render claims 37 and 38 obvious for the reasons explained above. The secondary references

merely teach that LY294002 is a PI3 kinase inhibitor. Such disclosure does not cure the defects in the Examiner's arguments based on the primary references.

C. The rejection of claim 39 under 35 U.S.C. § 103 over Bonjouklian in view of Arnold and Volinia and further in view of (in the alternative) Xiao or Skorski; and further in view of June

The rejection of claim 39 as allegedly unpatentable over Bonjouklian, Arnold, Volinia, and Xiao or Skorski as applied to claims 37 and 38 above, and further in view of June is also being appealed. June is characterized by the Examiner as describing that LY294002 is a preferred PI 3 kinase inhibitor and that LY294002 inhibits proliferation of a T cell (May 10, 2007 Office Action, page 9). The Examiner contends that claim 39 is obvious, as one of skill would have been motivated to use LY294002 based on the teachings of June. However, the cited primary references (Bonjouklian, Arnold, Volinia, and Xiao or Skorski) fail to render claims 37 and 38 obvious for the reasons explained above. The secondary reference merely teaches that LY294002 is a preferred PI3 kinase inhibitor. Such disclosure does not cure the defects in the Examiner's arguments based on the primary references.

D. The rejection of claim 39 under 35 U.S.C. § 103 over Bonjouklian in view of Arnold and Volinia and further in view of (in the alternative) Xiao or Skorski; and further in view of Lavin.

The rejection of claim 39 as allegedly unpatentable over Bonjouklian, Arnold, Volinia, and Xiao or Skorski as applied to claims 37 and 38 above, and further in view of Lavin is also being appealed. Lavin is characterized by the Examiner as describing that LY294002 is an effective PI 3 kinase inhibitor and abrogated the ability of NGF to prevent apoptosis in PC-12 cells, suggesting an important role of PI 3 kinase is to ensure cell survival by preventing apopotosis (May 10, 2007 Office Action, page 10). The Examiner contends that claim 39 is obvious, as one of skill would have been motivated to use LY294002 based on the teachings of Lavin. However, the cited primary references (Bonjouklian, Arnold, Volinia, and Xiao or Skorski) fail to render claims 37 and 38 obvious for the reasons explained above. The secondary

reference merely teach that LY294002 is an effective PI3 kinase inhibitor. Such disclosure does not cure the defects in the Examiner's arguments based on the primary references.

8. CONCLUSION

For the reasons explained above, the art cited by the Examiner does not lead to Appellants' invention. It is respectfully submitted that all of the rejections should be reversed.

Respectfully submitted,

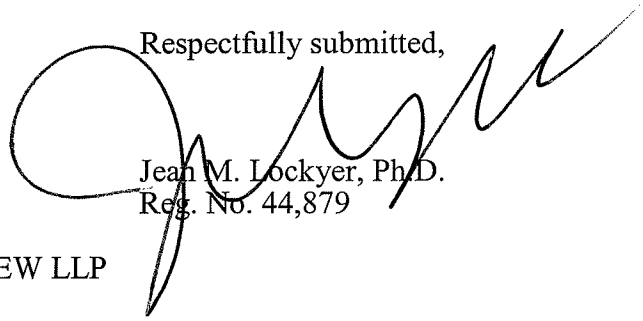

Jean M. Lockyer, Ph.D.
Reg. No. 44,879

TOWNSEND and TOWNSEND and CREW LLP
Two Embarcadero Center, Eighth Floor
San Francisco, California 94111-3834
Tel: 415-576-0200
Fax: 415-576-0300

62185084 v1

9. CLAIMS APPENDIX

1.-36. (cancelled)

37. (previously presented) A method of inhibiting the pathological proliferation of ovarian cancer cells in a patient, the method comprising:

detecting the presence of an amplification of PIK3CA in ovarian cancer cells from the patient; and

administering a therapeutically effective dose of an inhibitor of PI3 kinase to the patient, wherein the inhibitor inhibits PI3 kinase enzymatic activity.

38. (previously presented) The method of claim 37, wherein the inhibitor of PI3 kinase is a non-peptidic inhibitor of PI3 kinase phosphoinositide phosphorylation activity.

39. (previously presented) The method of claim 38, wherein the non-peptidic inhibitor is LY294002.

40. (cancelled)

10. EVIDENCE APPENDIX

A. Declaration under 37 C.F.R. § 1.132 by Joe W. Gray, Ph.D.

a) filed with Appellants' response filed January 8, 2007 to a non-final Office Action. (Signed version filed February 28, 2007.)

b) The Final Office Action mailed May 10, 2007 acknowledged the filed Declaration.

B. Declaration under 37 C.F.R. § 1.132 by Joe W. Gray, Ph.D.

a) filed with Appellants' response with RCE filed June 16, 2008 to the May 10, 2007 Final Office Action.

b) The Final Office Action mailed November 9, 2008 acknowledged the filed Declaration.

Evidence Appendix

A. Declaration by Joe W. Gray filed January 8, 2007

I hereby certify that this correspondence ... being ~~deposited with the United States Postal Service as first class mail in an envelope addressed to:~~

~~Mail Stop Amendment~~
~~Commissioner for Patents~~
~~P.O. Box 1450~~
~~Alexandria, VA 22313-1450~~

filed via EFS-Web w/USPTO

On 28 Feb. 2007

TOWNSEND and TOWNSEND and CREW LLP

By: Malinda Waght

PATENT
Attorney Docket No.: 02307O-067720US
Client Ref. No.: 96-215-3

IN THE UNITED STATES PATENT AND TRADEMARK OFFICE

In re application of:	Confirmation No. 5513
LALEH SHAYESTEH et al.	Examiner: Jehanne Souaya Sitton
Application No.: 08/905,508	Technology Center/Art Unit: 1634
Filed: August 4, 1997	DECLARATION UNDER 37 CFR 1.132
For: GENETIC ALTERATIONS ASSOCIATED WITH CANCER	
Customer No.: 20350	

Commissioner for Patents
P.O. Box 1450
Alexandria, VA 22313-1450

Sir:

1. I, Joe W. Gray, am Director, Division of Life Sciences, Lawrence Berkeley National Laboratory and an Adjunct Professor of Laboratory Medicine at the University of California San Francisco. I am a co-inventor of the subject matter disclosed and claimed in the above-referenced patent application.

2. I received a Ph.D. in Physics in 1972 from Kansas State University. My field of expertise is cancer, molecule cytogenetics, and genomics. I have been in this field for over 30 years and have authored over 300 publications in this area.

3. I have read and am familiar with the contents of the above-referenced patent application and claimed subject matter. I understand that the Examiner has rejected the current claims as allegedly unpatentable over the combination of the prior art teachings of Bonjouklian, *et al.* (U.S. Patent No. 5,378,725, "Bonjouklian") in view of Arnold, *et al.* (*Genes,*

Chromosomes, and Cancer 16:46-54, 1996, "Arnold") and Volinia, *et al.* (*Genomics* 24:472-477, 1994, "Volinia") and further in view of Xiao, *et al.* (*International Journal of Oncology* 6:405-411, 1995, "Xiao") or alternatively, Skorski, *et al.* (*Blood* 86:726-736, 1995, "Skorski"). In particular, it is my understanding that the rejection is based on the following arguments.

4. Bonjouklian is characterized by the Examiner as describing administration of a phosphatidyl inositol 3 (PI3) kinase inhibitor, *e.g.*, wortmannin, to treat a PI3 kinase-dependent condition such as abnormal cell growth in a neoplasm such as ovarian cancer. Arnold is described in the rejection as teaching an increase in copy number of 3q26-qter in ovarian tumors. The Examiner alleges that it would have been obvious to one of ordinary skill in the art at the time of the invention to detect amplification of the gene encoding the catalytic subunit of PI3 kinase, *i.e.*, *PIK3CA*, in ovarian cancer cells in a patient and to administer the PI3 kinase inhibitor wortmannin. Specifically, the Examiner contends that it would have been obvious because Arnold teaches that 3q26-qter is amplified in 42% of ovarian tumors that they analyzed and the *PIK3CA* gene is found at 3q26.3 (as taught by Volinia); and Bonjouklian teaches administration of a PI3 kinase inhibitor. The Examiner cites Xiao and Skorski as teaching that wortmannin inhibits proliferation of gastric cancer cell lines that overexpress PI3 kinase and of leukemia cells that require PI3 kinase for proliferation. It is the Examiner's position that Xiao and Skorski provide a basis for expecting that wortmannin treatment of ovarian cancer cells, as allegedly suggested by Bonjouklian, would inhibit proliferation.

5. This declaration is provided to show that the fact that the broad region of 3q26-qter was known to be amplified in ovarian cancer would not lead one of skill in the art to conclude that amplification of *PIK3CA*, which is one of numerous genes located in this broad region, leads to overexpression of PIK3CA and is therefore indicative of a role for PI3 kinase in oncogenesis in ovarian cancer cells that contain the amplified region.

6. Arnold describes a comparative genomic hybridization (CGH) study of forty nine ovarian cancer tumors. In this CGH analysis, differentially labelled total genomic DNA from a tumor sample and from a normal reference control sample were co-hybridized to normal metaphase chromosomes. The resulting ratio of the fluorescence intensities of the probes hybridized to the chromosomes is approximately proportional to the ratio of the copy numbers of

the corresponding DNA sequences in the tumor and normal reference genomes. Arnold identified the region of 3q26-qter as being increased in copy number in 42% of the ovarian tumors that were analyzed. However, although it was known in the art that the gene encoding the catalytic subunit of PI3 kinase (PIK3CA) is located at 3q26.3, the CGH study as performed by Arnold using metaphase chromosomes does not provide sufficient resolution to determine that the chromosomal subregion containing the PIK3CA locus is a focal point of amplification.

7. Furthermore, even though a gene may be present in an amplified chromosomal region, that fact alone does not lead one of skill to conclude that a particular gene is overexpressed. Many genes are present in chromosomal region 3q26-qter. For example the genome browser of the University of California, Santa Cruz (http://genome.ucsc.edu/cgi-bin/hgTracks?hgsid=83748260&clade=vertebrate&org=Human&db=hg18&position=3q26&pix=620&Submit=submit&hgsid=83748260, a print out of which is attached hereto, shows that numerous genes are located in the 3q26 region alone; however, there is no evidence that all or most of the products of these many genes are overexpressed in ovarian tumors.

8. It is my opinion as one who has practiced in this art for many years that although *PIK3CA* may have been identified as a potential gene of interest in the 3q26-qter region identified by Arnold due to its biological function in proliferation or its overexpression in other cancers, at the time of the invention one of skill could not have concluded that the mere presence of the gene in this broadly amplified region would predictably lead to a correlation with overexpression of the protein and an oncogenic role in ovarian cancer cell proliferation.

9. I further declare that all statements made herein of my knowledge are true and that all statements made on information and belief are believed to be true; and further that these statements are made with the knowledge that willful false statements and the like so made are punishable by fine or imprisonment or both (18 U.S.C. § 1001), and may jeopardize the validity of the patent application or any patent issuing thereon.

Dated: 4/26/07

Joe Gray, Ph.D.

Home Genomes Blat Tables Gene Sorter PCR DNA Convert Ensembl NCBI PDF/PS Help

UCSC Genome Browser on Human Mar. 2006 Assembly

move <<< << < > >> >>> zoom in 1.5x 3x 10x base zoom out 1.5x 3x 10x

position/search chr3:161,200,001-184,200,000 jump clear size 23,000,000 bp. configure

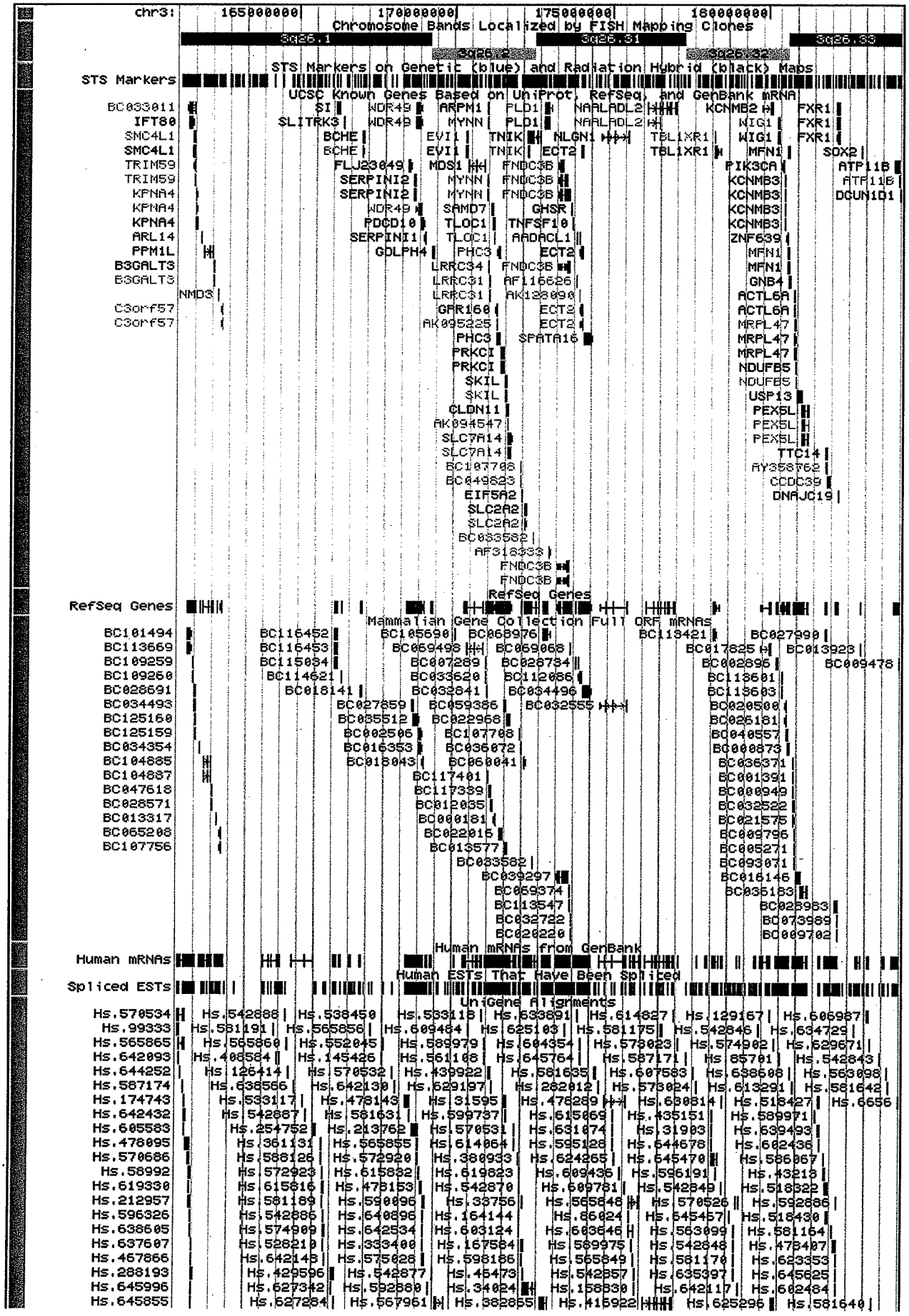
chr3:
165000000
170000000
175000000
180000000
Chromosome Bands Localized by FISH Mapping Clones
3q26.1
3q26.31
3q26.33
3q26.2
3q26.32
STS Markers on Genetic (blue) and Radiation Hybrid (black) Maps
STS Markers
UCSC Known Genes Based on UniProt, RefSeq, and GenBank mRNA
RefSeq Genes
Mammalian Gene Collection Full ORF mRNAs
Human mRNAs from GenBank
Human mRNAs
Human ESTs That Have Been Spliced
Spliced ESTs
UniGene Alignments

move start < 2.0 > Click on a feature for details. Click on base position to zoom in around cursor. Click on left mini-buttons for track-specific options. move end < 2.0 >

default tracks | hide all | add custom tracks | configure | refresh

Use drop down controls below and press refresh to alter tracks displayed.
Tracks with lots of items will automatically be displayed in more compact modes.

Mapping and Sequencing Tracks

Base Position dense	Chromosome Band pack	STS Markers dense	FISH Clones hide	Recomb Rate hide
Map Contigs hide	Assembly hide	Gap hide	Coverage hide	BAC End Pairs hide
Fosmid End Pairs hide	GC Percent hide	Short Match hide	Restr Enzymes hide	

Phenotype and Disease Associations

Locus Variants hide

Genes and Gene Prediction Tracks

Known Genes pack	RefSeq Genes dense	Other RefSeq hide	MGC Genes pack	Ensembl Genes hide
AceView Genes hide	N-SCAN hide	SGP Genes hide	Geneid Genes hide	Genscan Genes hide
Exoniphy hide	Superfamily hide	EvoFold hide	sno/miRNA hide	

mRNA and EST Tracks

Human mRNAs dense	Spliced ESTs dense	Human ESTs hide	Other mRNAs hide	Other ESTs hide
H-Inv hide	UniGene pack	Poly(A) hide		

Expression and Regulation

Affy HuEx 1.0 hide	Allen Brain hide	GNF Atlas 2 hide	GNF Ratio hide	Bertone Yale TAR hide
Affy U133 hide	Affy GNF1H hide	Affy U133Plus2 hide	Affy U95 hide	CpG Islands hide
FirstEF hide	TFBS Conserved hide	ORegAnno hide	7X Reg Potential hide	

Comparative Genomics

Conservation pack	Most Conserved hide	Fugu Chain hide	Fugu Net hide	Tetraodon Chain hide
Tetraodon Net hide	Tetraodon Ecores hide	Zebrafish chain hide	Zebrafish Net hide	X. tropicalis Chain hide
X. tropicalis Net hide	Chicken Chain hide	Chicken Net hide	Opossum Chain hide	Opossum Net hide
Cow Chain	Cow Net	Dog Chain	Dog Net	Rat Chain

hide	hide	hide	hide	hide
Rat Net hide	Mouse Chain hide	Mouse Net hide	Rhesus Chain hide	Rhesus Net hide
Chimp Chain hide	Chimp Net hide			

Variation and Repeats

SNPs dense	Segmental Dups hide	RepeatMasker dense	Simple Repeats hide	Microsatellite hide
Self Chain hide				

refresh

Evidence Appendix

B. Declaration by Joe W. Gray filed June 16, 2008

I hereby certify that this correspondence is being deposited with the United States Postal Service as first class mail in an envelope addressed to:

Mail Stop ~~Amendment~~ RCE
Commissioner for Patents
P.O. Box 1450
Alexandria, VA 22313-1450

On 13 June 2008

TOWNSEND and TOWNSEND and CREW LLP

By: Malinda Adagit

PATENT
Attorney Docket No.: 02307O-067720US
Client Ref. No.: 96-215-3

IN THE UNITED STATES PATENT AND TRADEMARK OFFICE

In re application of:	Confirmation No. 5513
LALEH SHAYESTEH et al.	Examiner: Jehanne Souaya Sitton
Application No.: 08/905,508	Technology Center/Art Unit: 1634
Filed: August 4, 1997	DECLARATION UNDER 37 CFR 1.132
For: GENETIC ALTERATIONS ASSOCIATED WITH CANCER	
Customer No.: 20350	

Commissioner for Patents
P.O. Box 1450
Alexandria, VA 22313-1450

Sir:

1. I, Joe W. Gray, am Director, Division of Life Sciences, Lawrence Berkeley National Laboratory and an Adjunct Professor of Laboratory Medicine at the University of California San Francisco. I am a co-inventor of the subject matter disclosed and claimed in the above-referenced patent application.

2. This declaration follows my declaration filed January 8, 2007 relating to the obviousness rejection over Bonjouklian, *et al.* (U.S. Patent No. 5,378,725) that also cites Arnold, *et al.* (*Genes, Chromosomes, and Cancer* 16:46-54, 1996) and Volinia, *et al.* (*Genomics* 24:472-477, 1994, "Volinia") and is in response to the May 10, 2007 Office Action. My background is described in the previous declaration.

3. I have read and am familiar with the contents of the above-referenced patent application and claimed subject matter. I understand that the Examiner has maintained the

rejection of the claims for obviousness based on the same sets of references. My previous declaration summarizes the references and rejections.

4. It is my understanding that the Examiner has questioned my statement that the presence of a gene in an amplified chromosomal region does not lead one of skill to conclude that the gene is overexpressed and important in the pathophysiology of ovarian cancer.

5. This declaration provides additional evidence that one of skill in the art would not conclude that expression of a particular gene would be increased simply based on the observation that the gene is present in an amplified chromosomal region, as well as evidence that one of skill in the art would not conclude, based on the observation that a particular gene is overexpressed, that it would contribute to the pathophysiology of the disease. In support of this contention, I refer to Chin *et al.* (2006) *Cancer Cell.* 10:529-41. [**Exhibit A**], Cheng *et al.,* (2004) *Nat Med.* 10:1251-6 [**Exhibit B**], Eder *et al* (2005) *Proc Natl Acad Sci U S A.* 102:12519-24 [**Exhibit C**], Nanjundan *et al.,* (2007) *Cancer Res.* 67:3074-84 [**Exhibit D**] and a Table of gene expression values from the regions of amplification at 3q26 in ovarian cancer [**Exhibit E**].

6. Chin addresses the issue of whether amplification of a gene correlates with increased expression. In doing so, the authors carried out comparative genomic hybridization (CGH) and gene expression analysis with breast cancer samples. As stated on the bottom of page 531 *"We tested associations between copy number and expression level for 186 genes in regions of amplification at 8p11-12, 11q13-q14, 17q11-12,and 20q13, and we identified 66 genes in these regions whose expression levels were correlated with copy number (FDR <0.01, Wilcoxon rank-sum test; Table 3). These genes define the transcriptionally important extents of the regions of recurrent amplification."* This reference in a top rank scientific journal demonstrates that, in reality, amplification of a chromosomal region does not lead one of skill in the art to conclude that a gene present in the amplified region is over expressed.

7. The Examiner cites Arnold *et al.*, which describes amplification of chromosome 3q26- 3qter in ovarian cancers. It is my understanding that the Examiner believes that there only 30- 50 genes in the region identified by Arnold *et al.* The Examiner contends that, given a finite number of identified, predictable solutions, a person of ordinary skill would

have good reason to pursue known options, and that this would represent nothing more than ordinary skill and common sense.

8. In my last declaration, I referred to the region of 3q26- 3qter as containing many genes. Provided herewith is a printout of information from the Ensembl genome browser that provides more detailed information as to the number of genes that have been identified in this chromosomal region. **Exhibit F** provides a graphic of the region of chromosome 3 from q26.1 through q29. **Exhibit F** also shows the gene contained within this region (Chromosome 3 162152104-199501827), of which there are hundreds. **Exhibit G** focuses on the 3q26 region, 3q26.1 through 3q26.33. A listing of the genes identified in that region (Chromosome 3 162152104-184145606) shows that there are over 80 genes in this region alone. Accordingly, the region identified by Arnold *et al.* as amplified in ovarian cancer, 3q26-3qter, in fact does contain a multitude of genes. This is further supported by **Exhibit E** which describes unpublished work from my laboratory in which demonstrates that the region of amplification at 3q26 that we identified as amplified in ovarian cancer encodes at least 68 genes. Of these, only 30 have expression levels that are associated with copy number ($p<0.05$, univariate t test).

9. The genes in this amplified region could not be characterized as "predictable solutions" to the problem of identifying and treating ovarian cancer. The functions of most of these genes in ovarian cells, and their roles in abnormal ovarian cancer cells, is not known. One of skill would not have a reasonable expectation that any of the genes in this region would necessarily be involved in ovarian cancer.

10. Regardless of how many genes are present in this region, one of skill could not conclude that amplification of *PIK3CA* in this region would lead to overexpression of *PIK3CA* and activation of phosphoinositide-3 kinase signaling. This stems from two facts:

(a) Transcriptional up regulation of a gene frequently does not lead to increased protein expression. We demonstrated that increased transcription of PIK3CA is associated with increased protein levels.

(b) The protein encoded by PIK3CA, the p110alpha catalytic subunit of phosphatidylinositol 3-kinase, must act in concert with the p85 adapter protein encoded by the gene PIK3R1. One skilled in the art would not conclude that expression of one subunit of a

signaling complex would necessarily lead to increased activity of the complex. We demonstrated that amplification and over expression of PIK3CA is associated with increased PI3-kinase activity AND that treatment with the PI3-kinase inhibitor LY294002 decreases proliferation and increases apoptosis. These studies, in combination, demonstrated the importance of *PIK3CA* as an oncogene that is a therapeutic target in ovarian cancer.

11. The publications of Cheng, Eder and Nanjundan indicate that other genes in the 3q26 amplification also play roles in the pathophysiology of ovarian cancer. These studies warranted publication in high rank journals. This again demonstrates the fact that simple presence in a region of amplification is not sufficient to lead one skilled in the art to conclude that the gene contributes to the pathophysiology of the cancer in which it is amplified, and it does not lead one with skill in the art to conclude that it is a useful therapeutic target.

12. I further declare that all statements made herein of my knowledge are true and that all statements made on information and belief are believed to be true; and further that these statements are made with the knowledge that willful false statements and the like so made are punishable by fine or imprisonment or both (18 U.S.C. § 1001), and may jeopardize the validity of the patent application or any patent issuing thereon.

Dated: 6/13/08

Joe Gray, Ph.D.

Exhibit A

Genomic and transcriptional aberrations linked to breast cancer pathophysiologies

Koei Chin,[1,5] Sandy DeVries,[1,5] Jane Fridlyand,[1,5] Paul T. Spellman,[2] Ritu Roydasgupta,[1] Wen-Lin Kuo,[1,2] Anna Lapuk,[1,2] Richard M. Neve,[1,2] Zuwei Qian,[4] Tom Ryder,[4] Fanqing Chen,[2] Heidi Feiler,[1,2] Taku Tokuyasu,[1] Chris Kingsley,[1] Shanaz Dairkee,[3] Zhenhang Meng,[3] Karen Chew,[1] Daniel Pinkel,[1] Ajay Jain,[1] Britt Marie Ljung,[1] Laura Esserman,[1] Donna G. Albertson,[1] Frederic M. Waldman,[1,6] and Joe W. Gray[1,2,6,*]

[1] Comprehensive Cancer Center, 2340 Sutter Street, University of California, San Francisco, San Francisco, California 94143
[2] Life Sciences Division, Lawrence Berkeley National Laboratory, One Cyclotron Road, Berkeley, California 94127
[3] California Pacific Medical Center, 475 Brannan Street, San Francisco, California 94107
[4] Affymetrix, Inc., 3450 Central Expressway, Santa Clara, California 95051
[5] These authors contributed equally to this work.
[6] These authors contributed equally to this work.
*Correspondence: jwgray@lbl.gov

Summary

This study explores the roles of genome copy number abnormalities (CNAs) in breast cancer pathophysiology by identifying associations between recurrent CNAs, gene expression, and clinical outcome in a set of aggressively treated early-stage breast tumors. It shows that the recurrent CNAs differ between tumor subtypes defined by expression pattern and that stratification of patients according to outcome can be improved by measuring both expression and copy number, especially high-level amplification. Sixty-six genes deregulated by the high-level amplifications are potential therapeutic targets. Nine of these (*FGFR1*, *IKBKB*, *ERBB2*, *PROCC*, *ADAM9*, *FNTA*, *ACACA*, *PNMT*, and *NR1D1*) are considered druggable. Low-level CNAs appear to contribute to cancer progression by altering RNA and cellular metabolism.

Introduction

It is now well established that breast cancers progress through accumulation of genomic (Albertson et al., 2003; Knuutila et al., 2000) and epigenomic (Baylin and Herman, 2000; Jones, 2005) aberrations that enable the development of aspects of cancer pathophysiology such as reduced apoptosis, unchecked proliferation, increased motility, and increased angiogenesis (Hanahan and Weinberg, 2000). Discovery of the genes that contribute to these pathophysiologies when deregulated by recurrent aberrations is important to understanding mechanisms of cancer formation and progression and to guide improvements in cancer diagnosis and treatment.

Analyses of expression profiles have been particularly powerful in identifying distinctive breast cancer subsets that differ in biological characteristics and clinical outcome (Perou et al., 1999, 2000; Sorlie et al., 2001, 2003). For example, unsupervised hierarchical clustering of microarray-derived expression data has identified intrinsically variable gene sets that distinguish five breast cancer subtypes—basal-like, luminal A, luminal B, ERBB2, and normal breast-like. The basal-like and ERBB2 subtypes have been associated with strongly reduced survival durations in patients treated with surgery plus radiation (Perou et al., 2000; Sorlie et al., 2001), and some studies have suggested that reduced survival duration in poorly performing subtypes is caused by an inherently high propensity to metastasize (Ramaswamy et al., 2003). These analyses already have led to the development of multigene assays that stratify patients into groups that can be offered treatment strategies based on risk of progression (Esteva et al., 2005; Gianni et al., 2005; van 't Veer et al., 2002; van de Vijver et al., 2002). However, the predictive power of these assays is still not as high as desired, and the assays have not been fully tested in patient populations treated with aggressive adjuvant chemotherapies.

Analyses of breast tumors using fluorescence in situ hybridization (Al-Kuraya et al., 2004; Kallioniemi et al., 1992; Press

SIGNIFICANCE

This study indicates that the accuracy with which breast patients can be stratified according to outcome can be improved by combining analyses of gene expression and genome copy number. Markers for high-level amplification and/or overexpression of genes at 8p11, 11q13, 17q12, and/or 20q13 are particularly strong predictors of reduced survival duration. Genes in these regions are high-priority therapeutic targets for treatment of patients that respond poorly to current aggressive therapies. The statistically significant deregulation of genes involved in RNA and cellular metabolism by low-level CNAs suggests that these events contribute to breast cancer progression by increasing basal metabolism.

et al., 2005; Tanner et al., 1994) and comparative genomic hybridization (Kallioniemi et al., 1994; Loo et al., 2004; Naylor et al., 2005; Pollack et al., 1999) show that breast tumors also display a number of recurrent genome copy number aberrations, including regions of high-level amplification that have been associated with adverse outcome (Al-Kuraya et al., 2004; Cheng et al., 2004; Isola et al., 1995; Jain et al., 2001; Press et al., 2005). This raises the possibility of improved patient stratification through combined analysis of gene expression and genome copy number (Barlund et al., 2000; Pollack et al., 2002; Ray et al., 2004; Yi et al., 2005). In addition, several studies of specific chromosomal regions of recurrent abnormality at 17q12 (Kauraniemi et al., 2001, 2003) and 8p11 (Gelsi-Boyer et al., 2005; Ray et al., 2004) show the value of combined analysis of genome copy number and gene expression for identification of genes that contribute to breast cancer pathophysiology by deregulating gene expression.

We have extended these studies by performing combined analyses of genome copy number and gene expression to identify genes that contribute to breast cancer pathophysiology, with emphasis on those that are associated with poor response to current therapies. By associating clinical endpoints with genome copy number and gene expression, we showed strong associations between expression subtype and genome aberration composition, and we identified four regions of recurrent amplification associated with poor outcome in treated patients. Gene expression profiling revealed 66 genes in these regions of amplification whose expression levels were deregulated by the high-level amplifications. We also found a surprising association between low-level CNAs and upregulation of genes associated with RNA and protein metabolism that may suggest a mechanism by which these aberrations contribute to cancer progression.

Results

We assessed genome copy number using BAC array CGH (Hodgson et al., 2001; Pinkel et al., 1998; Snijders et al., 2001; Solinas-Toldo et al., 1997) and gene expression profiles using Affymetrix U133A arrays (Ramaswamy et al., 2003; Reyal et al., 2005) in breast tumors from a cohort of patients treated according to the standard of care between 1989 and 1997 (surgery, radiation, hormonal therapy, and treatment with high-dose adriamycin and cytoxan as indicated). We measured genome copy number profiles for 145 primary breast tumors and gene expression profiles for 130 primary tumors, of which 101 were in common. We analyzed these data to identify recurrent genomic and transcriptional abnormalities, and we assessed associations with clinical endpoints to identify genomic events that might contribute to cancer pathophysiology.

Molecular characteristics and associations

Genome copy number and gene expression features

We found that the recurrent genome copy number and gene expression characteristics measured for the patient cohort in this study were similar to those reported in earlier studies. We summarize these briefly.

Figures 1A and 1B show numerous regions of recurrent genome CNA and nine regions of recurrent high-level amplification involving regions of chromosomes 8, 11, 12, 17, and 20, while Figure 2 shows that analysis of these data using unsupervised hierarchical clustering resolves these tumors into the "1q/16q" (or "simple"), "complex," and "amplifier" genome aberration subtypes (Fridlyand et al., 2006). The genomic extents of the regions of amplification are listed in Table 1. These were generally similar to those reported in earlier studies using chromosome (Kallioniemi et al., 1994) and array CGH (Loo et al., 2004; Naylor et al., 2005; Pollack et al., 1999, 2002). Several of these regions of amplification were frequently coamplified. Declaring a Fisher exact test p value of less than 0.05 for pairwise associations to be suggestive of possible significant coamplification, we found coamplification of 8q24 and 20q13 and coamplification of regions at 11q13-14, 12q13-14, 17q11-12, and 17q21-24. These analyses were underpowered to achieve significance with proper correction for multiple testing, so these associations are suggestive but not significant. However, these associations were consistent with the report of Al-Kuraya et al. (2004), who showed evidence for coamplification of genes in several of these regions of amplification including *ERBB2*, *MYC*, *CCND1*, and *MDM2*, and that of Naylor et al. (2005) showing coamplification of 17q12 and 17q25.

Figure S1 (in the Supplemental Data available with this article online) shows that unsupervised hierarchical clustering of intrinsically variable genes resolves the tumors in our study cohort into the luminal A, luminal B, basal-like, and ERBB2 expression subtypes previously reported for breast tumors (Perou et al., 1999, 2000; Sorlie et al., 2003). We assessed the genomic characteristics of these expression subtypes in subsequent analyses.

Associations between CNAs and expression

Combined analyses of genome copy number and expression showed that the recurrent genome CNAs differed between expression subtypes and identified genes whose expression levels were significantly deregulated by the CNAs. Figures 1C–1J show the recurrent CNAs for each expression subtype. In these analyses, we assigned each tumor to the expression subtype cluster (basal-like, ERBB2, luminal A, and luminal B) to which its expression profile was most highly correlated. We did not assess aberrations in normal-like tumors due to the small number of such tumors. Figure 1C shows that the basal-like tumors were relatively enriched for low-level copy number gains involving 3q, 8q, and 10p and losses involving 3p, 4p, 4q, 5q, 12q, 13q, 14q, and 15q, while Figure 1D shows that high-level amplification at any locus was infrequent in these tumors. Figure 1E shows that ERBB2 tumors were relatively enriched for increased copy number at 1q, 7p, 8q, 16p, and 20q and reduced copy number at 1p, 8p, 13q, and 18q. Figure 1F shows that amplification of *ERBB2* was highest in the ERBB2 subtype as expected, but amplification of noncontiguous, distal regions of 17q also was frequent as previously reported (Barlund et al., 1997). Figure 1G shows that increased copy number at 1q and 16p and reduced copy number at 16q were the most frequent abnormalities in luminal A tumors, while Figure 1H shows that high-level amplifications at 8p11-12, 11q13-14, 12q13-14, 17q11-12, 17q21-24, and 20q13 were relatively common in this subtype. Figure 1I shows that gains of chromosomes 1q, 8q, 17q, and 20q and losses involving portions of 1p, 8p, 13q, 16q, 17p, and 22q were prevalent in luminal B tumors, while Figure 1J shows that high-level amplifications involving 8p11-12, two regions of 8q, and 11q13-14 were frequent. Bergamaschi et al. (2006) have reported similar CNA patterns for the luminal A, luminal B, basal, and ERBB2 expression clusters.

In order to understand how the genome aberrations influence cancer pathophysiologies, we identified genes that were

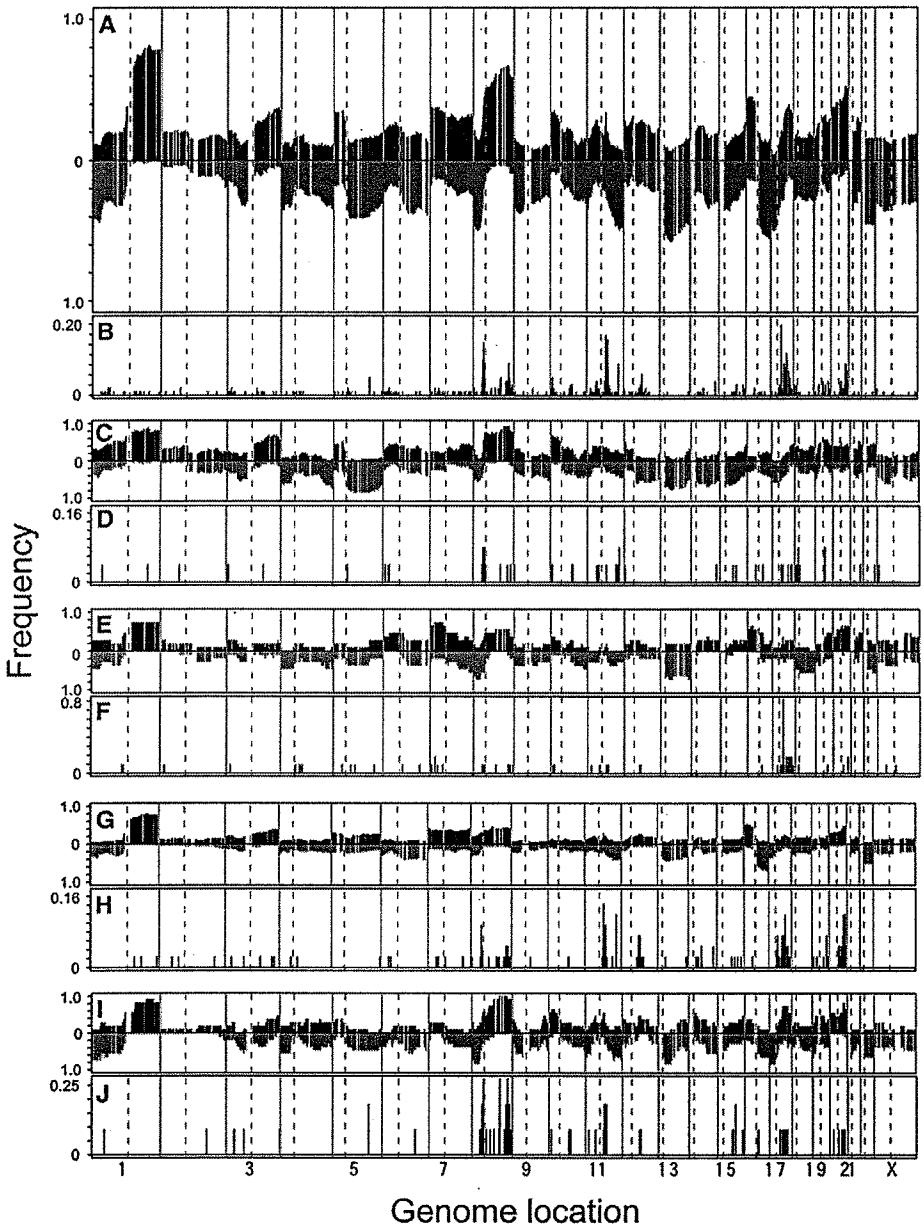

Figure 1. Recurrent abnormalities in 145 primary breast tumors

A: Frequencies of genome copy number gain and loss plotted as a function of genome location with chromosomes 1pter to the left and chromosomes 22qter and X to the right. Vertical lines indicate chromosome boundaries, and vertical dashed lines indicate centromere locations. Positive and negative values indicate frequencies of tumors showing copy number increases and decreases, respectively, with gain and loss as described in the Experimental Procedures.

B: Frequencies of tumors showing high-level amplification. Data are displayed as described in **A**.

C–J: Frequencies of tumors showing significant copy number gains and losses as defined in **A** (upper member of each pair) or high-level amplifications as defined in **B** (lower member of each pair) in tumor subtypes defined according to expression phenotype; **C** and **D**, basal-like; **E** and **F**, ERBB2; **G** and **H**, luminal A; **I** and **J**, luminal B. Data are displayed as described in **A**.

deregulated by recurrent genome CNAs. We took these genes to be those whose expression levels were significantly associated with copy number (Holm-adjusted p value < 0.05). These genes, which represent about 10% of the genome interrogated by the Affymetrix HGU133A arrays used in this study, and their copy number-expression level correlation coefficients are listed in Table S3. This extent of genome-aberration-driven deregulation of gene expression is similar to that reported in earlier studies (Hyman et al., 2002; Pollack et al., 1999). We tested associations between copy number and expression level for 186 genes in regions of amplification at 8p11-12, 11q13-q14, 17q11-12, and 20q13, and we identified 66 genes in these regions whose expression levels were correlated with copy number (FDR < 0.01, Wilcoxon rank-sum test; Table 3). These genes define the transcriptionally important extents of the regions of recurrent amplification. Twenty-three were from a 5.5 Mbp region at 8p11-12 flanked by *SPFH2* and *LOC441347*, ten were from a 6.6 Mbp region at 11q13-14 flanked by *CCND1* and *PRKRIR*, nineteen were from a 3.1 Mbp region at 17q12 flanked by *LHX1* and *NR1D1*, and fourteen were from a 5.4 Mbp region at 20q13 flanked by *ZNF217* and *C20orf45*.

Since the recurrent genome aberrations differed between expression subtypes, we explored the extent to which the expression subtypes were determined by genome copy number. Specifically, we applied unsupervised hierarchical clustering to intrinsically variable genes *after removing genes whose expression levels were correlated with copy number*. Figure 4 shows that the tumors still resolve into the basal-like and luminal classes. However, the ERBB2 cluster was lost.

Associations with clinical variables

Associations with histopathology

Figure 2 and Table 2 summarize associations of histopathological features with aspects of genome abnormality, including

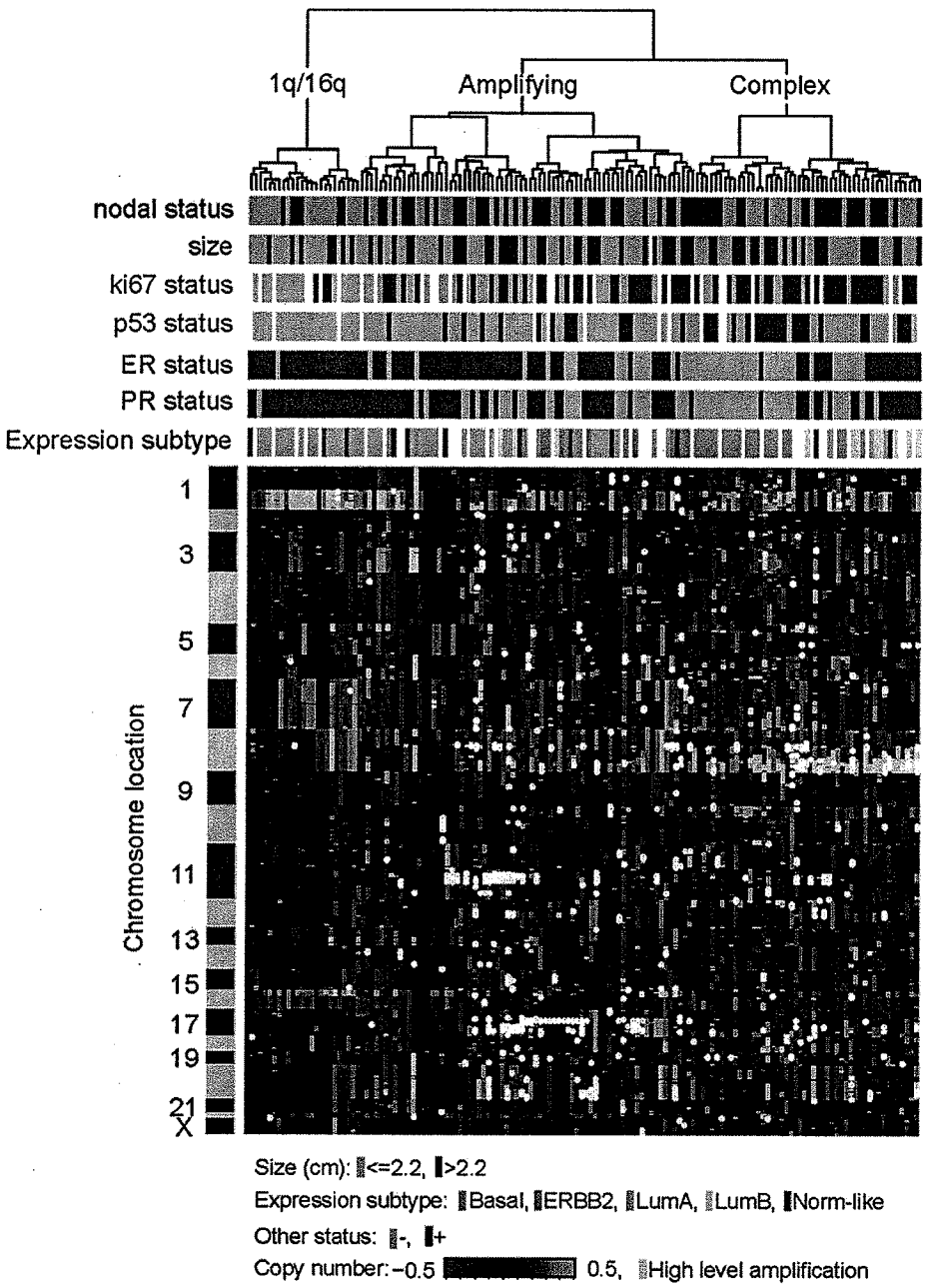

Figure 2. Unsupervised hierarchical clustering of genome copy number profiles measured for 145 primary breast tumors

Green indicates increased genome copy number, and red indicates decreased genome copy number. The three major genomic clusters from left to right are designated 1q/16q, complex, and amplifying. The bar to the left indicates chromosome locations with chromosome 1pter to the top and 22qter and X to the bottom. The locations of the odd-numbered chromosomes are indicated. The upper color bars indicate biological and clinical aspects of the tumors. Color codes are indicated at the bottom of the figure. Dark blue indicates positive status, and light blue indicates negative status for node, ER, PR, and p53 expression. For Ki67, dark blue indicates fraction >0.1, and light blue indicates fraction <0.1. For size, light blue indicates size <2.2 cm, and dark blue indicates size >2.2 cm. Color codes for the expression bar are as follows: orange, luminal A; dark blue, normal breast-like; light blue, ERBB2; green, basal-like; yellow, luminal B.

recurrent genome abnormalities, total number of copy number transitions, fraction of the genome altered (FGA), number of chromosomal arms containing at least one amplification, number of recurrent amplicons, and presence of at least one recurrent amplification. These analyses showed that ER/PR-negative tumors were predominantly found in the basal-like expression and "complex" genome aberration subtypes, respectively. Node-positive tumors had significantly more amplified arms and recurrent amplicons than node-negative samples but showed a much more moderate difference in terms of low-level copy number transitions. Stage 1 tumors had moderately fewer low- and high-level changes than higher-stage tumors. The number of low- and high-level abnormalities increased with SBR grade. Interestingly, the "complex" tumors showing many low-level abnormalities were more strongly associated with aberrant p53 expression than "amplifying" tumors. "Simple" tumors tended to have Ki67 proliferation indices <10%, while "complex" and "amplifying" tumors typically had Ki67 indices >10%. The number of amplifications increased significantly with tumor size, but the number of low-level changes did not. We observed no association of genomic changes with the age at diagnosis.

Associations with outcome

Figure 2 and Table S2 summarize associations between histopathological, transcriptional, and genomic characteristics and outcome endpoints identified using multivariate regression analysis. Histopathological features including size and nodal status were significantly associated with survival duration and/or disease recurrence in univariate analyses (Table S1) and were included in the multivariate regressions described below.

The tumor subtypes based on patterns of gene expression or genome aberration content showed moderate associations with

Table 1. Univariate and multivariate associations for individual amplicons and/or disease-specific survival and distant recurrence

Amplicon	Flanking clone (left)	Flanking clone (right)	Kb start	Kb end	p value, univariate		p value, luminal A, univariate		p value, multivariate	
					survival	recurrence	survival	recurrence	survival	recurrence
8p11-12	RP11-258M15	RP11-73M19	33579	43001	0.011	0.004	0.022	0.004	0.037	0.006
8q24	RP11-65D17	RP11-94M13	127186	132829	0.830	0.880	0.140	1.0	0.870	0.720
11q13-14	CTD-2080I19	RP11-256P19	68482	71659	0.540	0.410	0.016	0.240	0.660	0.440
11q13-14	RP11-102M18	RP11-215H8	73337	78686	0.230	0.150	0.016	0.240	0.360	0.190
12q13-14	BAL12B2624	RP11-92P22	67191	74053	0.250	0.260	0.230	0.098	0.920	0.960
17q11-12	RP11-58O8	RP11-87N6	34027	38681	0.004	0.004	1.0	1.0	0.022	0.008
17q21-24	RP11-234J24	RP11-84E24	45775	70598	0.960	0.920	0.610	0.290	0.530	0.630
20q13	RMC20B4135	RP11-278I13	51669	53455	0.340	0.800	0.048	0.140	0.590	0.970
20q13	GS-32I19	RP11-94A18	55630	59444	0.087	0.230	0.048	0.140	0.060	0.220
Any amplicon					0.005	0.003	0.024	0.120	0.034	0.009

Also shown are the chromosomal positions of the beginning and ends of the amplicons and the flanking clones. Associations are shown for the entire sample set and for luminal A tumors (univariate associations only).

outcome endpoints. For example, Figure 3A shows that patients with tumors classified as ERBB2 based on expression pattern had significantly shorter disease-specific survival than patients classified as luminal A or luminal B as previously reported (Perou et al., 2000; Sorlie et al., 2001). Unlike these earlier reports, patients with tumors classified as basal-like did not do significantly worse than patients with luminal or normal breast-like tumors, although there was a trend in that direction. In addition, Figure 3B indicates that patients with tumors classified as "1q/16q" based on genome aberration content tended to have longer disease-specific survival than patients with "complex" or "amplifier" tumors.

We found that high-level amplification was most strongly associated with poor outcome in this aggressively treated patient population. Amplification at any of the nine recurrent amplicons was an independent risk factor for reduced survival duration ($p < 0.04$) and distant recurrence ($p < 0.01$) in a multivariate Cox-proportional model that included tumor size and nodal status. Figure 3C, for example, shows that patients whose tumors had at least one recurrent amplicon survived a significantly shorter time than did patients with tumors showing no amplifications. More specifically, amplifications of 8p11-12 or 17q11-12 (*ERBB2*) were significantly associated with disease-specific survival and distant recurrence in all patients in multivariate regressions (Table 1). Importantly, we found that stratification according to amplification status allowed identification of patients with poor outcome even within an expression subtype. Figure 3D, for example, shows that patients with luminal A tumors and amplification at 8p11-12, 11q13-14, or 20q13 had significantly shorter disease-specific survival than patients without amplification in one of these regions (the number of samples in the luminal A subtype group was too small for multivariate regressions). Amplification at 8p11-12 was most strongly associated with distant recurrence in the luminal A subtype.

Considering the strong association between amplification and outcome, we explored the possibility that some of these genes were overexpressed in tumors in which they were not amplified and that overexpression was associated with reduced survival duration in those tumors. Increased expression levels of seven genes (see Table 3) were associated with reduced survival or distant recurrence at the $p < 0.1$ level, but only two, the growth factor receptor-binding protein GRB7 (17q) and the keratin-associated protein KTRAP5-9 (11q), at the $p < 0.05$ level. Interestingly, this analysis also revealed an unexpected association between *reduced* expression levels of genes from regions of amplification and poor outcome (either disease-free survival or distant recurrence) in tumors without relevant amplifications ($p < 0.05$). This was especially prominent for genes from the region of amplification at 8p11-12 (14 of 23 genes in this region showed this association), while only two genes from regions of adverse-outcome-associated amplifications on chromosomes 17q and 20q showed this association. Following this lead, we tested associations between outcome and reduced copy number at 8p11-12 in patients in tumors in which 8p11-12 was not

Table 2. Associations of genomic variables with clinical features

	Fraction of genome altered[1]	Total number of transitions[1]	Number of amplified arms[1]	Number of recurrent amplicons[1]	Presence of recurrent amplicons[2]
1. ER (negative versus positive)	<0.001	<0.001	0.376	0.147	0.482
2. PR (negative versus positive)	0.005	<0.001	<0.050	0.319	0.390
3. Nodes (positive versus negative)	0.053	0.106	0.012	0.012	0.008
4. Stage (>1 versus 1)	0.013	0.052	0.045	0.312	0.368
5. ERBB2 (positive versus negative)	0.650	0.830	0.015	<0.001	<0.001
6. Ki67 (>0.1 versus <0.1)	0.013	0.031	0.024	0.010	0.005
7. P53 (positive versus negative)	0.001	<0.001	0.043	0.573	0.171
8. Size	0.339	0.088	0.016	0.005	0.015
9. Age at Dx	0.767	0.361	0.223	0.905	0.947
10. SBR grade	<0.001	<0.001	0.008	0.206	0.035
11. Expression subtype	<0.001	<0.001	0.002	0.003	<0.001
12. Genomic subtype	<0.001	<0.001	<0.001	<0.001	<0.001

[1]Kruskal-Wallis test (1–7, 11, and 12), significance of robust linear regression standardized coefficient (8–10).
[2]Fisher exact test (1–7, 11, and 12), significance of robust linear regression standardized coefficient (8–10).

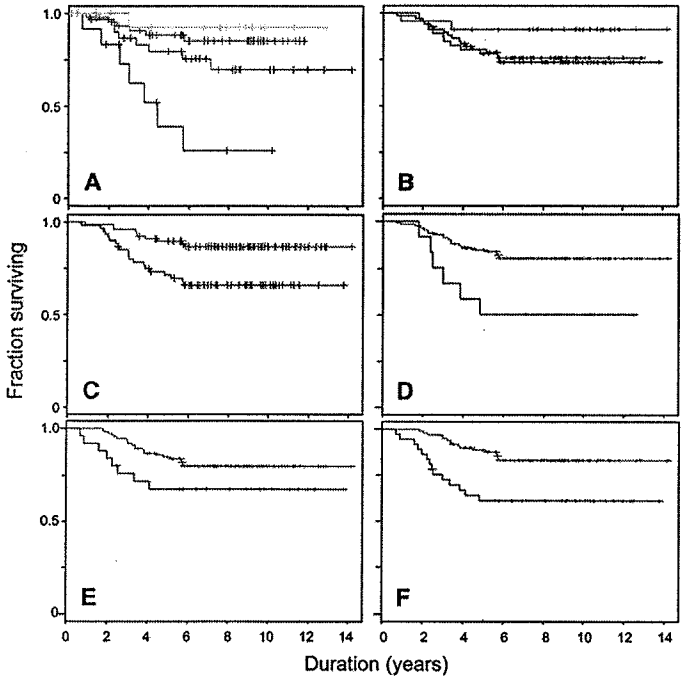

Figure 3. Kaplan-Meyer plots showing survival in breast tumor subclasses

A: Disease-specific survival in 130 breast cancer patients whose tumors were defined using expression profiling to be basal-like (green curve), luminal A (yellow curve), luminal B (orange curve), and ERBB2 (purple curve) class.

B: Disease-specific survival of patients with tumors classified by genome copy number aberration analysis as 1q/16q (green), complex (red), and amplifying (blue).

C: Survival of patients with (red curve) and without (green curve) amplification at any region of recurrent amplification.

D: Survival of patients whose tumors were defined using expression profiling to be luminal A tumors with (red curve) and without (green curve) amplification at 8p11-12, 11q13, and/or 20q.

E: Survival of patients whose tumors were not amplified at 8p11-12 and had normal (green curve) or reduced (red curve) genome copy number at 8p11-12.

F: Survival of patients whose tumors had normal (green curve) or abnormal (red curve) genome copy number at 8p11-12.

amplified. Figure 3E shows that patients with reduced copy number at 8p11-12 did worse than patients without a deletion in this region. Figure 3F shows that patients in the overall study with high-level amplification or deletion at 8p11-12 survived significantly shorter survival ($p = 0.0017$) than patients without either of those events.

We also tested for associations of low-level genome copy number changes with the outcome endpoints. The most frequent low-level copy number changes (e.g., increased copy number at 1q, 8q, and 20q or decreased copy number at 16q) were not significantly associated with outcome endpoints. However, we did find a significant association of the loss of a small region on 9q22 with adverse outcome, both disease-specific survival and distal recurrence, which persisted even after correction for multiple testing ($p < 0.05$, multivariate Cox regression). This region is defined by BACs, CTB-172A10, and RP11-80F13. We also found a marginally significant association between fraction of the genome lost and disease-specific survival in luminal A tumors ($p < 0.02$ and < 0.06 for univariate and multivariate regression, respectively, Cox-proportional regression).

We used the program GoStat (Beissbarth and Speed, 2004) to identify the Gene Ontology (GO) classes of 1444 unique genes (1734 probe sets) whose expression levels were preferentially modulated by low-level CNAs compared to 3026 probe sets whose expression levels did not show associations with copy number. The GO categories most significantly overrepresented in the set of genes with a dosage effect compared to genes with no or minimal dosage effect involved RNA processing (Holm adjusted p value < 0.001), RNA metabolism ($p < 0.01$), and cellular metabolism ($p < 0.02$).

Discussion

This paper describes a comprehensive analysis of gene expression and genome copy number in aggressively treated primary human breast cancers performed in order to (1) identify genomic events that can be assayed to better stratify patients according to clinical behavior, (2) develop insights into how molecular aberrations contribute to breast cancer pathogenesis, and (3) discover genes that might be therapeutic targets in patients that do not respond well to current therapies. An accompanying paper in this issue of *Cancer Cell* shows that many of these aberrations are found in subsets of breast cancer cell lines that can be manipulated to confirm functions suggested by associations with pathophysiology established here (Neve et al., 2006).

Molecular markers that predict outcome

Our combined analyses of genome copy number and gene expression focused on tumors from patients treated more aggressively than those in previously published studies (Perou et al., 2000; Sorlie et al., 2001) (i.e., with surgery, radiation of the surgical margins, hormonal therapy for ER-positive disease, and aggressive adjuvant chemotherapy as indicated) and revealed two important associations.

First, they showed that the survival of patients with tumors classified as basal-like according to expression pattern did not have significantly worse outcome than patients with luminal or normal-like tumors in this tumor set, unlike previous reports (Perou et al., 2000; Sorlie et al., 2001) (see Figure 3A), although there was a trend toward lower survival. However, patients with ERBB2-positive tumors did have significantly increased death from disease and shorter recurrence-free survival in accordance with the earlier studies. This may indicate that the aggressive chemotherapy employed for treatment of the predominantly ER-negative basal-like tumors increased survival duration in these patients relative to patients with tumors in the other subgroups. Thus, outcome for patients with basal-like tumors may not be as bad as indicated by earlier prognostic studies of patient populations that did not receive aggressive chemotherapy for progressive disease. Alternately, the differences may be due to differences in cohort selection. In either case, this result emphasizes the need to interpret the performance of molecular markers for patient stratification in the context of specific treatment regimens and in molecularly defined cohorts.

Second, we found that aggressively treated patients with high-level amplification had worse outcome than did patients without amplification (see Figure 3C). This is consistent with earlier CGH and single-locus analyses of associations of amplification with poor prognosis (Al-Kuraya et al., 2004; Blegen et al., 2003; Callagy et al., 2005; Gelsi-Boyer et al., 2005; Weber-Mangal et al., 2003). Moreover, the presence of high-level amplification was an indicator of poor outcome, even within patient subsets defined by expression profiling. This was particularly apparent

for luminal A tumors, as illustrated in Figure 3D, where patients whose tumors had high-level amplification at 8p11-12, 11q13-14, or 20q13 did significantly worse than patients without amplification. This suggests that stratification according to both expression level and copy number will identify patients that respond poorly to current therapeutic treatment strategies.

Mechanisms of disease progression

Our combined analyses of genome copy number and gene expression showed substantial differences in recurrent genome abnormality composition between tumors classified according to expression pattern and revealed that over 10% of the genes interrogated in this study had expression levels that were highly significantly associated with genome copy number changes. Most of the gene expression changes were associated with low-level changes in genome copy number, but 66 were deregulated by the high-level amplifications associated with poor outcome. These analyses provide insights into the etiology of breast cancer subtypes, suggest mechanisms by which the low-level copy number changes contribute to cancer pathogenesis, and identify a suite of genes that contribute to cancer pathophysiology.

Breast cancer subtypes

Figures 1 and 2 show that recurrent genome copy number aberrations differ substantially between tumors classified according to expression pattern as described previously (Perou et al., 1999). This is consistent with a model of cancer progression in which the expression subtype and genotype are determined by the cell type and stage of differentiation that survives telomere crisis and acquires sufficient proliferative advantage to achieve clonal dominance in the tumor (Chin et al., 2004). This model suggests that the genome CNA spectrum is selected to be most advantageous to the progression of the specific cell type that achieves immortality and clonal dominance. In this model, the recurrent genome CNA composition can be considered an independent subtype descriptor—much as genome CNA composition can be considered to be a cancer type descriptor (Knuutila et al., 2000). The independence of the genome CNA composition and basal and luminal expression subtypes is clear from Figure 4, which shows that the breast tumors divide into basal and luminal subtypes using unsupervised hierarchical clustering even after all transcripts showing associations with copy number are removed from the data set. Of course, the ERBB2 subtype is lost, since that subtype is strongly driven by ERBB2 amplification.

Low-level abnormalities

The most frequent low-level copy number changes were not associated with reduced survival duration, although some were associated with other markers usually associated with survival such as tumor size, nodal status, and grade (see Table 2). This raises the question of why the recurrent low-level CNAs are selected. GOstat analyses of the genes deregulated by these abnormalities showed that numerous genes involved in RNA and cellular metabolism were significantly upregulated by these events. Interestingly, we found these same GO classes to be significantly altered in a collection of breast cancer cell lines and in a study of ovarian cancer (W.-L.K., unpublished data). We also observed that many of the recurrent low-level aberrations matched the low-level copy number changes in the ZNF217-transfected human mammary epithelial cells that emerged after passage through telomere crisis having achieved clonal dominance in the culture (Chin et al., 2004; see Figure S2)—presumably because the aberrations they carried conferred a proliferative advantage. This suggests to us that the low-level CNAs are selected during early cancer formation because they increase basal metabolism, thereby providing a net survival/proliferative advantage to the cells that carry them. This idea is supported by a report that some of these same classes of genes were associated with proliferative fitness yeast (Deutschbauer et al., 2005). That study described analyses of proliferative fitness in the complete set of *Saccharomyces cerevisiae* heterozygous deletion strains and reported reduced growth rates for strains carrying deletions in genes involved in RNA metabolism and ribosome biogenesis and assembly.

High-level amplification

We found that high-level amplifications were associated with reduced survival duration and/or distant recurrence overall and within the luminal A expression subgroup. We identified 66 genes in these regions whose expression levels were correlated with copy number. GO analyses of those genes showed that they are involved in aspects of nucleic acid metabolism, protein modification, signaling, and the cell cycle and/or protein transport, and evidence is mounting that many if not most of these genes are functionally important in the cancers in which they are amplified and overexpressed (see Table 3). Indeed, published functional studies in model systems already have implicated eleven of these genes in diverse aspects of cancer pathophysiology. Six of these are encoded in the region of amplification at 8p11. These encode the RNA-binding protein LSM1 (Fraser et al., 2005), the receptor tyrosine kinase FGFR1 (Braun and Shannon, 2004), the cell-cycle-regulatory protein TACC1 (Still et al., 1999), the metalloproteinase ADAM9 (Mazzocca et al., 2005), the serine/threonine kinase IKBKB (Greten and Karin, 2004; Lam et al., 2005), and the DNA polymerase POLB (Clairmont et al., 1999). Functionally validated genes in the region of amplification at 11q13 include the cell-cycle-regulatory protein CCND1 (Hinds et al., 1994) and the growth factor FGF3 (Okunieff et al., 2003). Functionally important genes in the region of amplification at 17q include the transcription regulation protein PPARBP (Zhu et al., 2000), the receptor tyrosine kinase ERBB2 (Slamon et al., 1989), and the adaptor protein GRB7 (Tanaka et al., 2000), while the AKT-pathway-associated transcription factor ZNF217 (Huang et al., 2005; Nonet et al., 2001) and the RNA-binding protein REA1 (Babu et al., 2003) are functionally validated genes encoded in the region of amplification at 20q13. Further support for the functional importance of seven of these genes (*TACC1*, *ADAM9*, *IKBKB*, *POLB*, *CCND1*, *GRB7*, and *ZNF217*) in oncogenesis comes from the observation that they are within 100 Kbp of sites of recurrent tumorigenic viral integration in the mouse (Akagi et al., 2004), and three (*IKBKB*, *CCND1*, and *GRB7*) are within 10 Kbp of such a site. Taking proximity to a site of recurrent tumorigenic viral integration as evidence for a role in cancer genesis implicates an additional 13 genes or transcripts (see Table 3).

The biological roles of the genes deregulated by recurrent high-level amplification are diverse and vary between regions of amplification. For example, genes deregulated by amplification at 11q13 and 17q11-12 predominantly involved signaling and cell cycle regulation, while genes deregulated by amplification at 8p11-12 and 20q13 were of mixed function but were associated most frequently with aspects of nucleic acid metabolism. The predominance of genes involved in nucleic acid

Table 3. Functional characteristics of genes in recurrent amplicons associated with reduced survival duration in breast cancer

Gene	Ch	Mbp	p value, amplification	p value, disease free survival	p value, distant recurrence	Transcript description	Cancer function reference	Kbp to site of viral integration	Druggable?
SPFH2**	8	37.6	7.08E-07	0.053	0.003	chromosome 8 open reading frame 2			
PROSC**	8	37.7	2.28E-05	0.390	0.043	racemase and epimerase activity, energy metabolism			yes
BRF2**	8	37.8	1.20E-05	0.004	0.003	transcription factor regulating nucleic acid metabolism			
RAB11FIP1	8	37.8	7.77E-04	0.620	0.250	GTPase-activating protein involved in signal transduction			
ASH2L**	8	38.0	5.88E-06	0.036	0.002	DNA-binding protein involved in nucleic acid metabolism			
LSM1	8	38.0	6.79E-06	0.300	0.130	RNA-binding protein involved in nucleic acid metabolism	Fraser et al., 2005; Takahashi et al., 2002		
BAG4	8	38.1	8.73E-07	0.330	0.063	BCL2-associated chaperone protein involved in apoptosis	Gehrmann et al., 2005		
DDHD2**	8	38.1	4.40E-06	0.008	0.006	phospholipase involved in energy metabolism			
WHSC1L1	8	38.2	9.04E-06	0.760	0.730	nucleic acid binding			
FGFR1**	8	38.3	1.04E-04	0.025	0.540	receptor tyrosine kinase involved in signal transduction	Braun and Shannon, 2004; Ray et al., 2004		yes/ PD173074
TACC1**	8	38.7	6.72E-03	0.020	0.043	cell cycle control protein associated with signal transduction	Still et al., 1999	44.1/Plekha2	
ADAM9	8	38.9	1.91E-04	0.930	0.960	metalloproteinase associated with protein metabolism	Mazzocca et al., 2005	75/Plekha2	yes
GOLGA7	8	41.4	7.10E-05	0.140	0.170	integral membrane protein associated with transport			
SLD5	8	41.4	1.41E-03	0.780	0.460	unknown			
MYST3**	8	41.8	5.74E-05	0.006	0.022	transcription-regulatory protein involved in nucleic acid metabolism			
AP3M2**	8	42.0	4.43E-05	0.038	0.220	adapter protein associated with transport			
IKBKB**	8	42.1	7.73E-05	0.002	0.002	serine/threonine kinase associated with signal transduction	Greten and Karin, 2004; Lam et al., 2005	3.1/AK018683	yes/ PS-1145
POLB**	8	42.2	2.15E-04	0.001	0.008	DNA polymerase involved in nucleic acid metabolism	Clairmont et al., 1999	70.1/AK018683	
VDAC3**	8	42.3	9.93E-05	0.056	0.290	voltage-dependent anion channel associated with transport			
SLC20A2	8	42.3	1.98E-03	0.170	0.240	membrane transport protein			
THAP1**	8	42.7	7.13E-03	0.190	0.097	unknown			
FNTA**	8	42.9	3.13E-03	0.067	0.370	prenyltransferase associated with protein metabolism			yes
LOC441347	8	43.0	7.77E-04	0.180	0.810	unknown			
CCND1	11	69.2	1.50E-06	0.560	0.770	cell cycle control protein involved in signal transduction	Hinds et al., 1994	0.4/Fgf3	
FGF3	11	69.4	1.84E-03	0.920	0.420	growth factor involved in signal transduction	Okunieff et al., 2003		
FADD	11	70.0	7.42E-03	0.200	0.250	adapter molecule associated with signal transduction			
PPFIA1	11	70.0	1.53E-05	0.670	0.550	anchor protein associated with cell growth and/or maintenance			
CTTN*	11	70.0	2.69E-04	0.450	0.100	cytoskeletal protein associated with cell growth and/or maintenance			
NADSYN1	11	70.9	3.42E-04	0.290	0.990	unknown			
KRTAP5-9*	11	71.0	3.72E-03	0.035	0.050	cytoskeletal protein associated with cell growth and/or maintenance			
FOLR3	11	71.6	1.54E-03	0.730	0.490	cell surface receptor associated with signal transduction			
NEU3	11	74.4	9.73E-03	0.460	0.370	neuraminidase associated with protein metabolism			
N-PAC**	11	75.8	4.39E-03	0.110	0.038	protein kinase			
LHX1*	17	35.5	1.41E-03	0.250	0.018	transcription factor associated with nucleic acid metabolism			

Table 3. *Continued*

Gene	Ch	Mbp	p value, amplification	p value, disease free survival	p value, distant recurrence	Transcript description	Cancer function reference	Kbp to site of viral integration	Druggable?
ACACA	17	35.6	8.24E-03	0.850	0.850	carboxylase associated with energy metabolism			yes
DDX52	17	36.2	3.47E-04	0.300	0.560	RNA-binding protein associated with nucleic acid metabolism			
TBC1D3	17	36.7	5.25E-05	0.170	0.170	unknown			
SOCS7	17	36.9	4.00E-03	0.450	0.600	adapter molecule associated with signal transduction			
PCGF2	17	37.3	3.10E-04	0.760	0.850	transcription-regulatory protein associated with nucleic acid metabolism		5.4/Lasp1	
PSMB3	17	37.3	8.01E-03	0.390	0.810	ubiquitin proteasome system protein associated with protein metabolism		24.4/Lasp1	
PIP5K2B	17	37.3	5.07E-03	0.400	0.380	lipid kinase associated with signal transduction		47.5/Lasp1	
FLJ20291	17	37.3	3.14E-03	0.850	0.920	unknown		72.4/Lasp1	
PPARBP*	17	37.9	2.13E-04	0.089	0.260	transcription-regulatory protein associated with signal transduction	Zhu et al., 2000		
STARD3	17	38.2	3.40E-09	0.420	0.820	mitochondrial carrier protein associated with transport		52.1/Znfn1a3	
TCAP	17	38.2	1.26E-05	0.640	0.700	structural protein associated with cell growth and/or maintenance		23.1/Znfn1a3	
PNMT*	17	38.2	2.02E-06	0.630	0.010	methyltransferase associated with metabolism and energy		21.1/Znfn1a3	yes
PERLD1	17	38.2	3.41E-09	0.930	0.840	membrane protein of unknown function		18.2/Znfn1a3	
ERBB2	17	38.2	3.41E-09	0.110	0.560	receptor tyrosine kinase associated with signal transduction	Slamon et al., 1989		yes/ trastuzumab, lapatinib
GRB7*	17	38.3	7.28E-08	0.044	0.300	adapter molecule associated with signal transduction	Tanaka et al., 2000	10.8/Znfn1a3	
GSDML	17	38.4	8.36E-06	0.710	0.690	unknown		48.8/Znfn1a3	
PSMD3	17	38.5	4.25E-03	0.250	0.510	ubiquitin proteasome system protein associated with protein metabolism		32.8/Znfn1a3	
NR1D1	17	38.6	1.28E-03	0.210	0.750	nuclear receptor associated with signal transduction		73.4/Cdc6	yes
ZNF217	20	52.9	5.02E-06	0.650	0.650	transcription factor associated with signal transduction	Nonet et al., 2001	39.3/Zfp217	
BCAS1	20	53.2	4.93E-03	0.290	0.140	unknown		70.9/Zpf217	
CSTF1	20	55.7	7.15E-03	0.150	0.330	pre-mRNA processing			
RAE1	20	56.6	3.56E-05	0.360	0.420	RNA-binding protein associated with nucleic acid metabolism	Babu et al., 2003		
RNPC1	20	56.6	1.19E-03	0.750	0.830	RNA-binding protein associated with nucleic acid metabolism			
PCK1	20	56.8	9.78E-03	0.250	0.330	phosphotransferase associated with energy and metabolism			
TMEPAI*	20	56.9	1.21E-04	0.085	0.077	unknown			
RAB22A	20	57.6	3.15E-05	0.990	0.340	GTPase associated with signal transduction			
VAPB	20	57.6	3.78E-05	0.360	0.260	membrane transport protein			
STX16	20	57.9	2.63E-05	0.220	0.790	transport/cargo protein			
NPEPL1	20	57.9	3.35E-05	0.270	0.800	aminopeptidase associated with protein metabolism			
GNAS**	20	58.1	6.60E-03	0.052	0.058	G protein associated with signal transduction			
TH1L	20	58.2	1.14E-04	0.530	0.800	transcription-regulatory protein associated with nucleic acid metabolism		36.7/Thil	
C20orf45	20	58.3	6.29E-04	0.970	0.790	unknown		88.7/Th1l	

Functional annotation was based on the Human Protein Reference Database (http://hprd.org/). Genes marked with an asterisk are associated with reduced survival duration or distant recurrence when overexpressed in nonamplifying tumors. Genes marked with two asterisks are significantly associated with reduced survival duration or distant recurrence ($p < 0.05$) when downregulated in nonamplifying tumors. Distances to sites of recurrent viral integration were determined from published information (Akagi et al., 2004). The last column identifies genes that have predicted protein folding characteristics that suggest that they might be druggable (Russ and Lampel, 2005).

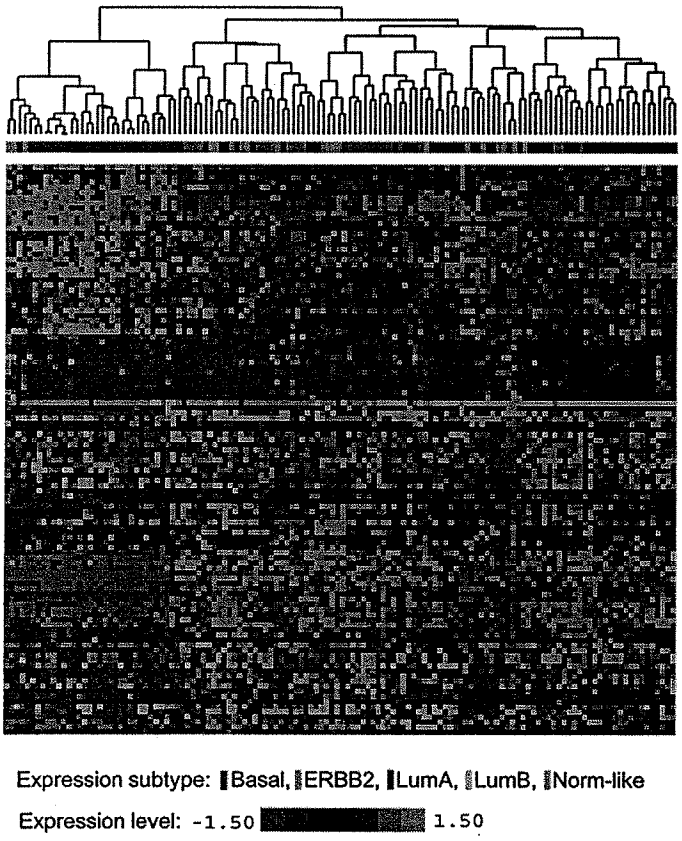

Figure 4. Results of unsupervised hierarchical clustering of 130 breast tumors using intrinsically variable gene expression but excluding any transcripts whose levels were significantly associated with genome copy number

Red indicates increased expression, and green indicates reduced expression. An annotated version is provided as Figure S3.

metabolism in the region of amplification at 8p11-12 was especially strong. Interestingly, the region of recurrent amplification at 8p11-12 described above was *reduced* in copy number in some tumors, and this event also was associated with poor outcome. This raises the possibility that poor clinical outcome in tumors with 8p11-12 abnormalities is due to increased genome instability/mutagenesis resulting from either up- or downregulation of genes encoded in this region. This concept is supported by studies in yeast showing that up- or downregulation of genes involved in chromosome integrity and segregation can produce similar instability phenotypes (Ouspenski et al., 1999).

Therapeutic targets

The 66 genes we found to be deregulated by the high-level amplifications associated with poor outcome are particularly interesting as therapeutic targets for treatment of patients that are refractory to current therapies. Small-molecule or antibody-based inhibitors have already been developed for *FGFR1* (PD173074; Ray et al., 2004), *IKBKB* (PS-1145; Lam et al., 2005), and *ERBB2* (Trastuzumab; Vogel et al., 2002), and six others (*PROCC*, *ADAM9*, *FNTA*, *ACACA*, *PNMT*, and *NR1D1*) are considered to be druggable based on the presence of predicted protein folds that favor interactions with drug-like compounds (Russ and Lampel, 2005). Taking *ERBB2* as the paradigm (recurrently amplified, overexpressed, associated with outcome and with demonstrated functional importance in cancer) suggests *FGFR1*, *TACC1*, *ADAM9*, *IKBKB*, *PNMT*, and *GRB7* as high-priority therapeutic targets in these regions of amplification.

Experimental procedures

Tumor characteristics

Frozen tissue from UC San Francisco and the California Pacific Medical Center collected between 1989 and 1997 was used for this study. Tissues were collected under IRB-approved protocols with patient consent. Tissues were collected, frozen over dry ice within 20 min of resection, and stored at −80°C. An H&E section of each tumor sample was reviewed, and the frozen block was manually trimmed to remove normal and necrotic tissue from the periphery. Clinical follow-up was available with a median time of 6.6 years overall and 8 years for censored patients. Tumors were predominantly early stage (83% stage I and II) with an average diameter of 2.6 cm. About half of the tumors were node positive, 67% were estrogen receptor positive, 60% received tamoxifen, and half received adjuvant chemotherapy (typically adriamycin and cytoxan). Clinical characteristics of the individual tumors are provided together with expression and array CGH profiles in the CaBIG repository and at http://cancer.lbl.gov/breastcancer/data.php.

Array CGH

Each sample was analyzed using Scanning and OncoBAC arrays. Scanning arrays were comprised of 2464 BACs selected at approximately megabase intervals along the genome as described previously (Hodgson et al., 2001; Snijders et al., 2001). OncoBAC arrays were comprised of 960 P1, PAC, or BAC clones. About three-quarters of the clones on the OncoBAC arrays contained genes and STSs implicated in cancer development or progression. All clones were printed in quadruplicate. DNA samples for array CGH were labeled generally as described previously (Hackett et al., 2003; Hodgson et al., 2001; Snijders et al., 2001). Briefly, 500 ng each of cancer and normal female genomic DNA sample was labeled by random priming with CY3- and CY5-dUTP, respectively; denatured; and hybridized with unlabeled Cot-1 DNA to CGH arrays. After hybridization, the slides were washed and imaged using a 16-bit CCD camera through CY3, CY5, and DAPI filters (Pinkel et al., 1998).

Expression profiling

Expression profiling was accomplished using the Affymetrix High Throughput Array (HTA) GeneChip system, in which target preparations, washing, and staining were carried out in a 96-well format. Detailed methods are described in the Supplemental Data.

Statistical considerations

Data processing

Array CGH data image analyses were performed as described previously (Jain et al., 2002). In this process, an array probe was assigned a missing value for an array if there were fewer than two valid replicates or the standard deviation of the replicates exceeded 0.2. Array probes missing in more than 50% of samples in OncoBAC or scanning array data sets were excluded in the corresponding set. Array probes representing the same DNA sequence were averaged within each data set and then between the two data sets. Finally, the two data sets were combined, and the array probes missing in more than 25% of the samples, unmapped array probes, and probes mapped to chromosome Y were eliminated. The final data set contained 2149 unique probes. For Affymetrix data, multichip robust normalization was performed using RMA software (Irizarry et al., 2003). Transcripts assessed on the arrays were classified into two groups using Gaussian model-based clustering by considering the joint distribution of the median and standard deviation of each probe set across samples. During this process, computational demands were reduced by randomly sampling and clustering 2000 probe intensities using *mclust* (Yeung et al., 2001, 2004) with two clusters and unequal variance. Next, the remaining probe intensities were classified into the newly created clusters using linear discriminant analysis. The cluster containing probe intensities with smaller mean and variance was defined as "not expressed," and the second cluster was defined as "expressed."

Characterizing copy number changes

The sample profiles were segmented into the levels of equal copy number common to the whole genome, and the copy number transitions,

amplifications, and frequency of alterations were determined using previously described methodologies (Snijders et al., 2003; Fridlyand et al., 2006). The detailed approaches are described in the Supplemental Data.

Clustering of genome copy number profiles

Genome copy number profiles were clustered using smoothed imputed data with outliers present. Agglomerative hierarchical clustering with Pearson's correlation as a similarity measure and the Ward method to minimize sum of variances were used to produce compact spherical clusters (Hartigan, 1975). The number of groups was assessed qualitatively by considering the shape of the clustering dendogram.

Expression subtype assignment

Tumors were classified according to expression phenotype (basal, ERBB2, luminal A, luminal B, and normal-like) by assigning each tumor to the subtype of the cluster defined by hierarchical clustering of expression profiles for 122 samples published by Sorlie et al. (2003) to which it had the highest Pearson's correlation. The correlation was computed using the subset of Stanford intrinsically variable genes common to both data sets. For details, refer to the Supplemental Data.

Association of copy number with survival

Stage 4 samples were excluded from all the outcome-related analyses, and disease-specific survival and time to distant recurrence were used as the two endpoints. Significance of the standardized regression coefficient Cox-proportional model was used to determine clinical (univariate and multivariate analyses) and genomic variables (individual clones, instability summary measures, and recurrent amplicon status) associated with outcome. p values for individual clones were adjusted using FDR. The significance was declared at $p < 0.05$. For details, see the Supplemental Data.

Association of copy number with expression

The presence of an overall dosage effect was assessed by subdividing each chromosomal arm into nonoverlapping 20 Mb bins and computing the average of cross-Pearson's-correlations for all gene transcript-BAC probe pairs that mapped to that bin. We also calculated Pearson's correlations and corresponding p values between expression level and copy number for each gene transcript. Each transcript was assigned an observed copy number of the nearest mapped BAC array probe. Eighty percent of gene transcripts had a nearest clone within 1 Mbp, and 50% had a clone within 400 Kbp. Correlation between expression and copy number was only computed for the gene transcripts whose absolute assigned copy number exceeded 0.2 in at least five samples. This was done to avoid spurious correlations in the absence of real copy number changes. We used conservative Holm p value adjustment to correct for multiple testing. Gene transcripts with an adjusted p value <0.05 were considered to have expression levels that were highly significantly affected by gene dosage. This corresponded to a minimum Pearson's correlation of 0.44.

Associations of transcription and CNA in regions of amplification with outcome in tumors without particular amplicons

We assessed the associations of levels of transcripts in regions of amplifications with survival or distant recurrence in tumors without amplifications in order to find genes that might contribute to progression when deregulated by mechanisms other than amplification (e.g., we assessed associations between expression levels of the genes mapping to the 8p11-12 amplicon and survival in samples without 8p11-12 amplification). We performed separate Cox-proportional regressions for disease-specific survival and distant recurrence. Stage 4 samples were excluded from all analyses.

Testing for functional enrichment

We used the gene ontology statistics tool GoStat (Beissbarth and Speed, 2004) to test whether the gene transcripts with the strongest dosage effects were enriched for particular functional groups. The p values were adjusted using false discovery rate. The categories were considered significantly overrepresented if the FDR-adjusted p value was less than 0.001. Since expressed genes were significantly more likely to show dosage effects than nonexpressed genes (p value < 2.2E-16, Wilcoxon rank-sum test), GoStat comparisons were performed only for expressed genes. Specifically, GO categories for 1734 expressed probes with significant dosage effect (Holm p value < 0.05) were compared with those for 3026 expressed probes with no dosage effect (Pearson's correlation < 0.1).

Microarray data

The raw data for expression profiling are available at ArrayExpress (http://www.ebi.ac.uk/arrayexpress/) with accession number E-TABM-158.

Clinical characteristics of the individual tumors as well as array CGH and expression profiles are available in the CaBIG repository (http://caarraydb.nci.nih.gov/caarray/publicExperimentDetailAction.do?expId=1015897589973255), at http://cancer.lbl.gov/breastcancer/data.php, and in the Supplemental Data.

Supplemental data

The Supplemental Data include Supplemental Experimental Procedures, three supplemental figures, and three supplemental tables and can be found with this article online at http://www.cancercell.org/cgi/content/full/10/6/529/DC1/.

Acknowledgments

This work was supported by the NIH (CA58207, CA90421, and CA101359), the Office of Health and Environmental Research of the U.S. Department of Energy (contract DE-AC03-76SF00098), and the Avon Foundation. The content of this publication does not necessarily reflect the views or policies of the Department of Health and Human Services, nor does mention of trade names, commercial products, or organizations imply endorsement by the U.S. Government. For full disclaimer, see http://www-library.lbl.gov/public/tmRco/howto/RcoBerkeleyLabDisclaimer.htm.

Received: May 3, 2006
Revised: August 19, 2006
Accepted: October 6, 2006
Published: December 11, 2006

References

Akagi, K., Suzuki, T., Stephens, R.M., Jenkins, N.A., and Copeland, N.G. (2004). RTCGD: Retroviral tagged cancer gene database. Nucleic Acids Res. *32*, D523–D527.

Al-Kuraya, K., Schraml, P., Torhorst, J., Tapia, C., Zaharieva, B., Novotny, H., Spichtin, H., Maurer, R., Mirlacher, M., Kochli, O., et al. (2004). Prognostic relevance of gene amplifications and coamplifications in breast cancer. Cancer Res. *64*, 8534–8540.

Albertson, D.G., Collins, C., McCormick, F., and Gray, J.W. (2003). Chromosome aberrations in solid tumors. Nat. Genet. *34*, 369–376.

Babu, J.R., Jeganathan, K.B., Baker, D.J., Wu, X., Kang-Decker, N., and van Deursen, J.M. (2003). Rae1 is an essential mitotic checkpoint regulator that cooperates with Bub3 to prevent chromosome missegregation. J. Cell Biol. *160*, 341–353.

Barlund, M., Tirkkonen, M., Forozan, F., Tanner, M.M., Kallioniemi, O., and Kallioniemi, A. (1997). Increased copy number at 17q22-q24 by CGH in breast cancer is due to high-level amplification of two separate regions. Genes Chromosomes Cancer *20*, 372–376.

Barlund, M., Monni, O., Kononen, J., Cornelison, R., Torhorst, J., Sauter, G., Kallioniemi, O.-P., and Kallioniemi, A. (2000). Multiple genes at 17q23 undergo amplification and overexpression in breast cancer. Cancer Res. *60*, 5340–5344.

Baylin, S.B., and Herman, J.G. (2000). DNA hypermethylation in tumorigenesis: Epigenetics joins genetics. Trends Genet. *16*, 168–174.

Bergamaschi, A., Kim, Y.H., Wang, P., Sorlie, T., Hernandez-Boussard, T., Lonning, P.E., Tibshirani, R., Borresen-Dale, A.L., and Pollack, J.R. (2006). Distinct patterns of DNA copy number alteration are associated with different clinicopathological features and gene-expression subtypes of breast cancer. Genes Chromosomes Cancer *45*, 1033–1040.

Beissbarth, T., and Speed, T.P. (2004). GOstat: Find statistically overrepresented Gene Ontologies within a group of genes. Bioinformatics *20*, 1464–1465.

Blegen, H., Will, J.S., Ghadimi, B.M., Nash, H.P., Zetterberg, A., Auer, G., and Ried, T. (2003). DNA amplifications and aneuploidy, high proliferative activity and impaired cell cycle control characterize breast carcinomas with poor prognosis. Anal. Cell. Pathol. *25*, 103–114.

Braun, B.S., and Shannon, K. (2004). The sum is greater than the FGFR1 partner. Cancer Cell *5*, 203–204.

Callagy, G., Pharoah, P., Chin, S.F., Sangan, T., Daigo, Y., Jackson, L., and Caldas, C. (2005). Identification and validation of prognostic markers in breast cancer with the complementary use of array-CGH and tissue microarrays. J. Pathol. *205*, 388–396.

Cheng, K.W., Lahad, J.P., Kuo, W.L., Lapuk, A., Yamada, K., Auersperg, N., Liu, J., Smith-McCune, K., Lu, K.H., Fishman, D., et al. (2004). The RAB25 small GTPase determines aggressiveness of ovarian and breast cancers. Nat. Med. *10*, 1251–1256.

Chin, K., de Solorzano, C.O., Knowles, D., Jones, A., Chou, W., Rodriguez, E.G., Kuo, W.L., Ljung, B.M., Chew, K., Myambo, K., et al. (2004). In situ analyses of genome instability in breast cancer. Nat. Genet. *36*, 984–988.

Clairmont, C.A., Narayanan, L., Sun, K.W., Glazer, P.M., and Sweasy, J.B. (1999). The Tyr-265-to-Cys mutator mutant of DNA polymerase beta induces a mutator phenotype in mouse LN12 cells. Proc. Natl. Acad. Sci. USA *96*, 9580–9585.

Deutschbauer, A.M., Jaramillo, D.F., Proctor, M., Kumm, J., Hillenmeyer, M.E., Davis, R.W., Nislow, C., and Giaever, G. (2005). Mechanisms of haploinsufficiency revealed by genome-wide profiling in yeast. Genetics *169*, 1915–1925.

Esteva, F.J., Sahin, A.A., Cristofanilli, M., Coombes, K., Lee, S.J., Baker, J., Cronin, M., Walker, M., Watson, D., Shak, S., and Hortobagyi, G.N. (2005). Prognostic role of a multigene reverse transcriptase-PCR assay in patients with node-negative breast cancer not receiving adjuvant systemic therapy. Clin. Cancer Res. *11*, 3315–3319.

Fraser, M.M., Watson, P.M., Fraig, M.M., Kelley, J.R., Nelson, P.S., Boylan, A.M., Cole, D.J., and Watson, D.K. (2005). CaSm-mediated cellular transformation is associated with altered gene expression and messenger RNA stability. Cancer Res. *65*, 6228–6236.

Fridlyand, J., Snijders, A.M., Ylstra, B., Li, H., Olshen, A., Segraves, R., Dairkee, S., Tokuyasu, T., Ljung, B.M., Jain, A.N., et al. (2006). Breast tumor copy number aberration phenotypes and genomic instability. BMC Cancer *6*, 96.

Gehrmann, M., Marienhagen, J., Eichholtz-Wirth, H., Fritz, E., Ellwart, J., Jaattela, M., Zilch, T., and Multhoff, G. (2005). Dual function of membrane-bound heat shock protein 70 (Hsp70), Bag-4, and Hsp40: Protection against radiation-induced effects and target structure for natural killer cells. Cell Death Differ. *12*, 38–51.

Gelsi-Boyer, V., Orsetti, B., Cervera, N., Finetti, P., Sircoulomb, F., Rouge, C., Lasorsa, L., Letessier, A., Ginestier, C., Monville, F., et al. (2005). Comprehensive profiling of 8p11-12 amplification in breast cancer. Mol. Cancer Res. *3*, 655–667.

Gianni, L., Zambetti, M., Clark, K., Baker, J., Cronin, M., Wu, J., Mariani, G., Rodriguez, J., Carcangiu, M., Watson, D., et al. (2005). Gene expression profiles in paraffin-embedded core biopsy tissue predict response to chemotherapy in women with locally advanced breast cancer. J. Clin. Oncol. *23*, 7265–7277.

Greten, F.R., and Karin, M. (2004). The IKK/NF-κB activation pathway—A target for prevention and treatment of cancer. Cancer Lett. *206*, 193–199.

Hackett, C.S., Hodgson, J.G., Law, M.E., Fridlyand, J., Osoegawa, K., de Jong, P.J., Nowak, N.J., Pinkel, D., Albertson, D.G., Jain, A., et al. (2003). Genome-wide array CGH analysis of murine neuroblastoma reveals distinct genomic aberrations which parallel those in human tumors. Cancer Res. *63*, 5266–5273.

Hanahan, D., and Weinberg, R.A. (2000). The hallmarks of cancer. Cell *100*, 57–70.

Hartigan, J.A. (1975). Clustering Algorithms (New York: Wiley).

Hinds, P.W., Dowdy, S.F., Eaton, E.N., Arnold, A., and Weinberg, R.A. (1994). Function of a human cyclin gene as an oncogene. Proc. Natl. Acad. Sci. USA *91*, 709–713.

Hodgson, G., Hager, J.H., Volik, S., Hariono, S., Wernick, M., Moore, D., Nowak, N., Albertson, D.G., Pinkel, D., Collins, C., et al. (2001). Genome scanning with array CGH delineates regional alterations in mouse islet carcinomas. Nat. Genet. *29*, 459–464.

Huang, G., Krig, S., Kowbel, D., Xu, H., Hyun, B., Volik, S., Feuerstein, B., Mills, G.B., Stokoe, D., Yaswen, P., and Collins, C. (2005). ZNF217 suppresses cell death associated with chemotherapy and telomere dysfunction. Hum. Mol. Genet. *14*, 3219–3225.

Hyman, E., Kauraniemi, P., Hautaniemi, S., Wolf, M., Mousses, S., Rozenblum, E., Ringner, M., Sauter, G., Monni, O., Elkahloun, A., et al. (2002). Impact of DNA amplification on gene expression patterns in breast cancer. Cancer Res. *62*, 6240–6245.

Irizarry, R., Bolstad, B., Collin, F., Cope, L., Hobbs, B., and Speed, T. (2003). Summaries of Affymetrix GeneChip probe level data. Nucleic Acids Res. *31*, e15.

Isola, J.J., Kallioniemi, O.P., Chu, L.W., Fuqua, S.A., Hilsenbeck, S.G., Osborne, C.K., and Waldman, F.M. (1995). Genetic aberrations detected by comparative genomic hybridization predict outcome in node-negative breast cancer. Am. J. Pathol. *147*, 905–911.

Jain, A.N., Chin, K., Borresen-Dale, A.L., Erikstein, B.K., Eynstein Lonning, P., Kaaresen, R., and Gray, J.W. (2001). Quantitative analysis of chromosomal CGH in human breast tumors associates copy number abnormalities with p53 status and patient survival. Proc. Natl. Acad. Sci. USA *98*, 7952–7957.

Jain, A.N., Tokuyasu, T.A., Snijders, A.M., Segraves, R., Albertson, D.G., and Pinkel, D. (2002). Fully automatic quantification of microarray image data. Genome Res. *12*, 325–332.

Jones, P.A. (2005). Overview of cancer epigenetics. Semin. Hematol. *42*, S3–S8.

Kallioniemi, O.P., Kallioniemi, A., Kurisu, W., Thor, A., Chen, L.C., Smith, H.S., Waldman, F.M., Pinkel, D., and Gray, J.W. (1992). ERBB2 amplification in breast cancer analyzed by fluorescence in situ hybridization. Proc. Natl. Acad. Sci. USA *89*, 5321–5325.

Kallioniemi, A., Kallioniemi, O.P., Piper, J., Tanner, M., Stokke, T., Chen, L., Smith, H.S., Pinkel, D., Gray, J.W., and Waldman, F.M. (1994). Detection and mapping of amplified DNA sequences in breast cancer by comparative genomic hybridization. Proc. Natl. Acad. Sci. USA *91*, 2156–2160.

Kauraniemi, P., Barlund, M., Monni, O., and Kallioniemi, A. (2001). New amplified and highly expressed genes discovered in the ERBB2 amplicon in breast cancer by cDNA microarrays. Cancer Res. *61*, 8235–8240.

Kauraniemi, P., Kuukasjarvi, T., Sauter, G., and Kallioniemi, A. (2003). Amplification of a 280-kilobase core region at the ERBB2 locus leads to activation of two hypothetical proteins in breast cancer. Am. J. Pathol. *163*, 1979–1984.

Knuutila, S., Autio, K., and Aalto, Y. (2000). Online access to CGH data of DNA sequence copy number changes. Am. J. Pathol. *157*, 689.

Lam, L.T., Davis, R.E., Pierce, J., Hepperle, M., Xu, Y., Hottelet, M., Nong, Y., Wen, D., Adams, J., Dang, L., and Staudt, L.M. (2005). Small molecule inhibitors of IκB kinase are selectively toxic for subgroups of diffuse large B-cell lymphoma defined by gene expression profiling. Clin. Cancer Res. *11*, 28–40.

Loo, L.W., Grove, D.I., Williams, E.M., Neal, C.L., Cousens, L.A., Schubert, E.L., Holcomb, I.N., Massa, H.F., Glogovac, J., Li, C.I., et al. (2004). Array comparative genomic hybridization analysis of genomic alterations in breast cancer subtypes. Cancer Res. *64*, 8541–8549.

Mazzocca, A., Coppari, R., De Franco, R., Cho, J.Y., Libermann, T.A., Pinzani, M., and Toker, A. (2005). A secreted form of ADAM9 promotes carcinoma invasion through tumor-stromal interactions. Cancer Res. *65*, 4728–4738.

Naylor, T.L., Greshock, J., Wang, Y., Colligon, T., Yu, Q.C., Clemmer, V., Zaks, T.Z., and Weber, B.L. (2005). High resolution genomic analysis of sporadic breast cancer using array-based comparative genomic hybridization. Breast Cancer Res. *7*, R1186–R1198.

Neve, R.M., Chin, K., Fridlyand, J., Yeh, J., Baehner, F.L., Fevr, T., Clark, L., Bayani, N., Coppe, J.-P., Tong, F., et al. (2006). A collection of breast cancer cell lines for the study of functionally distinct cancer subtypes. Cancer Cell *10*, this issue, 515–527.

Nonet, G., Stampfer, M., Chin, K., Gray, J.W., Collins, C., and Yaswen, P. (2001). The ZNF217 gene amplified in breast cancers promotes immortalization of human mammary epithelial cells. Cancer Res. *61*, 1250–1254.

Okunieff, P., Fenton, B.M., Zhang, L., Kern, F.G., Wu, T., Greg, J.R., and Ding, I. (2003). Fibroblast growth factors (FGFS) increase breast tumor growth rate, metastases, blood flow, and oxygenation without significant change in vascular density. Adv. Exp. Med. Biol. *530*, 593–601.

Ouspenski, I.I., Elledge, S.J., and Brinkley, B.R. (1999). New yeast genes important for chromosome integrity and segregation identified by dosage effects on genome stability. Nucleic Acids Res. *27*, 3001–3008.

Perou, C.M., Jeffrey, S.S., van de Rijn, M., Rees, C.A., Eisen, M.B., Ross, D.T., Pergamenschikov, A., Williams, C.F., Zhu, S.X., Lee, J.C., et al. (1999). Distinctive gene expression patterns in human mammary epithelial cells and breast cancers. Proc. Natl. Acad. Sci. USA *96*, 9212–9217.

Perou, C.M., Sorlie, T., Eisen, M.B., van de Rijn, M., Jeffrey, S.S., Rees, C.A., Pollack, J.R., Ross, D.T., Johnsen, H., Akslen, L.A., et al. (2000). Molecular portraits of human breast tumours. Nature *406*, 747–752.

Pinkel, D., Segraves, R., Sudar, D., Clark, S., Poole, I., Kowbel, D., Collins, C., Kuo, W.L., Chen, C., Zhai, Y., et al. (1998). High resolution analysis of DNA copy number variation using comparative genomic hybridization to microarrays. Nat. Genet. *20*, 207–211.

Pollack, J.R., Perou, C.M., Alizadeh, A.A., Eisen, M.B., Pergamenschikov, A., Williams, C.F., Jeffrey, S.S., Botstein, D., and Brown, P.O. (1999). Genome-wide analysis of DNA copy-number changes using cDNA microarrays. Nat. Genet. *23*, 41–46.

Pollack, J.R., Sorlie, T., Perou, C.M., Rees, C.A., Jeffrey, S.S., Lonning, P.E., Tibshirani, R., Botstein, D., Borresen-Dale, A.L., and Brown, P.O. (2002). Microarray analysis reveals a major direct role of DNA copy number alteration in the transcriptional program of human breast tumors. Proc. Natl. Acad. Sci. USA *99*, 12963–12968.

Press, M.F., Sauter, G., Bernstein, L., Villalobos, I.E., Mirlacher, M., Zhou, J.Y., Wardeh, R., Li, Y.T., Guzman, R., Ma, Y., et al. (2005). Diagnostic evaluation of HER-2 as a molecular target: An assessment of accuracy and reproducibility of laboratory testing in large, prospective, randomized clinical trials. Clin. Cancer Res. *11*, 6598–6607.

Ramaswamy, S., Ross, K.N., Lander, E.S., and Golub, T.R. (2003). A molecular signature of metastasis in primary solid tumors. Nat. Genet. *33*, 49–54.

Ray, M.E., Yang, Z.Q., Albertson, D., Kleer, C.G., Washburn, J.G., Macoska, J.A., and Ethier, S.P. (2004). Genomic and expression analysis of the 8p11-12 amplicon in human breast cancer cell lines. Cancer Res. *64*, 40–47.

Reyal, F., Stransky, N., Bernard-Pierrot, I., Vincent-Salomon, A., de Rycke, Y., Elvin, P., Cassidy, A., Graham, A., Spraggon, C., Desille, Y., et al. (2005). Visualizing chromosomes as transcriptome correlation maps: Evidence of chromosomal domains containing co-expressed genes—A study of 130 invasive ductal breast carcinomas. Cancer Res. *65*, 1376–1383.

Russ, A.P., and Lampel, S. (2005). The druggable genome: An update. Drug Discov. Today *10*, 1607–1610.

Slamon, D.J., Godolphin, W., Jones, L.A., Holt, J.A., Wong, S.G., Keith, D.E., Levin, W.J., Stuart, S.G., Udove, J., Ullrich, A., et al. (1989). Studies of the HER-2/neu proto-oncogene in human breast and ovarian cancer. Science *244*, 707–712.

Snijders, A.M., Nowak, N., Segraves, R., Blackwood, S., Brown, N., Conroy, J., Hamilton, G., Hindle, A.K., Huey, B., Kimura, K., et al. (2001). Assembly of microarrays for genome-wide measurement of DNA copy number. Nat. Genet. *29*, 263–264.

Snijders, A.M., Fridlyand, J., Mans, D.A., Segraves, R., Jain, A.N., Pinkel, D., and Albertson, D.G. (2003). Shaping of tumor and drug-resistant genomes by instability and selection. Oncogene *22*, 4370–4379.

Solinas-Toldo, S., Lampel, S., Stilgenbauer, S., Nickolenko, J., Benner, A., Dohner, H., Cremer, T., and Lichter, P. (1997). Matrix-based comparative genomic hybridization: Biochips to screen for genomic imbalances. Genes Chromosomes Cancer *20*, 399–407.

Sorlie, T., Perou, C.M., Tibshirani, R., Aas, T., Geisler, S., Johnsen, H., Hastie, T., Eisen, M.B., van de Rijn, M., Jeffrey, S.S., et al. (2001). Gene expression patterns of breast carcinomas distinguish tumor subclasses with clinical implications. Proc. Natl. Acad. Sci. USA *98*, 10869–10874.

Sorlie, T., Tibshirani, R., Parker, J., Hastie, T., Marron, J.S., Nobel, A., Deng, S., Johnsen, H., Pesich, R., Geisler, S., et al. (2003). Repeated observation of breast tumor subtypes in independent gene expression data sets. Proc. Natl. Acad. Sci. USA *100*, 8418–8423.

Still, I.H., Hamilton, M., Vince, P., Wolfman, A., and Cowell, J.K. (1999). Cloning of TACC1, an embryonically expressed, potentially transforming coiled coil containing gene, from the 8p11 breast cancer amplicon. Oncogene *18*, 4032–4038.

Takahashi, S., Suzuki, S., Inaguma, S., Cho, Y.M., Ikeda, Y., Hayashi, N., Inoue, T., Sugimura, Y., Nishiyama, N., Fujita, T., et al. (2002). Down-regulation of Lsm1 is involved in human prostate cancer progression. Br. J. Cancer *86*, 940–946.

Tanaka, S., Sugimachi, K., Kawaguchi, H., Saeki, H., Ohno, S., and Wands, J.R. (2000). Grb7 signal transduction protein mediates metastatic progression of esophageal carcinoma. J. Cell. Physiol. *183*, 411–415.

Tanner, M.M., Tirkkonen, M., Kallioniemi, A., Collins, C., Stokke, T., Karhu, R., Kowbel, D., Shadravan, F., Hintz, M., Kuo, W.L., et al. (1994). Increased copy number at 20q13 in breast cancer: Defining the critical region and exclusion of candidate genes. Cancer Res. *54*, 4257–4260.

van de Vijver, M.J., He, Y.D., van 't Veer, L.J., Dai, H., Hart, A.A., Voskuil, D.W., Schreiber, G.J., Peterse, J.L., Roberts, C., Marton, M.J., et al. (2002). A gene-expression signature as a predictor of survival in breast cancer. N. Engl. J. Med. *347*, 1999–2009.

van 't Veer, L.J., Dai, H., van de Vijver, M.J., He, Y.D., Hart, A.A., Mao, M., Peterse, H.L., van der Kooy, K., Marton, M.J., Witteveen, A.T., et al. (2002). Gene expression profiling predicts clinical outcome of breast cancer. Nature *415*, 530–536.

Vogel, C.L., Cobleigh, M.A., Tripathy, D., Gutheil, J.C., Harris, L.N., Fehrenbacher, L., Slamon, D.J., Murphy, M., Novotny, W.F., Burchmore, M., et al. (2002). Efficacy and safety of trastuzumab as a single agent in first-line treatment of HER2-overexpressing metastatic breast cancer. J. Clin. Oncol. *20*, 719–726.

Weber-Mangal, S., Sinn, H.P., Popp, S., Klaes, R., Emig, R., Bentz, M., Mansmann, U., Bastert, G., Bartram, C.R., and Jauch, A. (2003). Breast cancer in young women ($\leq$35 years): Genomic aberrations detected by comparative genomic hybridization. Int. J. Cancer *107*, 583–592.

Yeung, K.Y., Fraley, C., Murua, A., Raftery, A.E., and Ruzzo, W.L. (2001). Model-based clustering and data transformations for gene expression data. Bioinformatics *17*, 977–987.

Yeung, K.Y., Medvedovic, M., and Bumgarner, R.E. (2004). From co-expression to co-regulation: How many microarray experiments do we need? Genome Biol. *5*, R48.

Yi, Y., Mirosevich, J., Shyr, Y., Matusik, R., and George, A.L., Jr. (2005). Coupled analysis of gene expression and chromosomal location. Genomics *85*, 401–412.

Zhu, Y., Kan, L., Qi, C., Kanwar, Y.S., Yeldandi, A.V., Rao, M.S., and Reddy, J.K. (2000). Isolation and characterization of peroxisome proliferator-activated receptor (PPAR) interacting protein (PRIP) as a coactivator for PPAR. J. Biol. Chem. *275*, 13510–13516.

Accession numbers

The raw data for expression profiling are available at ArrayExpress (http://www.ebi.ac.uk/arrayexpress/) with accession number E-TABM-158.

Exhibit B

nature medicine

The RAB25 small GTPase determines aggressiveness of ovarian and breast cancers

Kwai Wa Cheng[1], John P Lahad[1], Wen-lin Kuo[2], Anna Lapuk[2], Kyosuke Yamada[2], Nelly Auersperg[3], Jinsong Liu[4], Karen Smith-McCune[5], Karen H Lu[6], David Fishman[7], Joe W Gray[2] & Gordon B Mills[1]

High-density array comparative genomic hybridization (CGH)[1] showed amplification of chromosome 1q22 centered on the *RAB25* small GTPase[2], which is implicated in apical vesicle trafficking[3], in approximately half of ovarian and breast cancers. *RAB25* mRNA levels were selectively increased in stage III and IV serous epithelial ovarian cancers compared to other genes within the amplified region, implicating *RAB25* as a driving event in the development of the amplicon. Increased DNA copy number or RNA level of *RAB25* was associated with markedly decreased disease-free survival or overall survival in ovarian and breast cancers, respectively. Forced expression of *RAB25* markedly increased anchorage-dependent and anchorage-independent cell proliferation, prevented apoptosis and anoikis, including that induced by chemotherapy, and increased aggressiveness of cancer cells *in vivo*. The inhibition of apoptosis was associated with a decrease in expression of the proapoptotic molecules, BAK and BAX, and activation of the antiapoptotic phosphatidylinositol 3 kinase (PI3K) and AKT pathway, providing potential mechanisms for the effects of *RAB25* on tumor aggressiveness. Overall, these studies implicate *RAB25*, and thus the RAB family of small G proteins, in aggressiveness of epithelial cancers.

Ovarian cancer remains the fifth most frequent cause of cancer death in women. An improved understanding of the genetic aberrations in ovarian cancer may identify new etiologic, prognostic or therapeutic targets that can improve patient management. Several genes located at sites of DNA copy number aberrations in ovarian cancer, including *PIK3CA*[4], *ERBB2* (ref. 5), *MYC*[6], *EEF1A2* (ref. 7), *AKT2* (ref. 8) and *NCOA3* (ref. 9), have been implicated in the pathophysiology of ovarian cancer. Importantly, chromosome CGH analyses reveal other regions of recurrent abnormality in ovarian cancer, which may encode additional genes contributing to tumor behavior[10–12]. In particular, chromosome 1q is frequently increased in copy number in ovarian[11,12] and breast[13] cancers and Wilms[14] tumors; a high relapse rate in invasive ductal breast carcinomas[13] and Wilms tumors[14] are associated with increased DNA copy number on chromosome 1q, but the driver of the regional copy number increase at 1q has not been identified.

Using array CGH[1] to more precisely define region(s) of recurrent copy number increase on chromosome 1q, we delineated an increase (at least 1.3-fold) in DNA copy number in a 1.1-Mb region located on chromosome 1q22 in 28 of 52 (54%) of advanced serous epithelial ovarian cancers (Fig. 1a). Notably, ovarian cancer patients with elevated 1q22 (at least 1.5 copies of *RAB25*) either did not enter a disease-free state following surgery and chemotherapy or showed very short disease-free survival, implicating gene(s) in this region as potential oncogenes regulating the behavior of ovarian cancers (Fig. 1b).

The minimal region of copy number increase on 1q22 encompassed the region from position 152,377,895 to 153,495,551, which contains a total of 34 genes, including 22 known genes and 12 hypothetical proteins based on the July 2003 human reference sequence. Based on expression levels from our microarray data sets[15], the Gene Expression Omnibus and the Stanford Microarray Database, we eliminated 18 candidates that did not show a significant difference in RNA levels between normal ovarian epithelium (NOE) and ovarian cancers. We analyzed mRNA expression levels of the remaining 16 open reading frames located in this region using real-time quantitative PCR to identify potential drivers of the copy number increase at 1q22. Although mRNA levels of several of the genes in this region were modestly elevated in a fraction of ovarian cancers as compared to NOE or benign ovarian tumors, *RAB25* mRNA levels were markedly increased in 55 of 62 (88.7%) of ovarian cancers ($P < 0.001$; Fig. 1c,d). This observation was confirmed in an independent ovarian cancer data set[16] wherein *RAB25* transcript levels were increased in 35 of 44 (80%) ovarian cancer samples compared to NOE. The increase in *RAB25* expression was stage dependent, with stage III and stage IV cancers showing higher levels ($P < 0.01$; Fig. 1d) than early stage cancers, suggesting a potential role of *RAB25* in tumor progression. Sequencing of the open reading frame in 8 ovarian cancer samples did not identify mutations in *RAB25*, suggesting that mutation of *RAB25* rarely or never occurs in ovarian cancer. Linear regression analysis of 21 epithelial ovarian cancers for which both CGH and expression levels were available showed a direct relationship between copy number and expression of *RAB25* (Fig. 1e) with

[1]Department of Molecular Therapeutics, University of Texas MD Anderson Cancer Center, Houston, Texas 77054, USA. [2]Lawrence Berkley National Laboratory, Berkeley, California 94720, USA. [3]Department of Obstetrics and Gynecology, University of British Columbia, Vancouver, British Columbia V6H 3V5, Canada. [4]Department of Pathology, [6]Department of Gynecological Oncology, University of Texas MD Anderson Cancer Center, Houston, Texas, 77030, USA. [5]Department of Obstetrics and Gynecology, University of California, San Francisco, San Francisco, California 94143, USA.[7]Department of Obstetrics and Gynecology, School of Medicine, New York University, New York, New York 10016, USA. Correspondence should be addressed to G.B.M. (gmills@mdanderson.org).

Published online 24 October 2004; doi:10.1038/nm1125

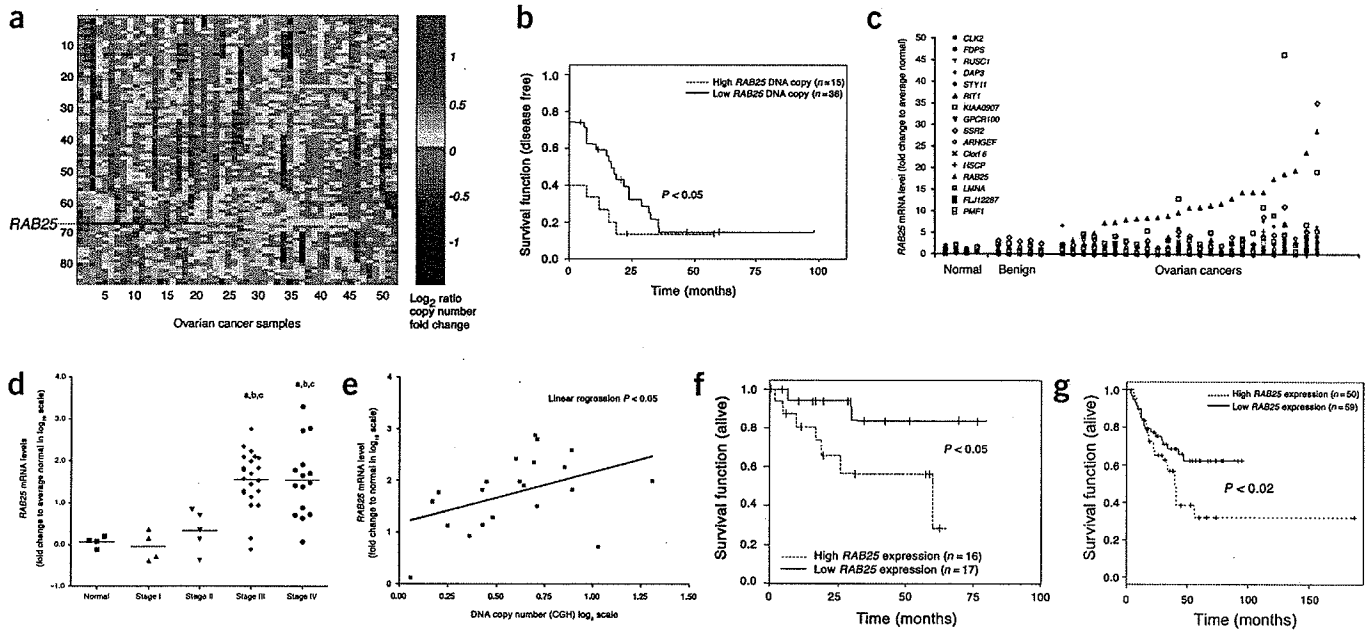

Figure 1 Genetic aberrations at chromosome 1q22. (**a**) Array CGH of chromosome 1 in ovarian cancer ordered by *RAB25*, with red and blue indicating increase and decrease in DNA copy number, respectively. (**b**) Disease-free survival in ovarian cancer patients with high *RAB25* DNA copy (at least 1.75-fold increase). (**c**) Real-time quantitative PCR of candidate genes from centromere to telomere in ovarian cancer. (**d**) Stage dependence of *RAB25* mRNA expression in ovarian cancer (**a**, $P < 0.001$ versus normal; **b**, $P < 0.001$ versus Stage I; **c**, $P < 0.01$ versus Stage II). (**e**) Correlation of *RAB25* DNA copy number and mRNA levels in ovarian cancer. (**f,g**) *RAB25* RNA levels on survival of ovarian cancer (**f**) and of breast cancer (**g**). Unless otherwise designated, ovarian cancers are epithelial serous Stage III–IV.

a Pearson coefficient value of 0.434 ($P < 0.05$) and a Spearman rank coefficient of 0.481 ($P < 0.05$). Of 53 patients with high *RAB25* mRNA (at least twofold increase) for which follow up data was available, 30 did not enter a disease-free interval (data not shown). As expected from CGH analysis (Fig. 1b), high *RAB25* mRNA expression (at least 40-fold increase compared to NOE, $P < 0.05$), assessed by real-time quantiative PCR and microarray[15], was associated with decreased survival (Fig. 1f) when comparing the top and bottom 30% of patients. When all patient samples ($n = 53$) were taken into consideration, a similar trend of correlation between high *RAB25* levels and outcome was observed (see Supplementary Fig. 1 online).

CGH analysis also indicated an increase (at least 1.3-fold) at 1q22 in the region of *RAB25* in 47% of breast cancers (JWG, unpublished data). In contrast to ovarian cancer, the regional increase in breast cancer is wide and encompasses the majority of 1q. Using an independent breast cancer microarray data set[17], 78 of 116 (66.7%) breast cancer patients showed an at least 1.7-fold increase in *RAB25* expression compared to normal breast tissue. Kaplan-Meier analysis of 109 breast cancer patients showed a correlation between high *RAB25* expression ($n = 50$; at least twofold higher than normal) and a decrease in both overall survival ($P < 0.02$, Fig. 1g) and disease-free survival ($P < 0.01$, Supplementary Fig. 2 online). *RAB25* levels were an independent indicator of disease-free interval and overall survival in breast cancer when the data were adjusted for tumor size, ER status and grade and stratified by metastases. Increased *RAB25* levels have previously been noted in prostate cancer[18], transitional cell carcinoma of the bladder[19] and invasive breast cancer[20], suggesting a pathological role for RAB25 in epithelial tumor development.

We evaluated the role of *RAB25* in the aggressiveness of ovarian and breast cancers by altering *RAB25* levels. Transient expression of *RAB25* in A2780, DOV13, HEY and OCC1 ovarian cancer cells markedly increased colony-forming activity under anchorage-dependent conditions (Fig. 2a). We thus established multiple breast and ovarian cancer cell lines that stably express *RAB25*. Stable expression of *RAB25* in ovarian T80 (SV-40– and telomerase-immortalized but nontumorigenic ovarian cancer cells[21]), A2780, OCC1, SKOV3 and HEY and breast MCF-7 cancer cells increased cell numbers under both low (1% fetal bovine serum (FBS)) and high (10% FBS) serum conditions (**Table 1, Supplementary Fig. 3** online). The ability of *RAB25* to increase cell number could result from either increased cell-cycle progression or reduced apoptosis. Our analyses did not detect a significant change in cell-cycle progression as assessed by propidium iodide staining; however, enforced expression of *RAB25* in immortalized ovarian cancer cells T80 and T29 (Fig. 2b), A2780 (Fig. 2b) and HEY (data not shown) was sufficient to increase cell survival under multiple stress conditions including serum starvation, anoikis (anchorage-independent stress), UV radiation and paclitaxel, suggesting that *RAB25* regulates cell survival. To verify the role of *RAB25* in regulating cell survival, we employed RNA interference (RNAi)[22] technology to knock down the expression of *RAB25*. RNAi transfection markedly decreased both *RAB25* mRNA levels (Fig. 2c) and protein levels (Fig. 2c). Decreasing *RAB25* levels consistently increased the number of apoptotic cells in control (no UV radiation) and UV-irradiated breast and ovarian cancer cells (Fig. 2d), confirming a role for *RAB25* in regulating cellular apoptosis. Similarly, RNAi transfection also resulted in a significant ($P < 0.05$) decrease in cell proliferation (**Supplementary Fig. 4** online), further confirming the role of *RAB25* in regulating cell survival.

Genes in the *BCL2* (B-cell lymphocyte/leukemia-2 gene) family[23], such as *BAK1* (Bcl-2 homologous antagonist/killer) and *BAX* (Bcl-2 associated protein x), have been shown to be central and key effectors of the mammalian apoptotic signaling cascade[24] and to regulate tumorigenesis[25]. Enforced *RAB25* expression decreased protein levels of BAK in A2780 and T29, whereas both BAX and BAK were

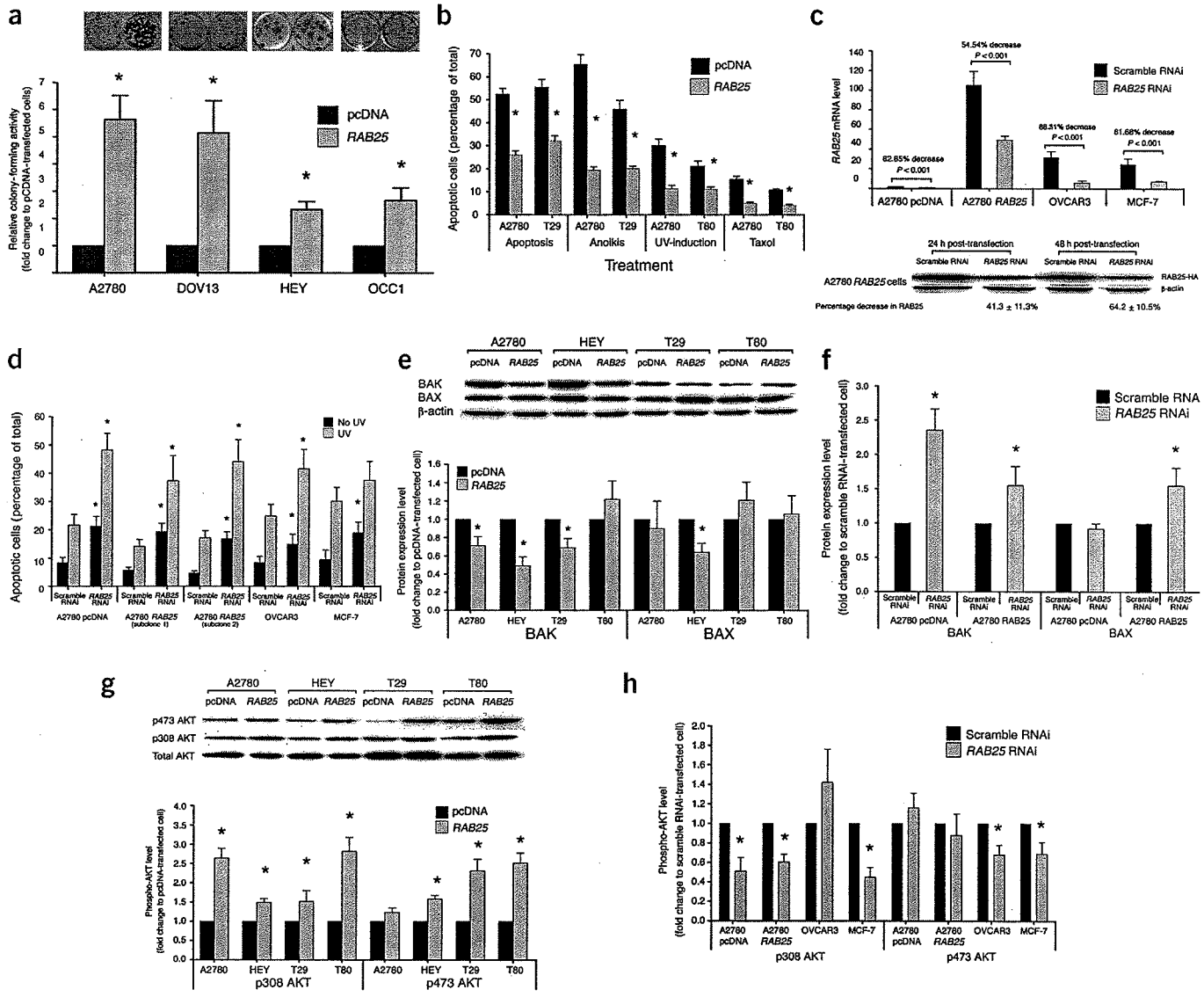

Figure 2 *RAB25* regulates cell proliferation and survival. **(a)** Effect of transient transfection of *RAB25* on colony formation. **(b)** Effect of stable expression of *RAB25* on apoptotic stress. *RAB25* siRNA decreases **(c)** *RAB25* mRNA (upper panel, measured as fold change to A2780 pcDNA scramble RNAi–transfected cells) and protein (lower panel) levels and **(d)** UV radiation–induced apoptosis. **(e,f)** Effect of *RAB25* stable expression **(e)** and *RAB25* RNAi **(f)** on BAK and BAX levels. **(g,h)** Effect of *RAB25* stable expression **(g)** and RNAi **(h)** on AKT phosphorylation. All results are mean ± s.d. of three individual experiments except colony formation, which is mean ± s.d. of triplicates in a representative experiment of three performed. At least two subclones of each line were assessed in each assay.

decreased in HEY ovarian cancer cells (Fig. 2e). Neither BAX nor BAK was decreased in T80, suggesting that mechanisms other than changes in BAX or BAK protein levels must also contribute to resistance to apoptosis in some cells. Nevertheless, downregulation of *RAB25* expression by RNAi reversed the RAB25-mediated inhibition of BAX and BAK levels in *RAB25*-overexpressing A2780 cells (Fig. 2f), supporting the potential involvement of *BCL2* family members in regulating *RAB25* action. Thus dependent on the genetic background of the cell, either BAX and BAK, or both (or potentially other apoptotic regulators), were decreased in *RAB25*-transfected cells.

The PI3K pathway, in particular AKT, has been implicated in cell survival[26,27], at least in part, through altered expression of *BCL2* family members[28]. Western blotting analysis showed higher levels of AKT phosphorylation, an indication of activation of the PI3K-AKT pathway, in A2780, HEY, T29 and T80 cells overexpressing *RAB25* (Fig. 2g). Similarly, *RAB25* knock-down by RNAi decreased AKT phosphorylation (Fig. 2h), confirming an interaction between *RAB25* and the PI3K pathway. Thus overexpression of *RAB25* increases signaling through the PI3K pathway and decreases expression of the

Table 1 Increase in cell proliferation by *RAB25* expression

	1% FBS		10% FBS	
Cell lines	pcDNA	*RAB25*	pcDNA	*RAB25*
A2780	37.5 ± 3.5	63.5 ± 7.8	100.5 ± 7.5	145 ± 6.2
OCC1	57 ± 6.3	82.5 ± 4.6	122.5 ± 9.8	181 ± 8.9
SKOV3	58.5 ± 7.2	96.5 ± 6.2	78.5 ± 9.2	128 ± 8.3
T80	95 ± 4.6	154.5 ± 6.8	171 ± 7.4	226 ± 9.3
HEY	119 ± 7.4	225 ± 5.7	348 ± 12.3	538 ± 28.9
MCF-7	60 ± 4.2	109 ± 10.5	142 ± 6.4	174 ± 4.4

Cell counts were performed on day 8 in stable cells lines. Numbers represent cell number × 10,000 cells/ml. Each sample is presented ± s.e.m. of three replicates from one of three representative experiments. Results were confirmed with multiple subclones of each cell line.

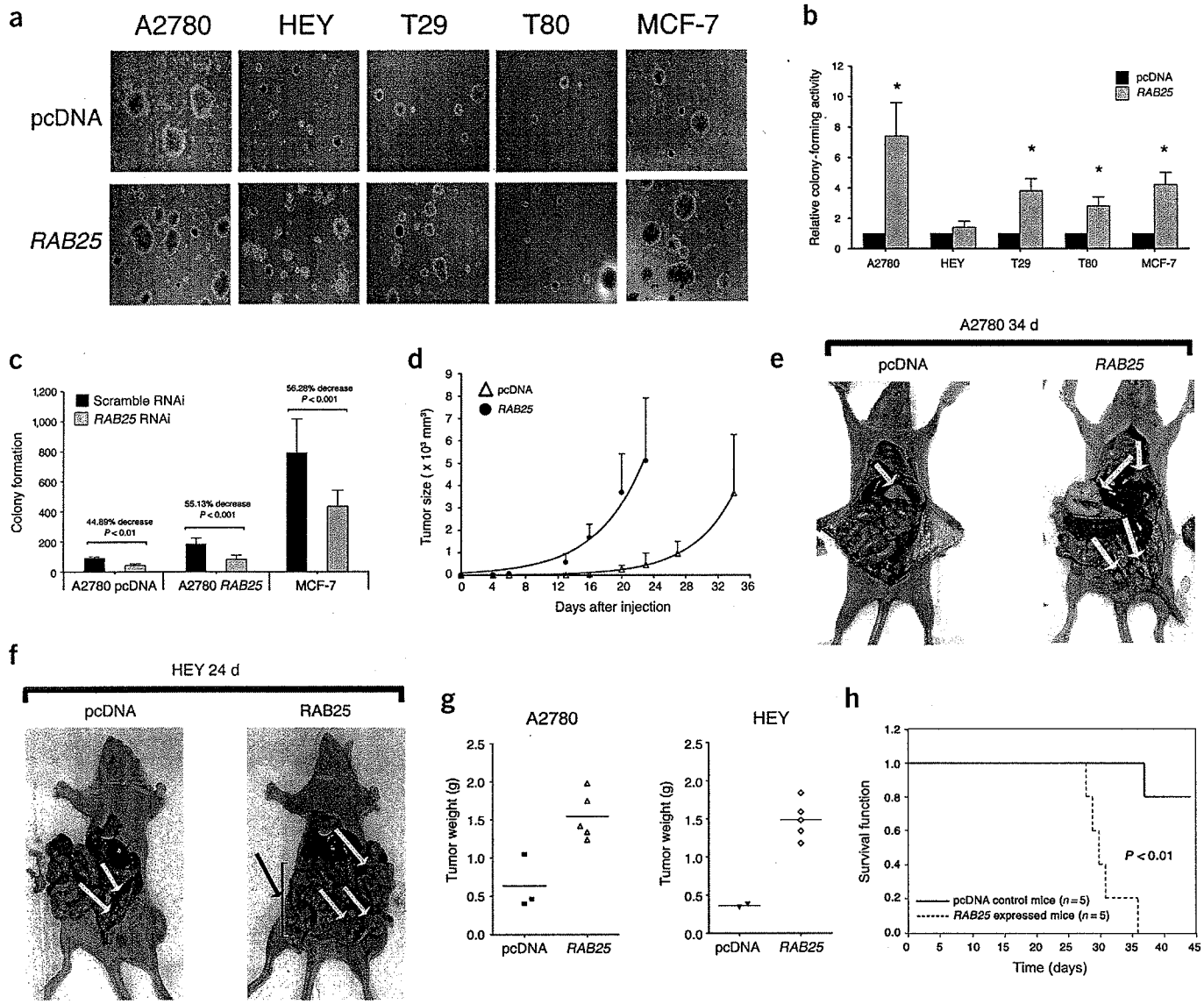

Figure 3 *RAB25* regulates tumorigenicity. Effect of stable *RAB25* (**a**,**b**) and RNAi (**c**) expression on anchorage-independent colony formation. The number of colonies (≥3 mm in diameter) per 10,000 cells plated in pcDNA-transfected cells was 130 ± 32 for A2780, 290 ± 46 for HEY, 68 ± 12 for T29, 28 ± 5 for T80 and 2034 ± 128 for MCF-7. (**d**) Effect of stable *RAB25* expression on subcutaneous growth of A2780 in nude mice. (**e**–**h**) Effect of stable *RAB25* expression on orthotopic intraperitoneal tumor growth (**e**,**f**), weight (**g**) and (**h**) survival (survival curve is from the results of **g**). All stable *RAB25*-transfected cell injections formed tumors, whereas only two and three pcDNA-transfected HEY and A2780 injections formed tumors, respectively). Results are mean ± s.d. from one representative experiment of three performed except mouse studies, which are from one of two experiments.

proapoptotic *BCL2* family members, which likely contributes to resistance to apoptotic stimuli. Although the mechanism by which *RAB25* alters AKT signaling and *BCL2* family expression remains to be fully elucidated, the recent demonstration that multiple signaling molecules, including AKT and small GTPases, associate in a complex on endocytic vesicles[29] provides a potentially unifying mechanism linking AKT with *RAB25*, and subsequent altered cell survival.

The ability of *RAB25* overexpression to block anoikis suggested that *RAB25* may increase the ability of cells to undergo anchorage-independent growth, an *in vitro* surrogate for *in vivo* tumor growth. Indeed, overexpression of *RAB25* markedly increased the number of colonies under anchorage-independent conditions in A2780, T29 and T80 ovarian cells (Fig. 3a,b). Although *RAB25* did not increase colony numbers with HEY cells (Fig. 3b), it did increase the size of HEY cell colonies (Fig. 3a). Similarly, overexpression of *RAB25* in MCF-7 breast cancer cells increased colony-forming activity (Fig. 3a,b). Compatible with a role for *RAB25* in survival under anchorage-independent conditions, a significant decrease in colony-forming activity was observed in *RAB25* RNAi-transfected cells (Fig. 3c, $P < 0.01$). Thus overexpression of RAB25 is sufficient to increase anchorage-independent growth in ovarian and breast epithelial cells.

The marked effects of *RAB25* on cell proliferation, anchorage-independent growth and cell survival suggested that *RAB25* might alter tumor growth *in vivo*. 100% of nude mice injected with *RAB25*-transfected cells developed subcutaneous tumors as compared to only 50% and 70% mice injected with vector transfected A2780 and HEY cells, respectively. Moreover, mice injected with *RAB25*-transfected A2780 and HEY cells developed larger tumors in a shorter time than

mice receiving vector transfected cells (Fig. 3d). *RAB25* overexpression also increased orthotopic intraperitoneal tumor growth (Fig. 3e–g). Further intraperitoneal injection of A2780 cells expressing *RAB25* resulted in rapid tumor accumulation and death compared with empty vector–expressing cells ($P < 0.01$, Fig. 3h). *RAB25* expressing T29 and T80 immortalized ovarian epithelial cells did not grow either subcutaneously or intraperitoneally in nude mice, indicating that *RAB25* is not sufficient to transform ovarian epithelial cells. Rather, *RAB25* increased rates of tumor growth and aggressiveness in already transformed lines. Our data strongly implicate *RAB25* in the aggressiveness of ovarian and breast carcinomas suggesting that *RAB25* could be used to predict patient outcome and may provide a novel therapeutic target. These studies also implicate *RAB25* and, by extension, the RAB GTPase family in tumor aggressiveness. This adds the genes encoding the RAB family to other members of the *RAS* oncogene superfamily as tumorigenic mediators.

METHODS

Patient samples. All patient samples and information were collected under Institutional Review Board–approved (LAB01-144) and HIPAA-compliant protocols at the MD Anderson Cancer Center. All patient samples contained ≥80% tumor on histologic inspection. We obtained NOE by directly scraping ovarian epithelial cells in the operating room into *RNA*later (Ambion). Analysis of the approach indicates that at least 90% of cells are of epithelial origin.

RNA isolation and real-time quantitative PCR. We isolated total RNA from normal ovarian surface epithelial cell preparations directly from the patient, and benign ovarian tumors and advanced (Stages III and IV) ovarian serous epithelial carcinomas by Trizol (Invitrogen) according to the manufacturer's protocol. Fluorogenic Taqman probes were designed based on sequences in GenBank. We determined mRNA levels for the genes of interest by Taqman real-time reverse transcription-PCR using the ABI PRISM 7700 Sequence Detection System (Applied Biosystems) through 40 cycles. We used β-actin as a reference.

Cell lines and transfection. We maintained ovarian caner cell lines in RPMI 1640 containing 10% FBS, and immortalized ovarian surface epithelial cells T29 and T80 in MCDB105:M199 (50:50) containing 10% FBS. We constructed a hemagglutinin-tagged *RAB25* expression vector by PCR amplification and confirmed it by sequencing. Stable *RAB25*-expressing clones were generated by transfection with hemagglutinin epitope–tagged *RAB25* constructs using FuGene 6 (Roche) and selected in G418 for 4 weeks by limiting dilution. We generated at least three clones for each cell line. We performed all experiments with multiple subclones in each cell line and results are representative of several subclones.

RNA interference. We purchased *RAB25*-specific siRNA (5′-GGAGCUCUAUGACCAUGCU-3′) from Xenigon and a scramble RNAi negative control from Ambion. We carried out RNAi transfection in solution T using a Nucleofector according to the manufacturer's protocol (catalog # 4611, Amaxa Biosystem).

Immunoblotting. We cultured cancer cell lines stably expressing *RAB25* in the absence of serum for at least 24 h before protein isolation. We used pcDNA-transfected cells as a control. The proteins were separated by SDS-PAGE and detected with anti-hemagglutinin (1;1000; Covance), anti-bak (1:1000), anti-BAX (1;1000), anti-phospho-AKT (1:1000 dilution, Ser473 or Thr308) or anti-AKT (1:1000 dilution) antibodies (Cell Signaling). We washed the membranes extensively, visualized the proteins by ECL (Amersham Biosciences) and quantified them using NIH image Version 1.61.

Cell proliferation and clonogenic assay. We plated cells stably expressing *RAB25* at a density of 1×10^5 cells/35-mm dish. Cells were then cultured in the presence of 1% or 10% FBS for 8 d. We harvested and counted total cells. We used pcDNA-transfected cells as a control. For anchorage-dependent colony formation, cells were transfected with either pcDNA 3.0 or *RAB25* expression vector. We trypsinized cells 48 h after transfection and replated them in 6 well/plates for 14 d in the presence of G418. Cells were stained with 0.1% Coomassie blue (Bio-Rad) in 30% methanol and 10% acetic acid. We counted the number of colonies formed and expressed the number as fold increase compared with pcDNA-transfected cells. To test the effect of *RAB25* expression on anchorage-independent colony formation, we suspended cells stably expressing pcDNA or *RAB25* at a density of 1×10^4 cells/ml in 1 ml of 0.3% agar dissolved in complete medium containing 25% FBS. Cells were plated in 35-mm dishes precoated with 1 ml of 0.6% agar base. We measured colony-forming efficiency 14–18 d after plating (≥50 cells/colony) and expressed the number as a fold increase related to control vector–transfected cells. All experiments with transfected cells were from multiple individual subclones.

Apoptosis assays. We measured apoptotic cells using paraformaldehyde-fixed cells with an APO-BrdU kit (Phoenix Flow Systems) with flow cytometry. In each experiment, we collected both floating and attached cells and washed them with PBS. We induced apoptosis by culturing cells in 0.1% serum for 48 h, with UV radiation (A2780: 300×100 μJ/cm^3; HEY 150×100 μJ/cm^3; IOSE: 50×100 μJ/cm^3) or paclitaxel (A2780: 200 ng/ml; HEY, T29 and T80: 50 ng/ml). For anoikis assays, we incubated cells on a rocker platform to prevent adhesion for 48 h.

Tumorigenicity in nude mice. To assess the impact of *RAB25* overexpression on tumorigenicity, BALB/c-nu/nu mice (female, 4 weeks old) were injected subcutaneously (above the left hind leg) or intraperitoneally with 5×10^6 *RAB25* overexpressing or control cells. We measured subcutaneous tumors with a digital caliper and killed the mice in compliance with MD Anderson Animal Care and Use Form (ACUF) rules. Intraperitoneal tumor mass was measured by dissection of tumor from the peritoneal cavity and weighing. We performed all animal protocols under an Association for Assessment and Accreditation of Laboratory Animal Care (AALAC)–approved protocol.

Statistical analysis. We statistically evaluated experimental results using the ANOVA test, simple *t*-test, or two-sided log-rank statistical test. Differences were considered significant if $P < 0.05$. Patients with no further follow-up information are represented by a vertical tick at last point of contact and are weighted in the Kaplan-Meier analysis.

URL. Human Genome Sequencing Consortium assembly http://genome.ucsc.edu/cgi-bin/hgGateway
Gene Expression Omnibus http://www.ncbi.hlm.nih.gov/geo/
Stanford Microarray Database http://genome-www5.stanford.edu/
Ovarian cancer data set[17] http://genome-www.stanford.edy/ovarian_cancer
Breast cancer microarray data set[19] http://genome.www.stanford.edu/breast_cancer/robustness/data.shtml

Note: Supplementary information is available on the Nature Medicine website.

ACKNOWLEDGMENTS

KWC was supported by the Odyssey Program of the Houston Endowment Scientific Achievement award from MD Anderson Cancer Center. We thank N. E. Atkinson's group for help and advice in statistical analysis. We thank R. Lapushin and H. Hall for their support. We thank R. Trost for obtaining patient follow up. We thank the staffs from the MD Anderson Cancer Center and University of California San Francisco ovarian tumor bank for providing ovarian carcinomas. This work is supported by National Institutes of Health SPORE (P50-CA83639) and PPG-PO1 CA64602 to GBM and JWG and P30 grant CA16672-28.

COMPETING INTERESTS STATEMENT

The authors declare that they have no competing financial interests.

Received 7 July; accepted 31 August 2004
Published online at http://www.nature.com/naturemedicine/

1. Pinkel, D. *et al.* High resolution analysis of DNA copy number variation using comparative genomic hybridization to microarrays. *Nat. Genet.* **20**, 207–211 (1998).
2. Goldenring, J.R., Shen, K.R., Vaughan, H.D. & Modlin, I.M. Identification of a small GTP-binding protein, Rab25, expressed in the gastrointestinal mucosa, kidney, and lung. *J. Biol. Chem.* **268**, 18419–18422 (1993).
3. Wang, X., Kumar, R., Navarre. J., Casanova, J.E. & Goldenring, J.R. Regulation of vesicle trafficking in Madin-Darby canine kidney cells by Rab11a and Rab25. *J. Biol. Chem.* **275**, 29138–29146 (2000).
4. Shayesteh, L. *et al.* PI3KCA is implicated as an oncogene in ovarian cancer. *Nat.*

Genet. **21**, 99–102 (1999).
5. Fukushi, Y., Sato, S., Yokoyama, Y., Kudo, K., Maruyama, H., & Saito, Y. Detection of numerical aberrations in chromosome 17 and c-erbB2 gene amplification in epithelial ovarian cancer using recently established dual color FISH. *Eur. J. Gynecol. Oncol.* **22**, 23–25 (2001).
6. Berchuck, A. & Carney, M. Human ovarian cancer of the surface epithelium. *Biochem. Pharmacol.* **54**, 541–544 (1997).
7. Anand, N. *et al.* Protein elongation factor EEF1A2 is a putative oncogene in ovarian cancer. *Nat. Genet.* **31**, 301–305 (2002).
8. Cheng, J.Q. *et al.* AKT2, a putative oncogene encoding a member of a subfamily of protein-serine/threonine kinases, is amplified in human ovarian carcinomas. *Proc. Natl. Acad. Sci. USA* **89**, 9267–9271 (1992).
9. Anzick, S.L. *et al.* AIB1, a steroid receptor co-activator amplified in breast and ovarian cancer. *Science* **277**, 965–967 (1997).
10. Suzuki, S. *et al.* An approach to analysis of large-scale correlations between genome changes and clinical endpoints in ovarian cancer. *Cancer Res.* **60**, 5382–5385 (2000).
11. Patael-Karasik, Y. *et al.* Comparative genomic hybridization in inherited and sporadic ovarian tumors in Israel. *Cancer Genet. Cytogenet.* **121**, 26–32 (2000).
12. Kiechle, M., Jacobsen, A., Schwarz-Boeger, U., Hedderich, J., Pfisterer, J. & Arnold, N. Comparative genomic hybridization detects genetic inbalance in primary ovarian carcinomas as correlated with grade of differentiation. *Cancer* **91**, 534–540 (2001).
13. Zudaire, I. *et al.* Genomic imbalances detected by comparative genomic hybridization are prognostic markers in invasive ductal breast carcinomas. *Histopathology* **40**, 547–555 (2002).
14. Lu, Y.J., Hing, S., Williams, R., Pinkerton, R., Shipley, J. & Pritchard-Jones, K. UK Children's Cancer Study Group Wilms' tumor group. Chromosome 1q expression profiling and relapse in Wilms' tumour. *Lancet* **9330**, 385–386 (2002).
15. Lu, K.H. *et al.* Selection of potential markers for epithelial ovarian cancer with gene expression arrays and recursive descent partition analysis. *Clin. Cancer Res.* **10**, 3291–3300 (2004).
16. Schaner, M.E. *et al.* Gene expression patterns in ovarian carcinomas. *Mol. Biol. Cell.* **14**, 4376–4386 (2003).
17. Sorlie, T. *et al.* Repeated observation of breast tumor subtypes in independent gene expression data sets. *Proc. Natl. Acad. Sci. USA* **100**, 8418–8423 (2003).
18. Calvo, A. *et al.* Alterations in gene expression profiles during prostate cancer progression: functional correlations to tumorigenicity and down-regulation of selenoprotein-P in mouse and human tumors. *Cancer Res.* **62**, 5325–5335 (2002).
19. Mor, O. *et al.* Molecular analysis of transitional cell carcinoma using cDNA microarray. *Oncogene* **22**, 7702–7710 (2003).
20. Wang, W. *et al.* Single cell behavior in metastatic primary mammary tumors correlated with gene expression patterns revealed by molecular profiling. *Cancer Res.* **62**, 6278–6288(2002).
21. Liu, J. *et al.* A genetically defined model for human ovarian cancer. *Cancer Res.* **64**, 1655–1663 (2004)
22. Milhavet, O., Gary, D.S. & Mattson, M.P. RNA interference in biology and medicine. *Pharmacol. Rev.* **55**, 629–648 (2003).
23. Gross, A., McDonnell, J.M. & Korsmeyer, S.J. BCL-2 family members and the mitochondria in apoptosis. *Genes Dev.* **13**, 1899–1911 (1999).
24. Wei, M. *et al.* Proapoptotic BAX and BAK: A requisite gateway to mitochondrial dysfunction and death. *Science* **292**, 727–730 (2001).
25. Degenhardt, K., Chen, G., Lindsten, T. & White, E. BAX and BAK mediate p53-independent suppression of tumorigenesis. *Cancer Cell* **2**, 193–203 (2002).
26. Lu, Y. *et al.* The PTEN/MMAC1/TEP tumor suppressor gene decreases cell growth and induces apoptosis and anoikis in breast cancer cells. *Oncogene* **18**, 7034–7045 (1999).
27. Mills, G.B. *et al.* Role of abnormalities of PTEN and the phosphatidylinositol 3′ kinase pathway in breast and ovarian tumorigenesis, prognosis and therapy. *Semin. Oncol.* **28**, S125–S141 (2001).
28. Kennedy, S.G. *et al.* The PI 3-kinase/Akt signaling pathway delivers an anti-apoptotic signal. *Genes Dev.* **11**, 701–713 (1997).
29. Delcroix, J.D., Valletta, J.S., Wu, C., Hunt, S.J., Kowal, A.S. & Mobley, W.C. NGF signaling in sensory neurons: evidence that early endosomes carry NGF retrograde signals. *Neuron* **39**, 69–84 (2003).

Exhibit C

Atypical PKCι contributes to poor prognosis through loss of apical–basal polarity and Cyclin E overexpression in ovarian cancer

Astrid M. Eder[†], Xiaomei Sui[†], Daniel G. Rosen[‡], Laura K Nolden[†], Kwai Wa Cheng[†], John P. Lahad[†], Madhuri Kango-Singh[§], Karen H. Lu[¶], Carla L. Warneke[‖], Edward N. Atkinson[‖], Isabelle Bedrosian[††], Khandan Keyomarsi[††], Wen-lin Kuo[‡‡], Joe W. Gray[‡‡], Jerry C. P. Yin[§§], Jinsong Liu[‡], Georg Halder[§], and Gordon B. Mills[†¶¶]

Departments of [†]Molecular Therapeutics, [‡]Pathology, [§]Biochemistry and Molecular Biology, [¶]Gynecologic Oncology, [‖]Biostatistics and Applied Mathematics, and [††]Experimental Radiation Oncology, M. D. Anderson Cancer Center, University of Texas, 1515 Holcombe Boulevard, Houston, TX 77030; [‡‡]Lawrence Berkeley National Laboratory, 84 One Cyclotron Road, Berkeley, CA 94720; and [§§]Departments of Genetics and Psychiatry, University of Wisconsin, 425 Henry Mall, Madison, WI 53706

Communicated by Louis Siminovitch, Mount Sinai Hospital, Toronto, ON, Canada, July 6, 2005 (received for review April 18, 2005)

We show that atypical PKCι, which plays a critical role in the establishment and maintenance of epithelial cell polarity, is genomically amplified and overexpressed in serous epithelial ovarian cancers. Furthermore, PKCι protein is markedly increased or mislocalized in all serous ovarian cancers. An increased *PKCι* DNA copy number is associated with decreased progression-free survival in serous epithelial ovarian cancers. In a *Drosophila in vivo* epithelial tissue model, overexpression of persistently active atypical PKC results in defects in apical–basal polarity, increased Cyclin E protein expression, and increased proliferation. Similar to the *Drosophila* model, increased PKCι proteins levels are associated with increased Cyclin E protein expression and proliferation in ovarian cancers. In nonserous ovarian cancers, increased PKCι protein levels, particularly in the presence of Cyclin E, are associated with markedly decreased overall survival. These results implicate PKCι as a potential oncogene in ovarian cancer regulating epithelial cell polarity and proliferation and suggest that PKCι is a novel target for therapy.

epithelial cell polarity | proliferation

Ovarian cancer remains the leading cause of death from gynecological malignancy among women in the U.S. (1). The prognosis for advanced disease has not improved significantly, suggesting that an improved understanding of the genetic aberrations in ovarian cancer is critical to identifying better ways to prevent, diagnose and treat this frequently fatal disease.

Atypical PKC (aPKC) ι is located at 3q26.2, the most frequent genomic amplicon in ovarian cancer (2), as indicated by array comparative genomic hybridization (3). PKCι is the sole catalytic component of the Par3–Par6–aPKC complex, which plays a critical role in the establishment and maintenance of epithelial cell polarity, tight junctions, and adherens junctions (4). In *Drosophila*, loss of the polarity-determining tumor suppressors Scribble, Discs large, and Lethal giant larvae contributes to tumor formation (5, 6). Importantly, loss of apical–basal cell polarity is required for epithelial–mesenchymal transition (EMT), which is a critical step in cellular motility and invasiveness (7). Loss of polarity also allows several growth factors and receptors, which are normally compartmentalized because of tight junctions in polarized cells, to mediate autocrine cell activation (8, 9). Thus, deregulation of PKCι, the key catalytic regulator of the formation and maintenance of polarity and tight junctions, could contribute to the pathophysiology of ovarian cancer.

Materials and Methods

Patients. Primary ovarian cancer patient samples (>80% tumor on histology), normal ovarian epithelium, and information were collected under Institutional Review Board-approved Health Insurance Portability and Accountability Act (HIPAA)- compliant protocols at M. D. Anderson Cancer Center; University of Toronto; Duke University; University of California, San Francisco; and Northwestern University.

Normal ovarian epithelium was obtained by directly scraping ovarian epithelial cells into RNAlater (Ambion, Austin, TX). At least 90% of cells isolated are of epithelial origin, as determined by staining for cytokeratins.

High-Density Array Comparative Genomic Hybridization. Bacterial artificial chromosome (BAC) DNA arrays were prepared and probed as described (3) by using 200 contiguous BAC clones covering ≈28 Mbp of 3q26-q28 centered on 3q26.2 at PKCι.

RNA Quantification. Total RNA was extracted from tissue samples by using TRIzol reagent (Invitrogen) according to the manufacturer's instructions. mRNA levels were determined by TaqMan RT-PCR, using 40 cycles with β-actin as reference.

Tissue Microarray Construction and Immunohistochemical Analysis. Tissue microarrays were generated from paraffin-embedded specimens of 441 cases of epithelial ovarian cancers with outcomes and 85 additional specimens reflecting specific histotypes of tumors at the University of Texas M. D. Anderson Cancer Center. Slides were stained with anti-PKCι (1:100, BD Transduction Laboratories), anti-phospho-PKCι (1:300, Abcam, Cambridge, MA), anti-Cyclin E (HE-12 1:100, Santa Cruz Biotechnology), anti-E cadherin (1:100, BD Transduction Laboratories), or anti-Ki67 (1:100, DakoCytomation, Carpinteria, CA) antibodies. Staining was detected by streptavidin–biotin–peroxidase and 3,3′-diaminobenzidine. E cadherin was detected by using FITC-labeled goat anti-mouse antibody (Caltag, Burlingame, CA). Nuclei were stained with DAPI (Sigma). We defined the Ki67 labeling index with >15% as high and ≤15% as low. Cyclin E was judged to be positive when >10% of nuclei stained. Anti-PKCι was shown to be specific for PKCι by Western blotting of tumor tissue and COS7 cells transfected with plasmids encoding PKCι or PKCζ. The anti-phospho-PKCι antibody crossreacts with phospho-PKCζ according to the manufacturer. However, ovarian cancers contain little to no detect-

Freely available online through the PNAS open access option.

Abbreviations: EMT, epithelial–mesenchymal transition; aPKC, atypical PKC; DaPKM, *Drosophila* atypical protein kinase M; rPKCζ*, persistently active rat PKCζ; LMP, low malignant potential; LMW, low molecular weight.

[¶¶]To whom correspondence should be addressed. E-mail: gmills@mdanderson.org.

able PKCζ; thus, the anti-phospho-PKCι antibody detects primarily phospho-PKCι.

Western Blot Analysis. Western blot analysis was performed as described (10) by using Cyclin E, PKCι, and Actin monoclonal antibodies (Roche Molecular Biochemicals).

Fly Stocks. *Drosophila* atypical protein kinase M (DaPKM) in UAS-DaPKM starts at Met-223 within the hinge region of *Drosophila* PKC (DaPKC) (11). Persistently active rat PKCζ (rPKCζ*) with a 5-aa deletion within the pseudosubstrate domain (residues 117–121) (12) was cloned into the XbaI site of pUAST (13). Eight independent transgenic rPKCζ* lines gave a similar phenotype. Other stocks were *yw*; *GMR-GAL4, UAS-GFP* and *GMR-GAL4* and *GMR-hid-Ala-5* and *UAS-p35* and *yw*; *dpp-GAL4, UAS-GFP/TM6B*.

Immunohistochemistry and Cell Death Assay of *Drosophila* Imaginal Discs. Imaginal discs were stained as described (14) with the following antibodies (dilutions): rabbit anti-PKCζ C20 (1:500; Santa Cruz Biotechnology), rat anti-Elav (1:60; Developmental Studies Hybridoma Bank, University of Iowa, Iowa City), rabbit anti-Patj (1:400; K. Choi, Baylor College of Medicine, Houston), and mouse anti-BrdUrd (1:50; Becton Dickinson). Donkey Fab fragment secondary antibodies were from Jackson ImmunoResearch. BrdUrd incorporation was for 1 h (14). Apoptosis (TUNEL) was detected by using an *in situ* cell death detection kit (Roche Applied Science, Indianapolis).

Statistical Analysis. Experiment results were analyzed with χ^2 test of independence, Spearman correlation, Kruskal–Wallis test, Mann–Whitney test, or Wilcoxon rank sum test, as appropriate. Survival rates were calculated by using Kaplan–Meier analysis (15). Differences in survival were analyzed by using the log-rank test and univariate and multivariate Cox proportional hazards models (16). All tests were two-tailed and were considered statistically significant if $P < 0.05$.

Results

Amplification of PKCι Contributes to Increased PKCι Expression and Reduced Progression-Free Survival in Ovarian Cancer. By using a high-density chromosome 3q array comparative genomic hybridization contig, the *PKCι* DNA copy number was increased in >70% of serous epithelial ovarian cancers (Fig. 1*a*) and was associated with a significantly shorter progression-free survival duration ($P = 0.0006$) (Fig. 1*b*). Similarly, PKCι RNA levels were increased in >80% of serous epithelial ovarian cancers, as compared with normal ovarian surface epithelial cells (17, 18), with the magnitude and frequency of PKCι RNA increases being higher in serous epithelial ovarian cancers than in other histotypes of ovarian cancer and tumor lineages (Fig. 1*c*). As indicated by TaqMan RT-PCR, PKCι mRNA levels were markedly increased in advanced (Stage III/IV) ovarian cancers as compared with normal ovarian surface epithelial cells, benign epithelial tumors, or early (Stage I/II) ovarian cancers (Fig. 6 *a* and *b*, which is published as supporting information on the PNAS web site). Although the magnitude of the RNA increase was consistently greater than the DNA copy number increase, *PKCι* DNA and RNA levels were correlated in serous epithelial ovarian cancers ($P = 0.05$, Fig. 6*c*), indicating that the increase in DNA copy number contributes to the elevated RNA levels.

Ectopic Expression of Persistently Active aPKC in *Drosophila* Imaginal Eye Discs Results in Loss of Cell Polarity. We evaluated the potential mechanisms by which increased levels of PKCι contribute to transformation of epithelial cells by overexpressing two persistently active forms of aPKC in epithelial tissues in the model organism *Drosophila*: (*i*) DaPKM (11), which produces a naturally occurring

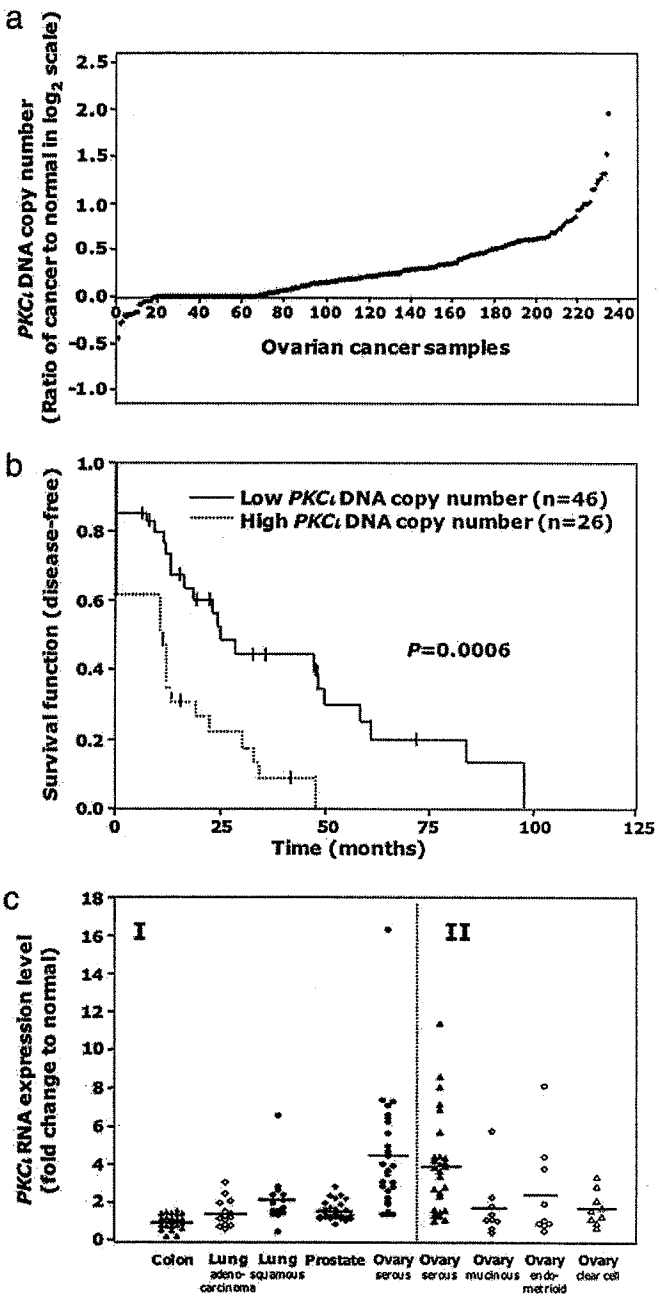

Fig. 1. Amplification of the *PKCι* gene and increased PKCι RNA expression in ovarian cancer. (*a*) Array comparative genomic hybridization analysis of *PKCι* DNA copy number in 235 Grade 3 and Stage III or IV serous epithelial ovarian cancer samples ($\log_2$ ratio of cancer patient DNA to normal DNA). (*b*) Increase in *PKCι* DNA copy number is associated with a decreased progression-free survival period. For patients where followup information was available, progression-free survival in patients with high *PKCι* DNA copy number ($n = 26$) was significantly worse ($P = 0.0006$) than in patients with low *PKCι* copy number ($n = 46$) (cutoff at 0.37 $\log_2$). Vertical lines indicate censored patients, i.e., patients for whom no further followup information was available after the indicated time points. (*c*) Microarray analysis of *PKCι* gene expression. Two different studies using Affymetrix DNA microarray analysis (17, 18) show marked elevation of *PKCι* gene expression in serous epithelial ovarian cancers as compared with pooled (I) and normal ovarian (II) epithelium.

active form of DaPKC lacking the Par6-binding site (19) and the aPKC pseudosubstrate site (20), and (*ii*) rPKCζ*, with a 5-aa deletion within the pseudosubstrate site (12). There is only one aPKC in *Drosophila* (DaPKC), allowing these two constructs to

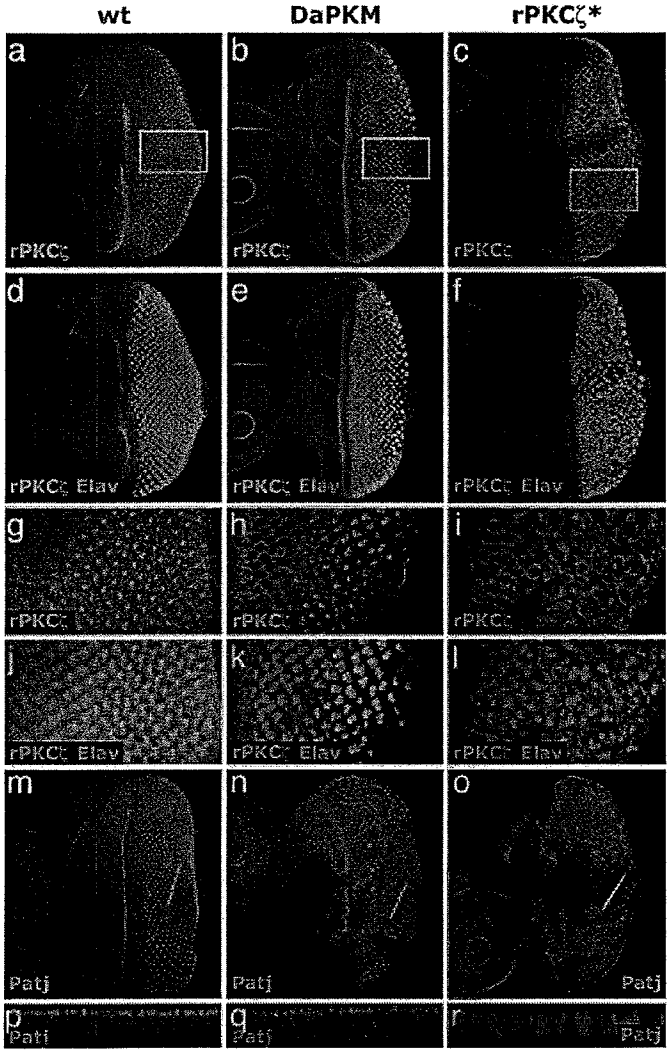

Fig. 2. Ectopic expression of persistently active aPKC in *Drosophila* third-instar larval eye discs causes defects in apical–basal polarity and tissue architecture. Transgenes were expressed in cells posterior to the morphogenetic furrow by using the UAS-GAL4 two-component system (13). Wild-type (*a*, *d*, *g*, and *j*), DaPKM-transgenic (*b*, *e*, *h*, and *k*), and rPKCζ*-transgenic (*c*, *f*, *i*, and *l*) eye discs stained for aPKC/aPKM (red) and Elav (green) are shown. Boxes in *a–c* indicate areas of magnified views in *g–l*. Wild-type eye disc (*m* and *p*), DaPKM-transgenic eye disc (*n* and *q*), and rPKCζ*-transgenic eye disc (*o* and *r*) stained for Pals-associated tight junction protein (Patj) are shown. Lines in planar views (*m–o*) indicate location of cross-section views in *p–r*. Anterior is to the left for all discs.

represent the effects of PKCι, the aPKC amplified in ovarian cancer. Endogenous DaPKC is an apical cell polarity marker in wild-type eye imaginal discs (21) (Fig. 2 *a*, *d*, *g*, and *j*). Both DaPKM (Fig. 2 *b*, *e*, *h*, and *k*) and rPKCζ* (Fig. 2 *c*, *f*, *i*, and *l*) were mislocalized in transgenic eye discs. Polarization of endogenous Pals-associated tight junction protein (Patj) (22, 23), an apical cell polarity marker (Fig. 2 *m* and *p*), was decreased in DaPKM-transgenic eye discs (Fig. 2 *n* and *q*) and completely lost in rPKCζ*-transgenic eye discs (Fig. 2 *o* and *r*). Thus, overexpression of persistently active aPKC is sufficient to induce defects in apical–basal polarity in *Drosophila* epithelial cells.

Persistently Active aPKC Induces Proliferation, Increases in Cyclin E, and Disorganization of Cellular Architecture Without Increasing Apoptosis in *Drosophila* Epithelial Cells. In wild-type eye discs, cell proliferation, as indicated by BrdUrd incorporation, was ran-

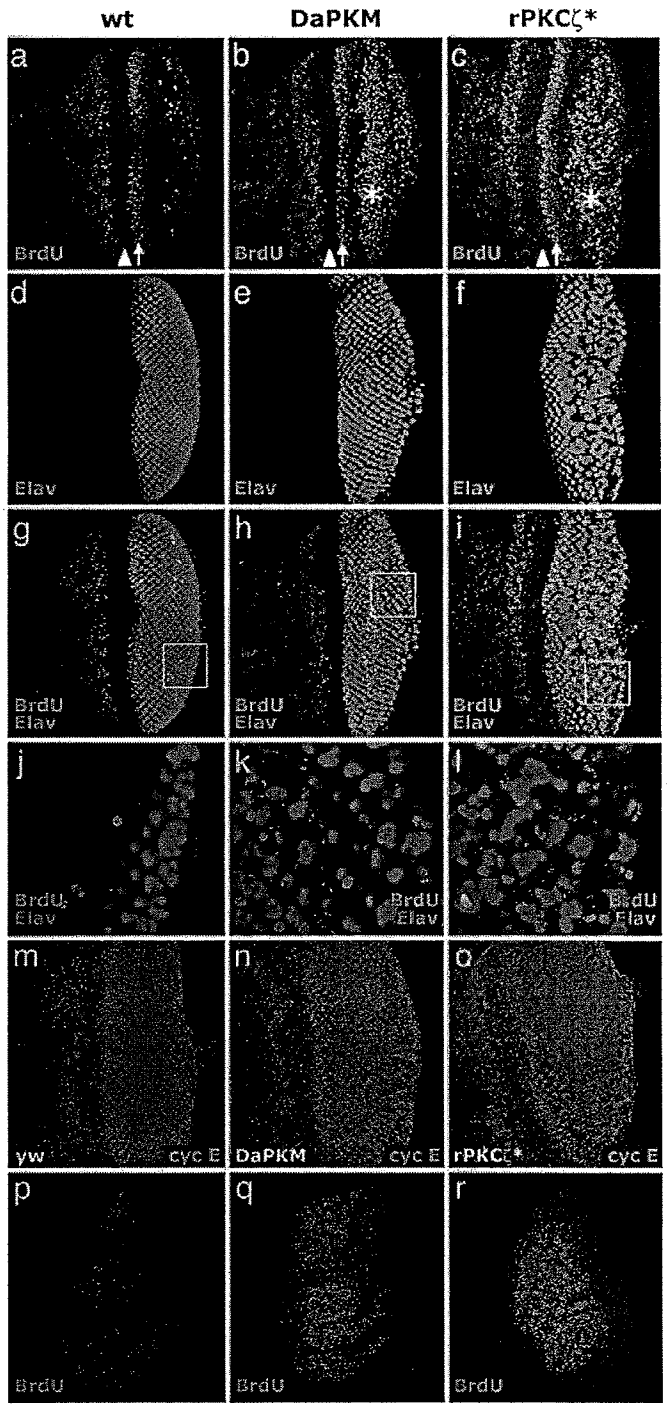

Fig. 3. Ectopic expression of persistently active aPKC in third-instar larval eye and wing discs induces proliferation, disorganization, and up-regulation of Cyclin E protein. (*a–c*) Wild-type (*a*) and DaPKM-transgenic (*b*) or rPKCζ*-transgenic (*c*) eye discs under control of the GMR-GAL4 driver (45), stained for BrdUrd incorporation. (*d–f*) Wild-type (*d*) and DaPKM-transgenic (*e*) or rPKCζ*-transgenic (*f*) eye discs stained for neuronal marker Elav. (*g–i*) Overlay of BrdUrd and Elav staining. White boxes indicate the location of higher-magnification views in *j–l*. (*m–o*) Cyclin E expression: wild-type (*m*), and DaPKM-transgenic (*n*) or rPKCζ*-transgenic (*o*) eye discs, stained for Cyclin E. (*p–r*) Wing discs: wild-type (*p*) and DaPKM-transgenic (*q*) or rPKCζ*-transgenic (*r*) wing discs under control of the dpp-GAL4 driver, resulting in transgene expression in a band of cells along the anteroposterior compartment boundary of the wing, stained for BrdUrd incorporation. The confocal images shown in *a–l* and *p–r* are extended field views, and the images in *m–o* are views of single focal planes. Arrowheads indicate the morphogenetic furrow. Arrows indicate the second mitotic wave. Anterior is to the left for all eye discs.

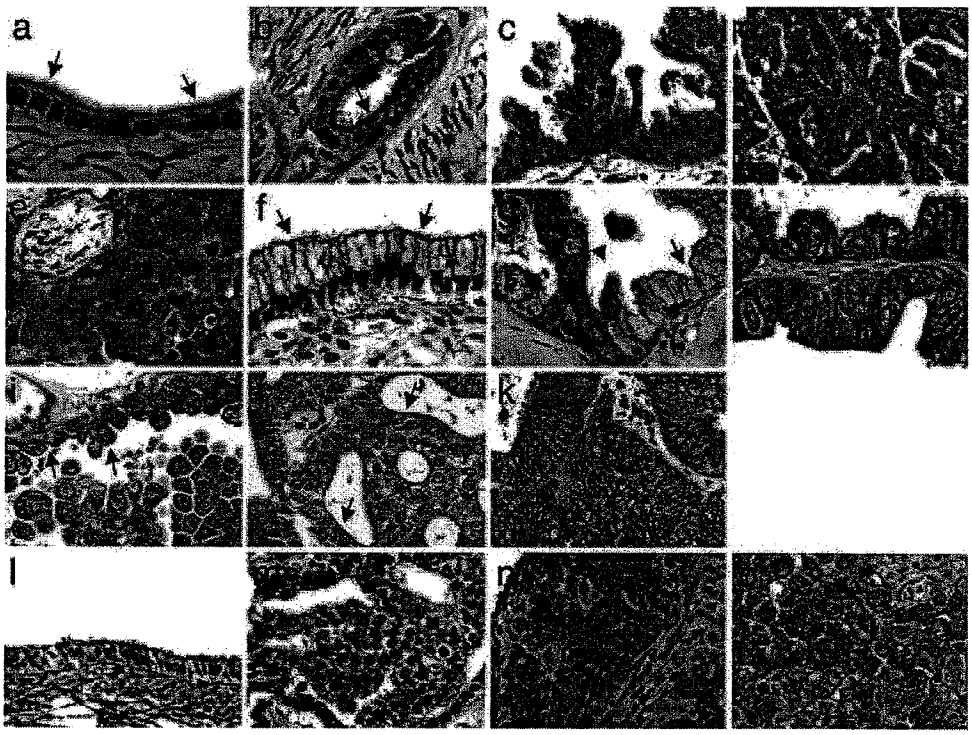

Fig. 4. Histotype- and progression-dependent mislocalization and overexpression of PKCι and phospho-PKCι. (*a–k*) Immunohistochemical staining of PKCι ($P = 0.0036$). Normal ovarian surface epithelial cells (*a*) and serous (*b*) and mucinous (*f*) inclusion cysts showing apical PKCι (arrows) are shown. Serous LMP (*c*), low- (*d*) and high-grade (*e*) serous, and mucinous (*h*) carcinoma with cytoplasmic PKCι, with loss of apical PKCι are also shown. (*g*) Mucinous LMP showing regions of apical PKCι (arrow) or cytoplasmic PKCι with loss of apical localization (arrowhead). (*i* and *j*) Clear cell (*i*) and low-grade (*j*) endometrioid carcinomas showing cytoplasmic PKCι with areas of cell membrane PKCι (arrows). (*k*) High-grade endometrioid carcinoma with cytoplasmic PKCι. (*l–o*) Immunohistochemical staining of phospho-PKCι. (*l–n*) Serous inclusion cyst (*l*) and low-grade (*m*) and high-grade (*n*) serous carcinoma with cytoplasmic PKCι. (*o*) High-grade serous carcinoma with membranous PKCι. Arbitrary optic density units ± SD for antiphospho-PKCι samples are 79 ± 3 for normal ovarian epithelium, 71.3 ± 5.7 for serous cysts, 123.6 ± 22.4 for low-grade serous carcinomas, and 107 ± 22.8 for high-grade serous carcinomas ($P = 0.0036$).

domly distributed anterior to the morphogenetic furrow, a dorsal–ventral groove marking the boundary of photoreceptor differentiation, arrested in G_1 in the furrow (Fig. 3*a*, arrowhead) and underwent an additional round of cell division referred to as the second mitotic wave posterior to the furrow (Fig. 3*a*, arrow). Posterior to the second mitotic wave, cells cease proliferation and differentiate into photoreceptor, cone, pigment, and bristle cells (24). Only rare BrdUrd-positive cells were found in the posterior area of wild-type eye discs, where photoreceptor cells express the neuronal marker Elav (25) (Fig. 3 *a* and *g*). In contrast to wild-type eye discs, DaPKM- or rPKCζ*-transgenic eye discs showed massive incorporation of BrdUrd posterior to the second mitotic wave (Fig. 3 *b* and *c*, asterisk). DaPKM-transgenic (Fig. 3 *e* and *h*) and rPKCζ*-transgenic (Fig. 3 *f* and *i*) eye discs, in contrast to wild-type eye discs (Fig. 3 *d* and *g*), displayed pronounced changes in the spacing, patterning, and size of photoreceptor clusters posterior to the second mitotic wave. In DaPKM-transgenic and rPKCζ*-transgenic eye discs (Fig. 3 *k* and *l*), the BrdUrd-positive DNA-synthesizing cells posterior to the second mitotic wave were Elav-negative. Thus, the DNA-synthesizing cells either have lost Elav expression or are nonneural cells. Increased proliferation induced by DaPKM or rPKCζ* was not limited to imaginal eye discs, because there was a dramatic increase in the number of BrdUrd-incorporating cells in transgenic (Fig. 3 *q* and *r*), as compared with wild-type (Fig. 3*p*) wing discs.

In imaginal disc cells, Cyclin E is limiting for S-phase initiation (26). Concurrent with the increase in proliferation, Cyclin E protein levels were dramatically increased in DaPKM-transgenic and rPKCζ*-transgenic eye disc cells posterior to the second mitotic wave (Fig. 3 *n* and *o*), as compared with wild-type eye discs (Fig. 3*m*). Coexpression of the Cyclin E antagonist Dacapo, which is the *Drosophila* $p21^{CIP}/p27^{Kip1}$ cyclin-dependent kinase inhibitor ortholog, results in amelioration of the DaPKM/rPKCζ* phenotype (data not shown), indicating a critical role of Cyclin E in mediating the DaPKM/rPKCζ* phenotype.

DaPKM-transgenic and rPKCζ*-transgenic eye discs did not show an increase in apoptosis by TUNEL using expression of activated *Drosophila* proaptotic Hid as a positive control (Fig. 7, which is published as supporting information on the PNAS web site, and data not shown). Furthermore, expression of p35, a pan-caspase inhibitor, failed to alter the morphological effects of overexpression of DaPKM and rPKCζ* in eye discs (data not presented). Thus, although aPKC increases cell cycle progression, it does not increase apoptosis in *Drosophila* epithelial tissue.

PKCι Protein Is Mislocalized and Overexpressed in Ovarian Cancer. Informed by the studies in *Drosophila*, we assessed whether increased *PKCι* DNA and RNA levels in ovarian cancer cells were associated with changes in polarity, Cyclin E expression, and cell proliferation and, furthermore, whether this constellation of effects contributes to the prognosis of epithelial ovarian cancer.

PKCι was present at the apical membrane and absent from the basal membrane in normal ovarian surface epithelial cells and in benign serous and mucinous cysts (Fig. 4 *a*, *b*, and *f*). In serous low malignant potential (LMP), although PKCι levels were modestly elevated (Fig. 8, which is published as supporting information on the PNAS web site), membrane localization of PKCι was lost in >85% (Fig. 4*c*). As with mRNA levels, PKCι protein was increased in >85% of low- and high-grade serous epithelial ovarian cancers, as compared with normal ovarian

surface epithelial cells (Table 1, which is published as supporting information on the PNAS web site). Strikingly, apical membrane location of PKCι was abrogated in all (322) serous epithelial ovarian cancers analyzed (Fig. 4 *d* and *e*). Similar to the mRNA data, PKCι protein was increased in a smaller percentage of nonserous ovarian cancers (50%) than serous cancers (Table 1). In contrast to serous LMP, PKCι was absent from the membrane in only 20% of mucinous LMP tumors. However, PKCι no longer localized to the membrane in 90% of mucinous carcinomas, 80–90% of clear cell carcinomas, 60–70% of low-grade endometrioid ovarian carcinomas, and all high-grade endometrioid ovarian carcinomas (Fig. 4 *f–k*). As expected from RNA analysis (Fig. 6 *a–c*), PKCι protein levels were significantly associated with histotype ($P < 0.00001$), stage ($P < 0.00001$), and grade ($P = 0.01$) (Table 1).

The pattern of localization of the adherens junction marker E-cadherin (27) was concordant with that of PKCι being localized to the apical–lateral membrane domain in serous and mucinous cysts and mucinous LMP, while being predominantly cytoplasmic in serous LMP as well as in low- and high-grade serous and mucinous carcinomas (Fig. 9, which is published as supporting information on the PNAS web site). This is compatible with the effects of PKCι overexpression in ovarian cancer contributing to aberrant E-cadherin and adherens junction function.

Activated PKCι Is Overexpressed and Mislocalized in the Cytoplasm in Ovarian Cancer. Activated PKCι levels, assessed by using an antibody recognizing the autophosphorylation site of PKCι and thus reflecting PKCι activity, are increased in ovarian carcinomas as compared with normal ovarian surface epithelial cells and cysts ($P = 0.0036$) (Fig. 4 *l–o*). A small group of serous high-grade carcinomas demonstrated membranous localization of phospho-PKCι (20/376) (Fig. 4*o*); however, it was mislocalized in all other conditions (Fig. 4 *l–n*). Similar to total PKCι, PKCι activity is an indicator of outcomes with 70/245 (28.6%) patients with low phospho-PKCι protein levels being alive at 5 years vs. 8/58 (13.8%) patients with high phospho-PKCι levels ($P = 0.03$).

High Levels of PKCι and Cyclin E Protein Contribute to Outcomes in Nonserous Epithelial Ovarian Cancer. Based on the effect of the aPKC transgenes on *Drosophila* epithelia, we assessed the interactions among PKCι, Cyclin E, and Ki67 and their contribution to patient outcomes. Elevated PKCι protein levels were associated with elevated levels of low molecular weight (LMW) forms of Cyclin E (10) protein in 16 of 18 ovarian cancer patient samples (Fig. 5*a*). In tissue microarrays, PKCι correlated with Cyclin E (using an antibody that recognizes all forms of Cyclin E because antibodies specific to LMW Cyclin E are not available) protein levels ($P = 0.01$) and proliferation (Ki67 levels, $P = 0.02$). Ki67 and Cyclin E levels were also highly correlated ($P < 0.0001$). Four transcriptional profiling data sets comprising a total of 215 ovarian cancer patient samples of mixed histology, grade, and stage demonstrated a direct Spearman correlation [$P < 0.001$ (in-house data set), $P < 0.002$ (17), $P < 0.05$ (28), and $P < 0.05$ (29)], with a positive linear regression on three of the four data sets [$P < 0.01$ (in house), and $P < 0.05$ (28, 29)]. PKCι levels, alone or in combination with Cyclin E levels, were indicative of prognosis in nonserous epithelial ovarian cancers (Fig. 5 *b* and *c*). Indeed, nonserous epithelial ovarian cancers with low levels of both Cyclin E and PKCι demonstrated a remarkably good prognosis with almost 90% of patients being alive at 5 years, whereas patients with high levels of both demonstrated a poor prognosis with <20% alive at 5 years. Univariate Cox proportional hazards models (16) showed that patients with nonserous tumors with high PKCι levels had a higher likelihood of death (Table 2, which is published as supporting information on the PNAS web site). This finding is compatible with a previous small study demonstrating an association of PKCι protein levels with outcome (30) and with studies indicating an association of Cyclin E with outcome (10, 31). In a multivariate model that included both PKCι and Cyclin E levels as independent variables, the association between overall survival and PKCι levels remained significant in nonserous epithelial tumors (Table 2). PKCι was either mislocalized or overexpressed in all serous epithelial ovarian cancers, suggesting that the processes normally regulated by PKCι, likely apical–basal polarity, are functionally aberrant in all serous epithelial ovarian cancers. Indeed, supporting this contention, PKCι levels were not predictive of outcomes in serous epithelial ovarian cancers.

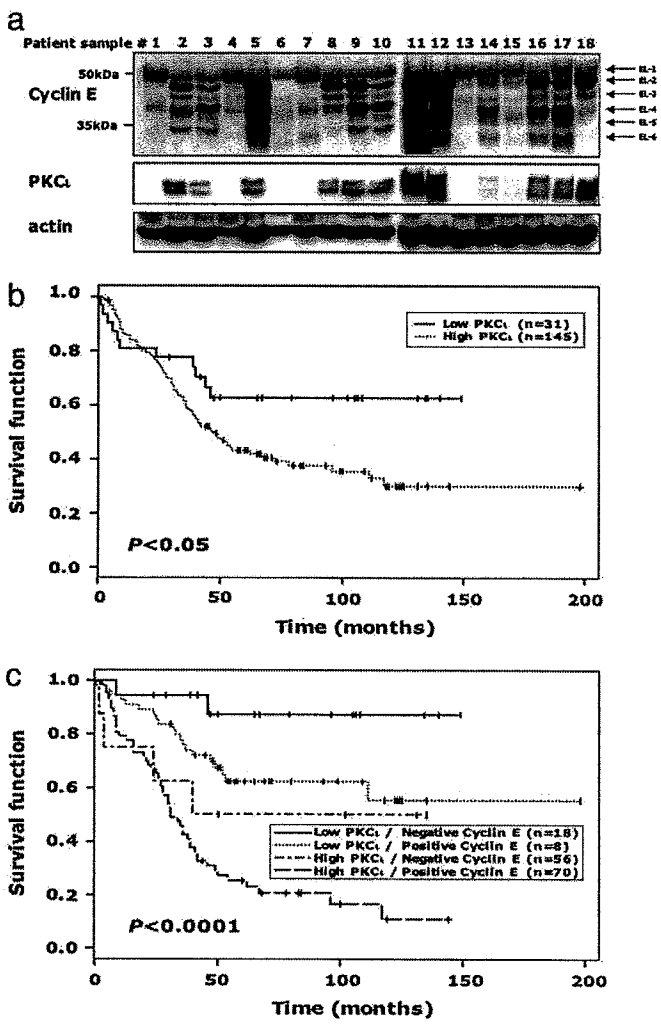

Fig. 5. Association of increased PKCι and Cyclin E protein levels with decreased survival in ovarian cancer patients. (*a*) Cyclin E and PKCι levels in 18 high-grade and Stage III or IV serous ovarian epithelial tumors were analyzed by Western blotting. EL-1 represents full-length Cyclin E, and EL-2–6 represent LWM forms of Cyclin E. Samples 1–10 and 11–18 are from independent gels with two extraneous lanes removed from gel 2. (*b*) Increase in PKCι protein level is associated with a decreased overall survival period in nonserous epithelial ovarian cancer patients. (*c*) Increases in both PKCι and Cyclin E protein levels are associated with a decreased overall survival period in nonserous epithelial ovarian cancer patients. Vertical lines indicate censored patients.

Discussion

We show that, in ovarian cancer patients, high PKCι levels correlate with defects in polarity, increased Cyclin E protein expression, and increased proliferation. aPKC levels must apparently be maintained within critical boundaries for the establishment and maintenance of

epithelial cell polarity, because both increase and loss of aPKC result in defects in apical–basal polarity in *Drosophila* (our data and refs. 32 and 33). Although the tumor suppressors Discs large, Lethal giant larvae, and Scribble regulate apical–basal polarity, cell survival, and cellular proliferation (34, 35), loss of polarity is not sufficient to induce cellular proliferation, at least in part because of altered cell survival (32, 36). In contrast, overexpression of activated aPKC was sufficient to induce cellular proliferation in *Drosophila* epithelial tissues, potentially because of a failure of overexpressed aPKC to induce apoptosis.

Many receptors are located in different compartments and are separated by tight junctions or specifically localized to and activated at junctional complexes (8, 9). Under conditions such as wounding, where polarity and junctional complexes are abrogated, an autocrine interaction between growth factors and receptors contributes to wound healing. In ovarian cancer, the disruption of polarity as a consequence of overexpression and activation of PKCι could result in aberrant autocrine signaling. Furthermore, polarity defects could cause mislocalization of intracellular signal transduction components (37). Thus, a loss of polarity due to overexpression of PKCι could directly lead to increased proliferation contributing to tumorigenesis. Loss of E-cadherin, which plays a pivotal role in epithelial organization and suppresses aberrant proliferation (7, 38), from adherens junctions because of aberrant PKCι activity and subsequent loss of polarity could also contribute to increased proliferation. Indeed, E-cadherin is mislocalized and associated with outcomes in ovarian cancer (39, 40). The tumor suppressor Disabled-2, originally identified in *Drosophila*, mediates basement membrane attachment of ovarian epithelial cells, thus ensuring correct positioning, emphasizing the critical importance of maintenance of polarity (41).

The *Drosophila in vivo* epithelial model system informed subsequent human studies demonstrating an interaction between PKCι and Cyclin E levels and patient outcome. Because overexpression of aPKC is sufficient to increase Cyclin E protein in *Drosophila*, up-regulation of PKCι may play a causal role in Cyclin E deregulation in ovarian cancer. Strikingly, LMW forms of Cyclin E and PKCι were coordinately up-regulated in ovarian cancers. Because the LMW forms of Cyclin E are hyperactive, associated with resistance to p21 and p27 and with genomic instability (10, 42, 43), the interaction between PKCι and LMW Cyclin E may play a role in the initiation and progression of ovarian cancer as well as in patient outcomes. Although increased Cyclin E levels had been shown to be associated with a worsened outcome in ovarian cancers (10, 31), concurrent analysis of Cyclin E and PKCι levels provides a superior predictor of outcome in nonserous ovarian cancers than either alone, indicating an interaction between these two determinants. Cyclin E levels are increased in a number of ovarian cancers without elevated PKCι, suggesting that additional mechanisms must regulate Cyclin E protein levels. Once again, a convergence of studies in *Drosophila* and human ovarian cancer may be informative, because Archipelago, which has been demonstrated to regulate Cyclin E degradation in *Drosophila*, is mutationally inactivated in a fraction of ovarian cancers (44).

PKCι protein levels and the incidence of PKCι mislocalization increase with stage and grade, suggesting that PKCι plays a role in tumor progression. PKCι contributes to tumor aggressiveness, because high PKCι protein levels are associated with reduced survival. Taken together, it appears that PKCι plays a role in the pathophysiology of ovarian cancer contributing to tumor progression and aggressiveness. Thus, PKCι should be explored as a marker of prognosis, in particular aggressiveness of ovarian cancers, and should be evaluated as a potential therapeutic target.

We thank P. Parker (Cancer Research UK, London Research Institute, London) for rPKCζ* and K.-W. Choi (Baylor College of Medicine, Houston) for antibody and discussion. This work was supported by National Cancer Institute Grants P50 CA083639, P30 CA16672 (to G.B.M.), and P01 CA64602 (to G.B.M. and J.W.G.) and in part by the U.S. Department of Energy, Office of Science, Office of Biological and Environmental Research (Contract DE-AC03-76SF00098, to J.W.G.).

1. Jemal, A., Murray, T., Ward, E., Samuels, A., Tiwari, R. C., Ghafoor, A., Feuer, E. J. & Thun, M. J. (2005) *CA Cancer J. Clin.* **55,** 10–30.
2. Suzuki, S., Moore, D. H., 2nd, Ginzinger, D. G., Godfrey, T. E., Barclay, J., Powell, B., Pinkel, D., Zaloudek, C., Lu, K., *et al.* (2000) *Cancer Res.* **60,** 5382–5385.
3. Pinkel, D., Segraves, R., Sudar, D., Clark, S., Poole, I., Kowbel, D., Collins, C., Kuo, W. L., Chen, C., Zhai, Y., *et al.* (1998) *Nat. Genet.* **20,** 207–211.
4. Macara, I. G. (2004) *Nat. Rev. Mol. Cell. Biol.* **5,** 220–231.
5. Woods, D. F., Hough, C., Peel, D., Callaini, G. & Bryant, P. J. (1996) *J. Cell Biol.* **134,** 1469–1482.
6. Bilder, D., Li, M. & Perrimon, N. (2000) *Science* **289,** 113–116.
7. Thiery, J. P. (2002) *Nat. Rev. Cancer* **2,** 442–454.
8. Balda, M. S., Garrett, M. D. & Matter, K. (2003) *J. Cell Biol.* **160,** 423–432.
9. Vermeer, P. D., Einwalter, L. A., Moninger, T. O., Rokhlina, T., Kern, J. A., Zabner, J. & Welsh, M. J. (2003) *Nature* **422,** 322–326.
10. Bedrosian, I., Lu, K. H., Verschraegen, C. & Keyomarsi, K. (2004) *Oncogene* **23,** 2648–2657.
11. Drier, E. A., Tello, M. K., Cowan, M., Wu, P., Blace, N., Sacktor, T. C. & Yin, J. C. (2002) *Nat. Neurosci.* **5,** 316–324.
12. Schonwasser, D. C., Marais, R. M., Marshall, C. J. & Parker, P. J. (1998) *Mol. Cell. Biol.* **18,** 790–798.
13. Brand, A. H. & Perrimon, N. (1993) *Development (Cambridge, U.K.)* **118,** 401–415.
14. Udan, R. S., Kango-Singh, M., Nolo, R., Tao, C. & Halder, G. (2003) *Nat. Cell Biol.* **5,** 914–920.
15. Kaplan, E. L., Meier, P. (1958) *J. Am. Stat. Assoc.* **53,** 457–481.
16. Cox, D. R. (1972) *J. R. Stat. Soc. Ser. B* **34,** 187–220.
17. Lu, K. H., Patterson, A. P., Wang, L., Marquez, R. T., Atkinson, E. N., Baggerly, K. A., Ramoth, L. R., Rosen, D. G., Liu, J., Hellstrom, I., *et al.* (2004) *Clin. Cancer Res.* **10,** 3291–3300.
18. Su, A. I., Welsh, J. B., Sapinoso, L. M., Kern, S. G., Dimitrov, P., Lapp, H., Schultz, P. G., Powell, S. M., Moskaluk, C. A., Frierson, H. F., Jr., *et al.* (2001) *Cancer Res.* **61,** 7388–7393.
19. Etienne-Manneville, S. & Hall, A. (2003) *Curr. Opin. Cell Biol.* **15,** 67–72.
20. Parker, P. J. & Murray-Rust, J. (2004) *J. Cell Sci.* **117,** 131–132.
21. Johnson, K. & Wodarz, A. (2003) *Nat. Cell Biol.* **5,** 12–14.
22. Bhat, M. A., Izaddoost, S., Lu, Y., Cho, K. O., Choi, K. W. & Bellen, H. J. (1999) *Cell* **96,** 833–845.
23. Pielage, J., Stork, T., Bunse, I. & Klambt, C. (2003) *Dev. Cell* **5,** 841–851.
24. Wolf, T. & Ready, D. F. (1993) in *The Development of Drosophila melanogaster,* eds. Bate, M, A. & Arias, A. M. (Cold Spring Harbor Lab. Press, Plainview, NY), pp. 1277–1326.
25. Antic, D. & Keene, J. D. (1997) *Am. J. Hum. Genet.* **61,** 273–278.
26. Richardson, H., O'Keefe, L. V., Marty, T. & Saint, R. (1995) *Development (Cambridge, U.K.)* **121,** 3371–3379.
27. Nelson, W. J., Shore, E. M., Wang, A. Z. & Hammerton, R. W. (1990) *J. Cell Biol.* **110,** 349–357.
28. Lancaster, J. M., Dressman, H. K., Whitaker, R. S., Havrilesky, L., Gray, J., Marks, J. R., Nevins, J. R. & Berchuck, A. (2004) *J. Soc. Gynecol. Invest.* **11,** 51–59.
29. Schwartz, D. R., Kardia, S. L., Shedden, K. A., Kuick, R., Michailidis, G., Taylor, J. M., Misek, D. E., Wu, R., Zhai, Y., Darrah, D. M., *et al.* (2002) *Cancer Res.* **62,** 4722–4729.
30. Weichert, W., Gekeler, V., Denkert, C., Dietel, M. & Hauptmann, S. (2003) *Int. J. Oncol.* **23,** 633–639.
31. Farley, J., Smith, L. M., Darcy, K. M., Sobel, E., O'Connor, D., Henderson, B., Morrison, L. E. & Birrer, M. J. (2003) *Cancer Res.* **63,** 1235–1241.
32. Rolls, M. M., Albertson, R., Shih, H. P., Lee, C. Y. & Doe, C. Q. (2003) *J. Cell Biol.* **163,** 1089–1098.
33. Sotillos, S., Diaz-Meco, M. T., Caminero, E., Moscat, J. & Campuzano, S. (2004) *J. Cell Biol.* **166,** 549–557.
34. Bilder, D. (2004) *Genes Dev.* **18,** 1909–1925.
35. Humbert, P., Russell, S. & Richardson, H. (2003) *BioEssays* **25,** 542–553.
36. Pagliarini, R. A. & Xu, T. (2003) *Science* **302,** 1227–1231.
37. Hoeller, D., Volarevic, S. & Dikic, I. (2005) *Curr. Opin. Cell Biol.* **17,** 107–111.
38. Tinkle, C. L., Lechler, T., Pasolli, H. A. & Fuchs, E. (2004) *Proc. Natl. Acad. Sci. USA* **101,** 552–557.
39. Marques, F. R., Fonsechi-Carvasan, G. A., De Angelo Andrade, L. A. & Bottcher-Luiz, F. (2004) *Gynecol. Oncol.* **94,** 16–24.
40. Faleiro-Rodrigues, C., Macedo-Pinto, I., Pereira, D. & Lopes, C. S. (2004) *Ann. Oncol.* **15,** 1535–1542.
41. Sheng, Z., Sun, W., Smith, E., Cohen, C. & Xu, X. X. (2000) *Oncogene* **19,** 4847–4854.
42. Wingate, H., Zhang, N., McGarhen, M. J., Bedrosian, I., Harper, J. W. & Keyomarsi, K. (2005) *J. Biol. Chem.* **280,** 15148–15157.
43. Akli, S., Zheng, P. J., Multani, A. S., Wingate, H. F., Pathak, S., Zhang, N., Tucker, S. L., Chang, S. & Keyomarsi, K. (2004) *Cancer Res.* **64,** 3198–3208.
44. Moberg, K. H., Bell, D. W., Wahrer, D. C., Haber, D. A. & Hariharan, I. K. (2001) *Nature* **413,** 311–316.
45. Moses, K. & Rubin, G. M. (1991) *Genes Dev.* **5,** 583–593.

Exhibit D

Amplification of MDS1/EVI1 and EVI1, Located in the 3q26.2 Amplicon, Is Associated with Favorable Patient Prognosis in Ovarian Cancer

Meera Nanjundan,[1] Yasuhisa Nakayama,[1] Kwai Wa Cheng,[1] John Lahad,[1] Jinsong Liu,[2] Karen Lu,[3] Wen-Lin Kuo,[4] Karen Smith-McCune,[5] David Fishman,[6] Joe W. Gray,[4] and Gordon B. Mills[1]

Departments of [1]Molecular Therapeutics, [2]Pathology, and [3]Gynecologic Oncology, M. D. Anderson Cancer Center, University of Texas, Houston, Texas; [4]Department of Laboratory Medicine, University of California, San Francisco, and the Lawrence Berkeley National Laboratory, Berkeley, California; [5]Department of Obstetrics, Gynecology, and Reproductive Sciences, University of California, San Francisco, California; and [6]New York University, New York, New York

Abstract

Increased copy number involving chromosome 3q26 is a frequent and early event in cancers of the ovary, lung, head and neck, cervix, and BRCA1 positive and basal breast cancers. The p110α catalytic subunit of phosphoinositide-3-kinase (PI3KCA) and protein kinase Cι (PKCι) have previously been shown as functionally deregulated by 3q copy number increase. High-resolution array comparative genomic hybridization of 235 high-grade serous epithelial ovarian cancers using contiguous bacterial artificial chromosomes across 3q26 delineated an ~2 Mb–wide region at 3q26.2 encompassing PDCD10 to MYNN (chr3:168722613-170908630). Ecotropic viral integration site-1 (EVI1) and myelodysplastic syndrome 1 (MDS1) are located at the center of this region, and their DNA copy number increases are associated with at least 5-fold increased RNA transcript levels in 83% and 98% of advanced ovarian cancers, respectively. Moreover, MDS1/EVI1 and EVI1 protein levels are increased in ovarian cancers and cancer cell lines. EVI1 and MDS1/EVI1 gene products increased cell proliferation, migration, and decreased transforming growth factor-β–mediated plasminogen activator inhibitor-1 promoter activity in ovarian epithelial cells. Intriguingly, the increases in EVI1 DNA copy number and MDS1/EVI1 transcripts are associated with improved patient outcomes, whereas EVI1 transcript levels are associated with a poor patient survival. Thus, the favorable patient prognosis associated with increased DNA copy number seems to be as a result of high-level expression of the fusion transcript MDS1/EVI1. Collectively, these studies suggest that MDS1/EVI1 and EVI1, previously implicated in acute myelogenous leukemia, contribute to the pathophysiology of epithelial ovarian cancer. [Cancer Res 2007;67(7):3074–84]

Introduction

In the United States in 2006, the American Cancer Society predicts that 20,180 women will develop ovarian cancer, and 15,310 will die of their disease. Ovarian cancer has proven to be a powerful model for the identification and characterization of aberrant genes contributing to the pathophysiology of ovarian cancer as well as multiple other cancer lineages. Thus, identification and characterization of genomic aberrations and of their drivers will increase our understanding of the initiation and progression of cancer as well as provide molecular markers that could improve early cancer detection, determining prognosis, and predicting response to therapy. Increased copy number involving chromosome 3q26 is a frequent and early event in a number of epithelial cancers, including squamous cell carcinomas (SCC) of the cervix (1), esophagus (2, 3), lung (1), head and neck (4), prostate cancer (5, 6), breast cancer (basal and BRCA1-associated; refs. 7, 8), and nasopharyngeal cancer (9), as well as in chronic myelogenous leukemia (10). The 3q amplification domain has been variously identified as 3q26 ~ 27, q25 ~ 26, and q26 ~ qter by various low-resolution methods with the minimum region of overlap identified spanning nearly 20 Mb, making it challenging to search for possible target genes.

A number of potential targets in the 3q26 amplicon have been identified in epithelial cancers through these low-resolution approaches, including PIK3CA [catalytic subunit of phosphoinositide-3-kinase (PI3K); ref. 11], protein kinase Cι (PKCι; refs. 12–14), eukaryotic initiation factor (15), ZASC1 (a novel Kruppel-like zinc finger protein; ref. 2), SnoN (3), SCC–related oncogene (16), and TERC (RNA component of human telomerase; ref. 17). These studies suggest that 3q26 may contain one or more putative oncogenes, which play important roles in the development or the progression of various solid tumors.

In ovarian cancers, the p110α catalytic subunit of PIK3CA (11) and PKCι (12) are functionally deregulated by 3q copy number increase. However, the 3q26 region contains other candidates, including ecotropic viral integration site-1 (EVI1). A recent report indicates that EVI1 is amplified at 3q26, resulting in increased RNA levels that may contribute to aberrant transforming growth factor-β (TGFβ) signaling in ovarian cancer (18). EVI1 has been implicated in acute myelogenous leukemia (AML) and myelodysplastic syndrome (MDS), where it is frequently activated due to intra- and interchromosome rearrangements. EVI1 has been implicated in proliferation of leukemic cells, transformation of Rat1 fibroblasts, inhibition of growth factor-mediated differentiation and survival, induction of neural and megakaryocyte differentiation, and inhibition of TGFβ signaling (19). EVI1 also

---

Note: Supplementary data for this article are available at Cancer Research Online (http://cancerres.aacrjournals.org/).

M. Nanjundan and Y. Nakayama contributed equally to this manuscript.

The M. D. Anderson Cancer Center, Department of Molecular Therapeutics, University of Texas and the Department of Laboratory Medicine, University of California San Francisco and the Lawrence Berkeley National Laboratory, Berkeley, California are equal contributors.

Current address for Y. Nakayama: Department of Pharmacology, Kansai Medical University, 10-15 Fumizono-cho, Moriguchi City, Osaka 570-8506, Japan.

Requests for reprints: Meera Nanjundan, M. D. Anderson Cancer Center, Department of Molecular Therapeutics, University of Texas, 1515 Holcombe Boulevard, Box 0950, Houston, TX 77054. Phone: 713-563-4225; Fax: 713-563-4235; E-mail: mnanjund@mdanderson.org.

doi:10.1158/0008-5472.CAN-06-2366

(*a*) blocks mothers against DPP homolog (SMAD)–induced gene transcription through binding to SMAD3, (*b*) enhances activator protein 1 activity, (*c*) blocks c-jun-NH_2-kinase and stress-induced apoptosis, (*d*) blocks the action of IFN by blocking promyelocytic leukemia (PML) function, and (*e*) binds the brahma-related tumor suppressor, BRG1 (19), and more recently, is implicated in signaling through the PI3K/AKT pathway (20). We now use a high-resolution array comparative genomic hybridization (CGH) bacterial artificial chromosome (BAC) contig to show that EVI1 is located at the most frequent point of genomic amplification at 3q26.2 in 235 advanced serous epithelial ovarian cancers. Specifically, we show that DNA copy number increase is associated with marked accumulation of MDS1/EVI1 (PRDM3) intergenic read-through transcripts and MDS1 and EVI1 transcripts. MDS1/EVI1 and EVI1 functionally dysregulate cellular proliferation, gene transcription, and cellular motility. Intriguingly, the increases in DNA copy number and MDS1/EVI1 transcripts are associated with improved patient outcomes, whereas EVI1 is associated with a worsened outcome. These studies show that MDS1/EVI1 and EVI1, previously implicated in AML, contribute to the pathophysiology of epithelial ovarian cancers.

Materials and Methods

Preparation of patient samples. Stages I to IV serous epithelial ovarian cancers were from the Ovarian Cancer Tumor Bank of the M.D. Anderson Cancer Center. Benign ovarian cysts and stages III and IV serous epithelial ovarian cancers were from the Basic Biology of Ovarian Cancer Program Project Grant Bank at the University of California, San Francisco. Benign ovarian cysts were macrodissected to increase the amount of epithelium present. Early-stage and late-stage ovarian cancers were macrodissected to contain >70% tumor. Normal ovarian epithelial scrapings were from the Northwestern University. Normal scrapings were collected using a cytobrush, and cells immediately suspended and frozen in RLT buffer (Qiagen, Valencia, CA). DNA was extracted as previously described (21). Total RNA was extracted from ovarian cancers and normal ovarian epithelial scrapings using the RNeasy Kit (Qiagen, Valencia, CA) according to the manufacturer's protocol. Institutional Review Board approval was obtained at each institution before the initiation of this study.

Comparative genomic hybridization and analysis. CGH was done with a 3q BAC contig as previously described (21). Only BACs with signals in 90% or greater of tumors are included. In the CGH data set presented in Fig. 1*A*, there were five BACs containing EVI1. The EVI1 signal is represented as the average copy number change across the five BACs. The values are depicted using a $\log_2$-based color scale (as indicated), such that the red reflects increased copy number and blue reflects decreased copy number. Light green indicates a null data point either as a result of poor hybridization and quality control or as a result of a probe not being analyzed for that sample.

***In vitro* methylation assay.** MDS1/EVI1-HA, EVI1-HA, and AKT-HA (used as negative control) were transiently expressed in COS7 cells and immunoprecipitated using HA antibody. Sepharose G-beads containing immunoprecipitates and GST-PRMT1 (used as positive control; kind gift of Dr. Mark Bedford, M.D. Anderson Cancer Center) were incubated with 2 μCi of 1 mCi/mL ^{3}H-*S*-adenosyl-L-methyl-^{3}H-methionine, 10 μg histones in Tris-HCl buffer for 2 h at 37°C. The reactions were terminated by adding SDS sample buffer and boiled. Samples were run on a 15% SDS-PAGE gel, which was stained with Gelcode Blue (Pierce, Rockford, IL), destained, soaked in Enhance (Perkin-Elmer, Waltham, MA), washed, vacuum dried, and then exposed to film overnight at −80°C.

Quantitative PCR analysis. Quantitative PCR was done using RNA isolated from normal, benign, early-stage (I and II), and advanced-stage (III and IV) patient ovarian samples using a one-step reverse transcription-PCR TaqMan master mix kit (Applied Biosystems, Foster City, CA) with the following primers and probes sets:

EVI1 exon III (detects both EVI1 and MDS1/EVI1): forward primer, CGAAGACTATCCCCATGAAACTATG; reverse primer, TCACAGTCTTCGCAGCGATATT; probe sequence: TCCACGAAGACGGA.

EVI1 exon I: (detects only EVI1) forward primer, TTGCCAAGTAACAGCTTTGCTG; reverse primer, CCAAAGGGTCCGAATGTGACTT; probe sequence: TCGCGAAGCAGCACAC.

MDS1/EVI1: forward primer, TCAAACCTGAAAGACCCCAGTTA; reverse primer, GCATCTATGCAGAACTTCACATTGT; probe sequence: TGGATGGGAGATCTT.

MDS1: forward primer, AACCTGAAAGACCCCAGTTATGG; reverse primer, CGCTTACCCTCCGAGACCTT; probe sequence: ATGGGAGGTACATCTT.

The MDS1 qPCR probe recognizes a domain that is not included in the MDS1/EVI1 fusion gene (see Fig. 1*B* for details). However, the EVI1 exon III qPCR probe recognizes both EVI1 and MDS1/EVI1 (designated as "EVI1 + MDS1/EVI1"). The MDS1/EVI1 qPCR probe recognizes the mRNA fusion site and is specific to MDS1/EVI1. The EVI1 exon I qPCR probe is designed to specifically recognize EVI1 and not the fusion transcript, MDS1/EVI1 (designated as "EVI1"). Primers/probes for all of the remaining genes in the EVI1 region were based on corresponding Genebank sequences (Applied Biosystems, Assays by Design). Using the correlative method, RNA-fold increase in expression was calculated as Ct of gene − Ct of β-actin to generate ΔCt from which ΔCt of the normal sample was subtracted. These values were then converted to $\log_2$ values.

Plasmid constructs. EVI1 and MDS1/EVI1-HA fusion constructs were provided kindly by Rotraud Wieser (KIMCL, Abteilung fuer Humangenetik, Medizinische Universitaet Wien, Wien, Austria; ref. 22). EVI1 was kindly provided by Dr. Hisamaru Hirai (23) and Dr. Mineo Kurokawa (Department of Hematology and Oncology, Graduate School of Medicine, University of Tokyo, Tokyo, Japan; ref. 23).

SDS-PAGE and Western blot analysis. Proteins were resolved on an 8% SDS-PAGE gel and electrophoretically transferred to polyvinylidene difluoride membranes. After blocking with 5% (w/v) milk, membranes were incubated overnight at 4°C with primary antibody and 1 h with appropriate horseradish peroxidase-conjugated secondary antibodies. Blots were developed using chemiluminescence substrates (GE Healthcare, Piscataway, NJ). Polyclonal EVI1 antibody was obtained from Dr. Hisamaru Hirai recognizing amino acid 1 to 263 (24) and from Dr. James Ihle (Department of Biochemistry, St. Jude Children's Research Hospital, Memphis, TN; ref. 25).

Proliferation and cellular migration assays. IOSE80 and IOSE29 htert immortalized ovarian cells (T80/T29) were transfected with EVI1 and MDS1/EVI1 by Nucleofector method using T solution (Amaxa, Gaithersburg, MD). The transfection efficiency was ~60% to 80% assessed by enhanced green fluorescent protein (EGFP) fluorescence. After 12 h, cells were counted, and 5,000 cells were plated in 96-well plates maintained in 0% or 10% fetal bovine serum (FBS). At various days, cells were fixed and stained with crystal violet solution, dissolved in Sorenson's buffer, and absorbance was measured at 570 nm. Twenty-four hours after transient transfection, cells were harvested, counted, and seeded into Boyden chamber inserts (BD Biosciences, San Jose, CA) in serum-free media. FBS in the lower chamber media was used as a chemoattractant. The cells that migrated onto the lower membrane were stained with crystal violet and counted.

Statistical analysis. Experimental results were statistically evaluated using Student's *t* test. Differences were considered significant if $P < 0.05$. Patients with no further follow-up information are represented by a vertical tick at last point contact and are weighed in the Kaplan-Meier analysis.

Results

Delineation of the 3q26.2 amplicon in ovarian cancer. Increased copy number involving chromosome 3q26.2 is a frequent and early event in ovarian cancer development and is found in a subset of other epithelial cancers. The driver(s) of the regional DNA copy number increase on chromosome 3q and in particular at 3q26

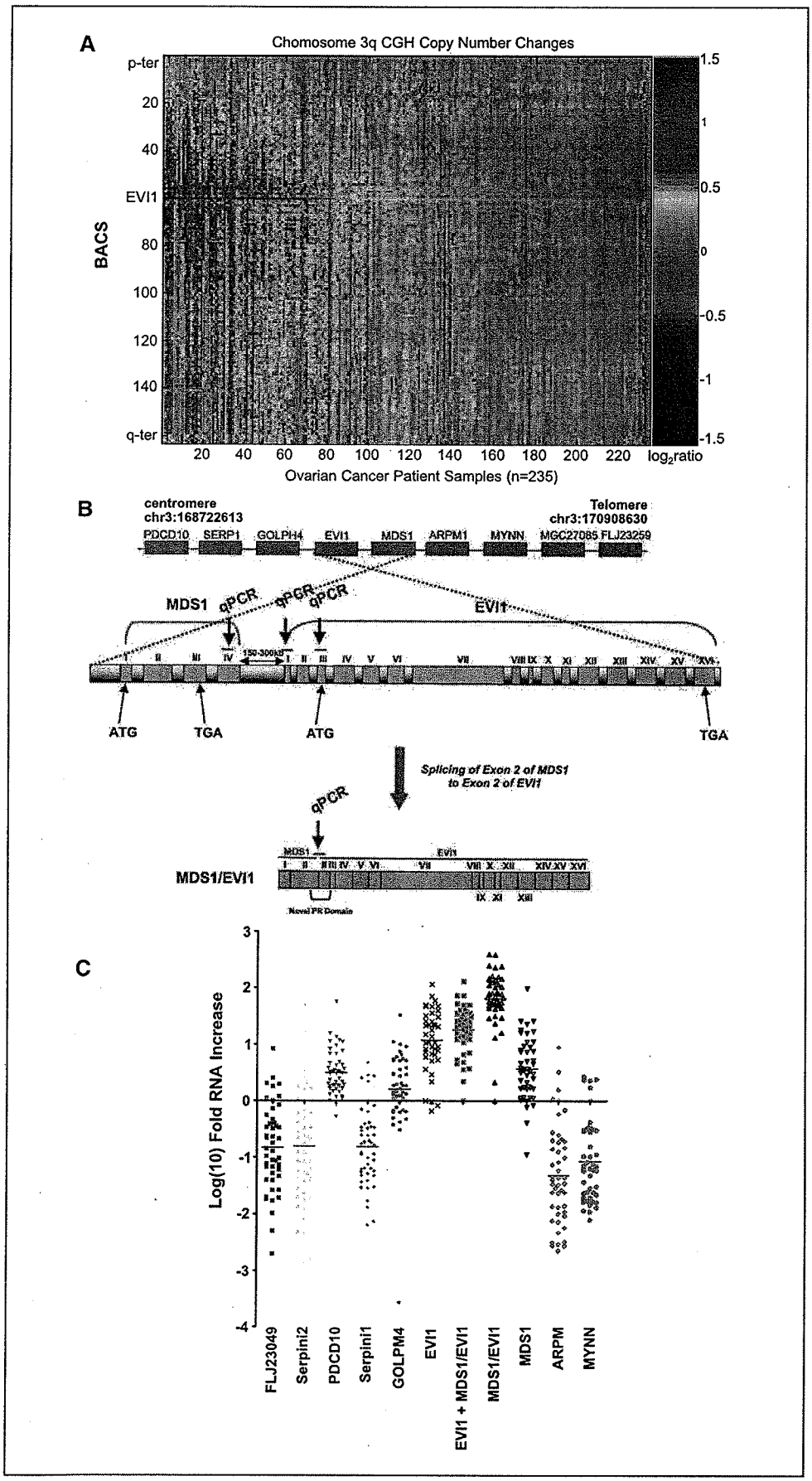

Figure 1. EVI1 genomic copy number increase is associated with a selective accumulation of EVI1 and MDS1/EVI1 transcripts. *A*, CGH analysis for 235 ovarian tumors using a contig encompassing 163 BACs probes on 3q is shown as a scaled image map. The signal for the EVI1 BAC is the maximum signal intensity across the group of BACs for EVI1 region. The patient samples are ordered with respect to decreasing EVI1 copy number alterations from left to right. The BACs on chromosome 3q are ordered by position along the chromosome. Parametric and nonparametric correlation analyses were done to delineate the region of highest correlation on 3q. Data vectors for each BAC on chromosome 3q were created, and correlation coefficients were determined for each BAC compared with every other BAC on the chromosome. The region on 3q from PDCD10 to MYNN (Chr3:168722613-170908630) was the most frequently altered area on 3q when compared with the frequency of change for other regions. In addition, BACs within this region exhibited the most statistically significant direct correlation with other BACs in the region. *B*, genomic organization surrounding MDS1 and EVI1. Open reading frames within the minimally aberrant region on 3q are organized from centromere to telomere. MDS1 and EVI1 as well as the MDS1/EVI1 intergenic read-through are shown in detail. The MDS1/EVI1 intergenic transcript contains exon I and exon II of the MDS1 coding sequence, followed by the untranslated region of EVI1 (exon II), respectively, giving rise to a novel PR domain and the complete open reading frame of EVI1. The location of the qPCR primers for MDS1 (exon IV), MDS1/EVI1 (PR domain), and EVI1 (two independent probe sets: one against exon I and the other against exon III) are indicated. *C*, RNA expression levels of genes surrounding EVI1 along chromosome 3q, from PDCD10 to MYNN, were assessed by quantitative PCR (qPCR) analysis in ovarian tissue samples. The results are displayed as $\log_{10}$-fold RNA alterations for NOE and advanced tumors (stages III and IV), compared with the average of the normal epithelium. The EVI1 exon I probe is specific for EVI1 alone (specifically EVI1d), the EVI1 exon III probe recognizes both EVI1 and MDS1/EVI1 levels (denoted as EVI1 + MDS1/EVI1), whereas the MDS1/EVI1 probe is specific to the fusion gene. *PDCD10*, programmed cell death 10; *Serpini1*, a serine/cysteine proteinase inhibitor, *GOLPH4*, Golgi phosphoprotein 4, *ARPM1*, an actin-related protein, and *MYNN*, myoneurin zinc finger protein.

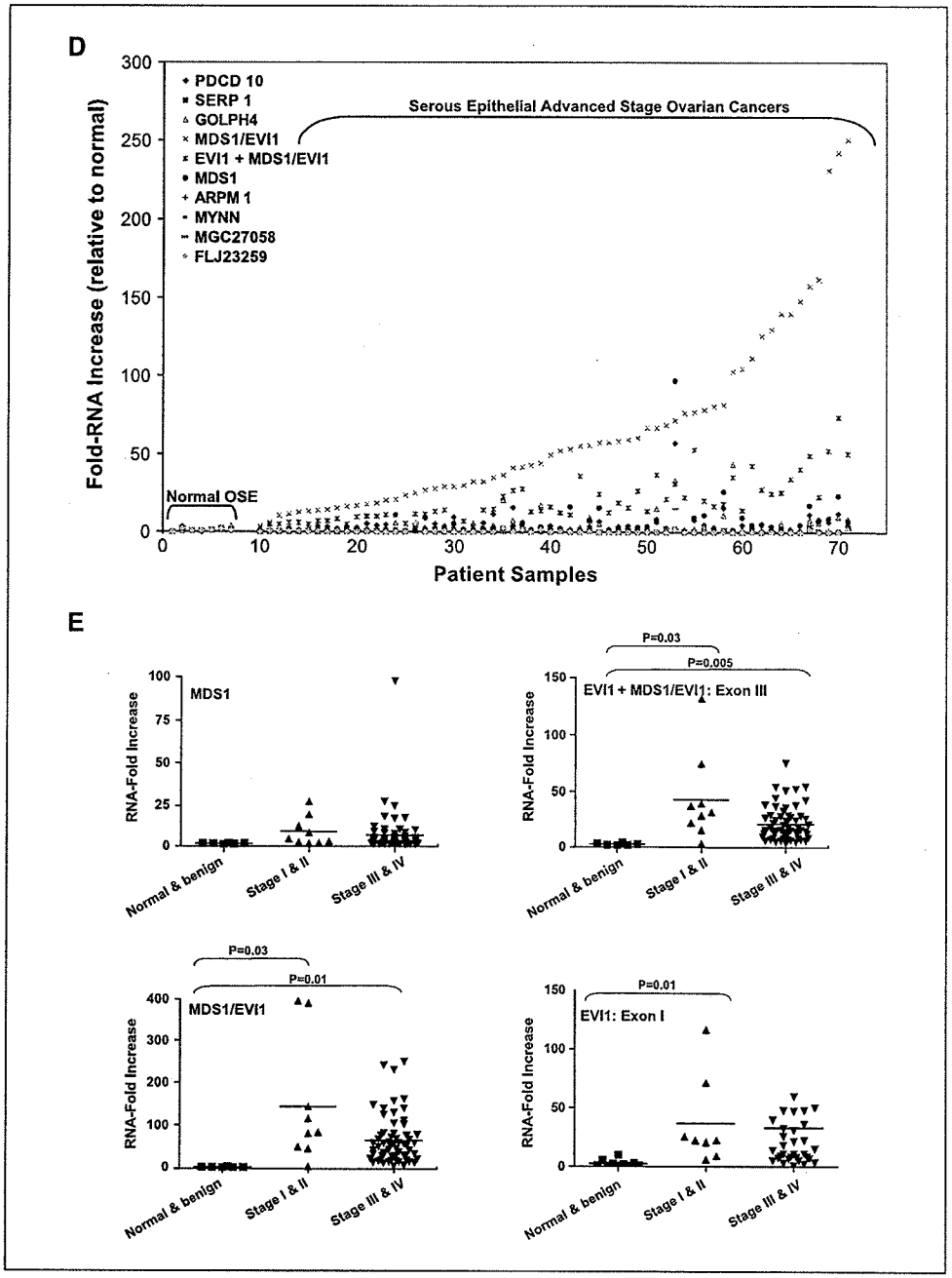

Figure 1 *Continued. D,* the results from (*C*) are displayed as fold RNA for normal OSE and serous epithelial advanced stage ovarian cancers. EVI1 in this graph is shown using exon III probe (*EVI1 + MDS1/EVI1*). *E,* RNA expression levels of total EVI1 and MDS1/EVI1 (exon III qPCR probes), EVI1 (exon I qPCR probes), MDS1/EVI1, and MDS1 were assessed by quantitative PCR analysis in ovarian tissue samples by stage as fold alterations in RNA expression compared with that of normal epithelium. Normal and benign cystadenomas, stages I and II, as well as stages III and IV, were grouped together to increase sample size. Both stage I/II and stage III/IV were significantly increased from normal/benign.

in epithelial cancers remain to be fully characterized. PI3K (11) and PKCι (12, 13) both have been reported to be elevated at the mRNA and protein levels in association with the 3q copy number increase in ovarian cancer. However, the region of copy number increase defined in earlier low-resolution CGH studies extended over much of 3q, suggesting that additional genes likely contribute to the selection of the amplicon.

Thus, to better define aberration structure within the 3q26 region, we applied high-resolution array CGH to 235 high-grade serous epithelial ovarian cancers using a contig encompassing 163 contiguous BACs across 3q (Fig. 1*A*). The levels of amplification and deletion varied dramatically between different patients, but several occurred frequently, suggesting that they contribute to the pathophysiology of ovarian cancer. The complex pattern of changes suggests that multiple different drivers exist for the 3q26 amplicon. We more clearly defined and narrowed the most frequent region of copy number increase in ovarian cancers to an ~2 Mb-wide region at 3q26.2 encompassing FLJ23049 to MYNN (chr3:168722613-170908630; Fig. 1*A*) that is aberrant in >70% of all serous epithelial ovarian cancers. As noted in Fig. 1*A*, aberrations involving other regions of 3q26 also were observed, including those present in tumors lacking the increase at 3q26.2 but at lower frequency than the aberration encompassing FLJ23049 to MYNN. MDS1 and EVI1 are located at the center of the chr3:168722613-170908630 region representing the most aberrant loci in the region. Three additional ovarian CGH data sets of 50, 72, and 86 patient samples confirmed that this region and specifically MDS1 and EVI1 showed selective amplification in ~70% of patients (data not

presented). In support, previous reports have indicated increased EVI1 DNA or RNA levels in ovarian cancer (18, 26).

To identify mutations within EVI1, we sequenced EVI1 from genomic DNA across its 16 exons in 48 ovarian cancer patients. Out of 48 patients, 2 patients had a nonsynonymous mutation in exon 14 of EVI1. In addition, a common synonymous mutation in exon 13 was observed in ~25% of the patients, which is a previously documented single nucleotide polymorphism. Thus, the frequency of mutations/sequence changes is <4%, with no obvious functional effect expected arising from the mutations in exon 14.

Increased EVI1 copy number is associated with elevated EVI1 and MDS1/EVI1 transcripts in ovarian cancers. To assess whether the observed DNA copy number increase in EVI1 corresponds to increased transcript levels, quantitative PCR (qPCR) analysis of nine genes encoded in chr3:168722613-170908630 in the 3q26.2 amplicon was done (see Fig. 1*B* for genomic organization of this region). In addition, we assessed the transcript expression level of the MDS1/EVI1 intergenic fusion transcript (see Fig. 1*B* for details). We designed several qPCR probes to assess the level of EVI1, MDS1, and the fusion transcript MDS1/EVI1. As shown in Fig. 1*B*, the EVI1 exon I probe specifically recognizes only EVI1, the MDS1 qPCR probe (against exon IV of MDS1) is specific for MDS1, EVI1 exon III recognizes EVI1 as well as MDS1/EVI1 (designated as EVI1 + MDS1/EVI1), whereas the MDS1/EVI1 probe is specific to the intergenic novel domain in the fusion transcript, MDS1/EVI1.

To determine whether the 3q26.2-amplified gene transcript levels were elevated in advanced-stage ovarian cancers relative to ovarian surface epithelium, we assessed their expression in 61 advanced-stage serous epithelial ovarian cancers (>70% tumor) and 7 normal ovarian epithelium (NOE) obtained by scraping epithelial cells directly into RNA later. Thus, comparing NOE to ovarian cancers, we observed a centromeric regional increase resulting in selective accumulation of EVI1, EVI1 + MDS1/EVI1, and MDS1/EVI1 intergenic fusion transcripts (Fig. 1*C*, presented as $\log_{10}$-fold RNA increases). Specifically, transcript levels of other genes assessed did not differ significantly between NOE and advanced-stage ovarian cancers other than a modest increase in MDS1, PDCD10, and GOLPH4. Thus, EVI1 and MDS1/EVI1 represent the most highly and frequently amplified transcripts within this region. MDS1/EVI1 and EVI1 exon III (EVI1 + MDS1/EVI1) RNA levels are increased up to 540- and 125-fold in the majority (98% and 83%) of ovarian cancers, respectively (Fig. 1*D*, presented as RNA-fold increases) relative to NOE. In addition, transcriptional profiling using probes that do not distinguish between EVI1 and MDS1/EVI1 in two independent data sets of 69 and 30 samples also indicated that total EVI1 and MDS1/EVI1 were the most frequently and markedly amplified transcripts in the 3q26.2 region (not presented). Furthermore, previous studies have indicated elevated RNA levels for EVI1 using approaches that would not distinguish between EVI1 and MDS1/EVI1 in ovarian cancer (18, 26).

To determine whether EVI1 mRNA was selectively elevated in ovarian cancer, we used probes to exon I (see Materials and Methods), which distinguishes between EVI1 and the fusion transcript MDS1/EVI1 (27) to assess EVI1d transcript levels (Fig. 1*C*). We found that the relative fold increases of the EVI1 exon I probe were similar to the EVI1 exon III probe. Thus, both EVI1 and MDS1/EVI1 transcripts are highly elevated in ovarian cancers.

RNA expression levels of EVI1 and MDS1/EVI1 were further assessed by qPCR analysis in ovarian tissue samples by stage. RNA levels for MDS1, EVI1, and MDS1/EVI1 were elevated compared with normal and benign cystadenomas in both early (stages I and II) and late stages of ovarian cancer (stages III and IV; Fig. 1*E*). Benign cystadenomas were macrodissected to enrich for epithelial cells; however, contamination with stromal cells is still present accounting for the majority of cells. Nonetheless, the comparison to cysts supplements the data from purified ovarian epithelial cells, indicating that EVI1 and MDS1/EVI1 levels are increased in ovarian cancers.

The increases in RNA levels for EVI1 and MDS1/EVI1 were much greater than the increases in DNA copy number in both magnitude and frequency (compare $\log_2$ scale in Fig. 1*A* to $\log_{10}$ scale in Fig. 1*C*). Thus, there exist additional alterations other than increased DNA copy number that may lead to the observed increased RNA expression levels, including rearrangements/mutations involving regulatory regions or epigenetic alterations. Nonetheless, the overall patterns of gene amplification and elevated gene expression are concordant where highly amplified genes are highly expressed. EVI1 and the MDS1/EVI1 "read-through" transcript seem to be major drivers of the 3q26.2 aberration and, thus, may play important roles in the initiation and/or progression of ovarian cancers. The MDS1/EVI1 fusion mRNA is selectively elevated in serous epithelial ovarian cancers, indicating that the MDS1/EVI1 fusion may play a novel role in ovarian cancer pathogenesis.

Increased EVI1 transcripts are associated with elevated EVI1 and MDS1/EVI1 protein in ovarian cancer cell lines and advanced cancers. To assess whether increased EVI1 and MDS1/EVI1 transcript levels result in an increase in protein, Western blot analysis was done across a series of ovarian cell lines and advanced-stage ovarian cancers. CGH profiles of SKOV3 and OVCAR8 cells are shown in Fig. 2*A*, where EVI1 is amplified at the 3q26.2 locus in SKOV3 cells and homozygously deleted in OVCAR8 cells, providing positive and negative controls. Western blot analysis was done in SV40/htert immortalized ovarian surface epithelial cells (T80), SKOV3, and OVCAR8 cell lines using a polyclonal antibody (from Dr. Hirai; ref. 23), recognizing both EVI1 and MDS1/EVI1 forms. EVI1 and MDS1/EVI1 protein were present at low levels in T80, markedly elevated in SKOV3, and absent in OVCAR8, which closely parallel transcript levels in cell lines (Fig. 2*B*).

Using an EVI1 polyclonal antibody (from Dr. J. Ihle; ref. 25), recognizing both EVI1 and MDS1/EVI1, we assessed protein expression level of EVI1 and MDS1/EVI1 in SKOV3, OVCA429, HEY, DOV13, OVCAR8, and T80 cells. Western blot analysis shows high-level EVI1 expression in SKOV3 cells, its absence in OVCAR8, and low expression in T80 cells. MDS1/EVI1 and EVI1 protein levels were found to closely parallel transcript levels and DNA copy number in a number of ovarian cancer cell lines as shown in the corresponding qPCR analysis with DNA copy number (by fluorescence *in situ* hybridization analysis; Fig. 2*C*).

In advanced ovarian patient samples, using the antibody from Hirai (23), densitometric analysis of EVI1 and MDS1/EVI1 levels in advanced-stage ovarian cancer patients showed that MDS1/EVI1 and EVI1 protein were increased relative to T80 (Fig. 2*D*). MDS1/EVI1 protein levels seem increased relative to wild-type EVI1 in these ovarian cancers, with most cancers expressing low to undetectable levels of wild-type EVI1. In these patient samples, EVI1 transcripts and protein correlated with MDS1/EVI1 transcripts ($P = 0.0001$) and protein ($P = 0.0031$) in contrast to MDS1 where there was no correlation (not presented). However, transcript levels did not correlate with protein levels for either EVI1 and MDS1/EVI1, suggesting that additional mechanisms exist accounting for the high levels of these proteins, including rearrangements, effects of enhancers and promoters, fusion products, mRNA, and

protein stability. Thus, the protein expression profiles support EVI1 and/or MDS1/EVI1 as contributing to the effect of the recurrent regional DNA copy number increase on chromosome 3q26.2 in the pathophysiology of ovarian cancer.

Short-term EVI1 overexpression promotes ovarian cell proliferation, migration, and represses TGFβ-mediated PAI-1 transcriptional regulation in ovarian cells. Because MDS1/EVI1 and EVI1 transcripts seemed to be the most abundant transcripts in advanced-stage ovarian cancers in the 3q26.2 amplicon, we next investigated whether certain components of the epithelial-mesenchymal transformation (EMT) process (cell proliferation and migration) required during epithelial tumor initiation and progression may be altered as a result of aberrant expression of EVI1 and MDS1/EVI1 in T80 cells. We first assessed the role of EVI1 and MDS1/EVI1 on ovarian cell proliferation by transient transfection by Nucleofector method into T80 cells. Transfection of HA-tagged EVI1 and MDS1/EVI1 into T80 cells was assessed by Western blot analysis (Fig. 3*A*) as well as nuclear fluorescence (transfection efficiency of ~60–80% based on nuclear EGFP fluorescence; Fig. 3*B*). We observed that wild-type EVI1 and MDS1/EVI1 increased cell proliferation and saturation density of cells grown in the presence (10%) or absence (0%) of FBS (Fig. 3*C*). Moreover, transient expression of EVI1 in the ovarian cancer cell line, OVCAR8 (with >50% transfection efficiency), which contains a deletion at the EVI1 locus, failed to alter growth or cell cycle relative to control transfected cells.

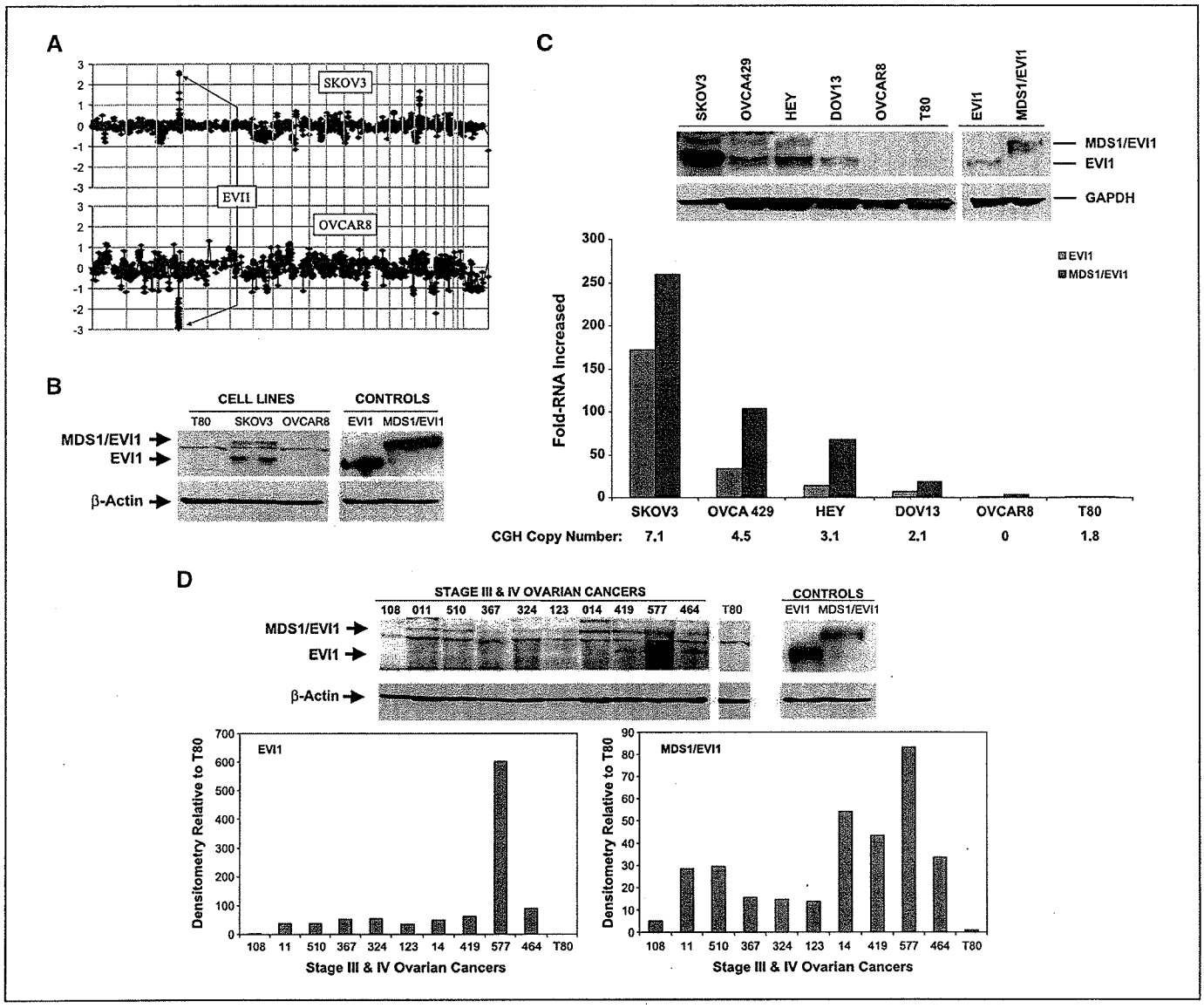

Figure 2. EVI1 genomic copy number increase is associated with a selective accumulation of EVI1 and MDS1/EVI1 protein. *A*, CGH profiles of SKOV3 and OVCAR8 cells are displayed showing EVI1 amplified at the 3q26.2 locus in SKOV3 cells and deleted in OVCAR8 cells. *B*, Western analysis was done in T80, SKOV3, and OVCAR8 cell lines and with EVI1 and MDS1/EVI1 transfected in T80 cells as positive controls (*CONTROLS*) using polyclonal antibody recognizing both EVI1 and MDS1/EVI1. β-Actin was used as loading control. *C*, Western analysis was done in SKOV3, OVCA429, HEY, DOV13, OVCAR8, and T80 cells and with EVI1 and MDS1/EVI1 transfected in T80 cells as positive controls (*CONTROLS*) using an antibody that recognizes both EVI1 and MDS1/EVI1. qPCR for EVI1 and MDS1/EVI1 was done in ovarian cell lines. The results are displayed as fold-RNA expression normalized to T80; CGH copy number for the cell lines is indicated below the lines. Experiments were done in triplicate. *D*, Western analysis of EVI1 was done using the antibody that recognizes both EVI1 and MDS1/EVI1 in advanced ovarian patient samples. T80 cells transfected with EVI1 and MDS1/EVI1 were used as positive controls. Densitometric analysis of EVI1 and MDS1/EVI1 levels in advanced-stage ovarian cancer patients normalized to T80 protein is presented.

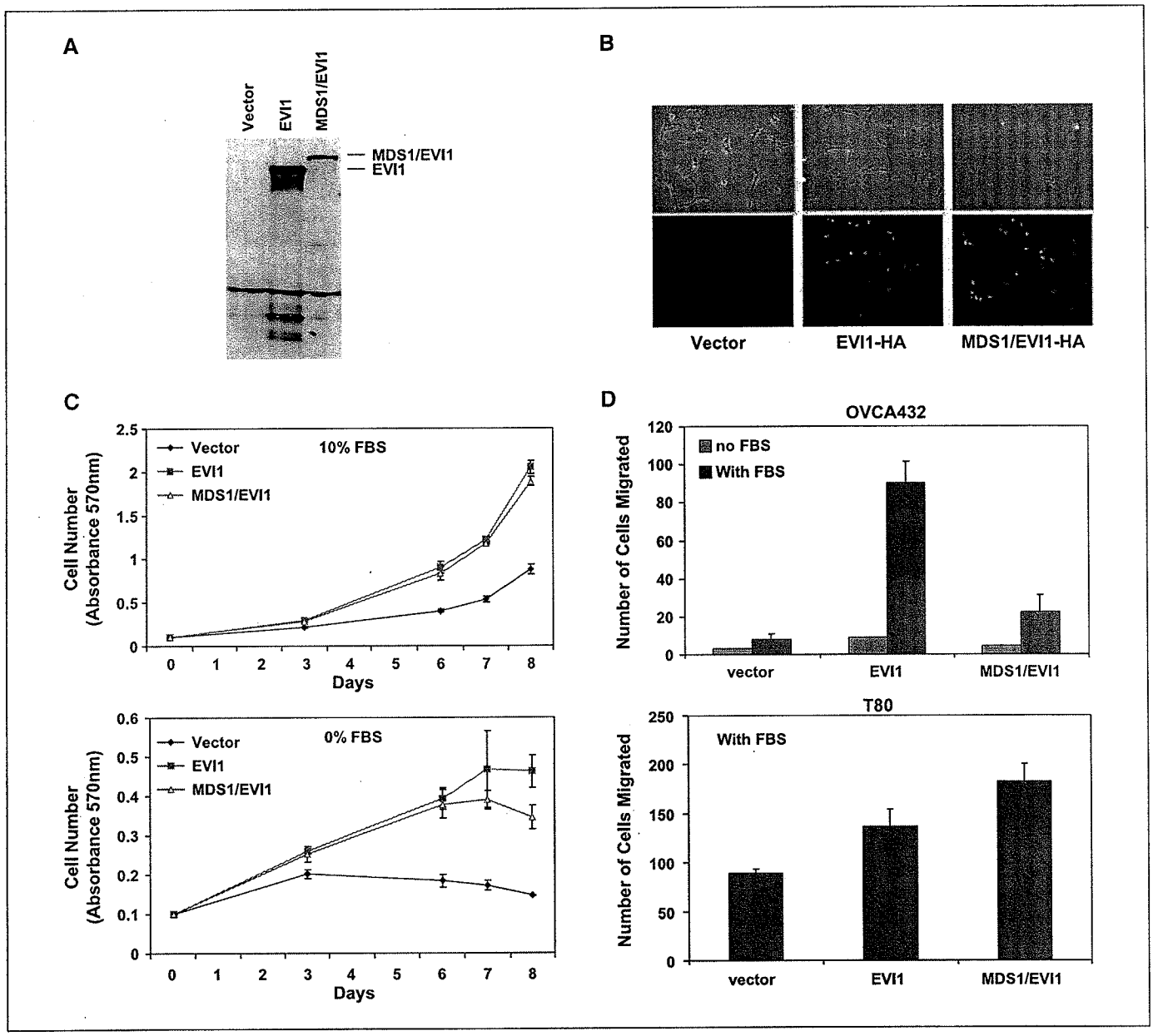

Figure 3. EVI1 and MDS1/EVI1 alter ovarian cell–proliferative and migratory responses. *A*, EVI1 and MDS1/EVI1 were overexpressed in T80 cells. Lysates were harvested, and Western analysis was done using Hirai's polyclonal antibody. *B*, EVI1-HA and MDS1/EVI1-HA were overexpressed in T80 cells and stained for HA to visualize nuclear overexpression. *C*, effect of EVI1 and MDS1/EVI1 on proliferation of T80 cells was done in 10% FBS (*top*) and 0% FBS (*bottom*). The growth assay was done in 96-well plates where cells were plated at 5,000 cells per well and grown in 10% FBS (*top*) and 0% FBS (*bottom*). Cells were stained in crystal violet solution and solubilized with Sorenson's buffer and quantitated at absorbance of 570 nm. Experiments were done in triplicate. *D*, the ability of EVI1 and MDS1/EVI1 to alter cellular migration was assessed in both serum-free and complete serum conditions in OVCA432 cells (*top*) and T80 cells (*bottom*). The cells that migrated onto the lower surface of the membrane were both photographed and counted. Experiments were done in triplicate.

The effects of MDS1/EVI1 and EVI1 on motility have not been previously reported. Thus, to investigate a potential role in cellular migration, we used both T80 (a normal ovarian immortalized cell line) as well as an ovarian cancer cell line (OVCA432 cells). OVCA432 cells had very low basal migration in the presence of FBS, which facilitates the detection of increases in cellular migration upon transfection with EVI1 and MDS1/EVI1. T80 and OVCA432 ovarian cancer cells were transiently transfected with EVI1 and MDS1/EVI1. Cells were plated into Boyden chambers to assess directional migration using 10% FBS as a chemoattractant. Both EVI1 and MDS1/EVI1 promoted ovarian cell migration, identifying a novel process not previously attributed to EVI1 (Fig. 3*D*, *top* and *bottom*). Thus, transient expression of EVI1 and MDS1/EVI1 exerts similar effects on proliferation and cell motility, increasing both coordinately. We also assessed other ovarian cell lines, including immortalized T29 ovarian epithelial cells, which had slightly increased growth with transfected EVI1; however, motility was not dramatically or significantly increased. T29 as compared with T80 have undergone many of the components of EMT being more fibroblastoid, motile, and invasive in matrigel, potentially contributing to the difference in response.

Because EVI1 inhibits TGFβ-mediated signaling (23), we addressed whether EVI1 and MDS1/EVI1 could modulate TGFβ-mediated plasminogen activator inhibitor-1 (PAI-1) expression,

which reduces cell migration and invasion in breast and gynecologic cancer cells (28), using TGFβ-responsive PAI-1 reporters (PAI-1 and CAGA). In T80 cells and T29 cells, we observed that enforced expression of both EVI1 and MDS1/EVI1 markedly inhibited TGFβ-mediated induction of the PAI-1 promoter (Supplementary Fig. S1) similar to results from others (18). However, enforced expression of MDS1/EVI1 in T29 cells (results not shown) not only did not repress TGFβ-induced CAGA luciferase activity, but increased TGFβ-induced CAGA activity in contrast to EVI1, which repressed the promoter. Because the PAI-1 promoter contains elements that are not present in the CAGA promoter and the CAGA promoter represents a multimerized sequence, the differential effects on the two promoters may be due to the presence of additional regulatory elements in the PAI-1 promoter.

Collectively, these data implicate an important and unexpected role for MDS1/EVI1 and EVI1 in epithelial-mesenchymal transformation in ovarian cancer, specifically the migration of ovarian epithelial cells possibly through induction of PAI-1, thus implicating these gene products in multiple roles in ovarian cancer metastasis.

The PR domain of MDS1/EVI1 is negative for methyltransferase activity. MDS1/EVI1 has been shown to exhibit similar functions or to act as an inhibitor of EVI1 depending on the system investigated (22, 29–31). MDS1/EVI1 (PRDM3) has a novel PR (PRD1-BF1-RIZ homology) domain not present in either MDS1 or EVI1, which has the potential to act as a protein methyltransferase (32). However, using free histones and [^{3}H]-*S*-adenosyl-methionine, we were unable to detect significant differences between the methyltransferase activity associated with MDS1/EVI1 and EVI1 following forced expression in COS7 cells (Fig. 4). In contrast, GST-PRMT1, a type I protein arginine methyltransferase, dramatically increased the methylation of free histone substrates. There was a weak methyltransferase activity associated with both MDS1/EVI1 and EVI1 immunoprecipitates that could be due to coimmunoprecipitation of components of the Swi/Snf complex including BRG1 (SMARCA4; ref. 33) that bind EVI1 and have methyltransferase activity. Together, the data suggest that the PR domain of MDS1/EVI1 does not have methyltransferase activity nor is inactive with the substrates assessed and under conditions where other PR domains are active. The PR domain in MDS1/EVI1 has been reported to inhibit oligomerization and CtBP recruitment (34) and, thus, the ability to inhibit TGFβ signaling in some models, suggesting an alternative mechanism for the differential effects of MDS1/EVI1 and EVI1.

EVI1 and MDS1/EVI1 DNA and RNA correlate with patient prognosis. It has been previously reported that high EVI1 expression in AML patients predicts poor survival in acute myeloid leukemia (AML), whereas MDS1/EVI1 expression correlates with improved outcomes (35). To determine whether overexpression of EVI1 and MDS1/EVI1 correlated with patient outcomes in ovarian cancers, Kaplan-Meier curves using EVI1 DNA and mRNA expression as a categorical variable were generated. We show that overall survival of ovarian cancer patients with elevated DNA copy number of EVI1 was significantly longer ($P < 0.03$) than patients with low levels (Fig. 5*A*). The 0.37 cutoff corresponds to a normalized gain of one copy of the DNA. Overall survival for patients with elevated total EVI1 and MDS1/EVI1 (using exon III probes) or MDS1/EVI1 RNA levels (using MDS1/EVI1-specific probe) was significantly longer ($P < 0.05$) than patients with low EVI1 and MDS1/EVI1 RNA levels (Fig. 5*B*), which is consistent with the CGH data. However, overall survival for patients with elevated EVI1 (using EVI1 exon I probe, which detects EVI1d specifically) was significantly shorter ($P < 0.05$) than patients with low EVI1 RNA levels (Fig. 5*B*), which is similar

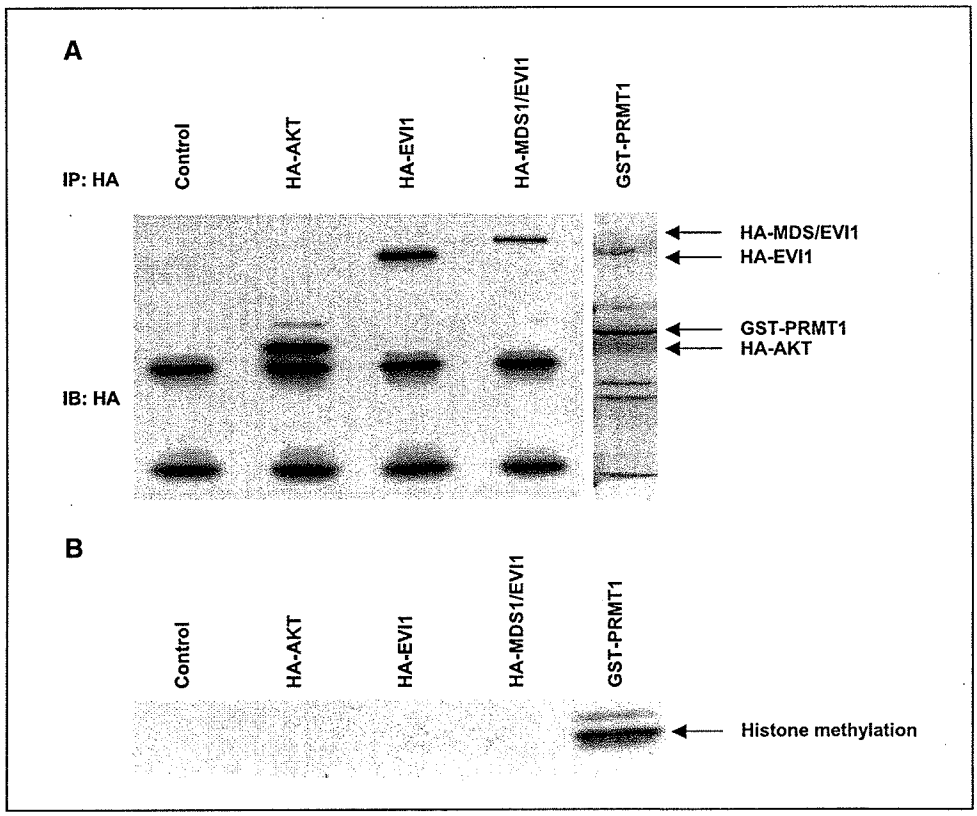

Figure 4. The PR domain of MDS1/EVI1 is negative for methyltransferase activity. *A*, transient transfection with HA-AKT, HA-EVI1, and HA-MDS1/EVI1 fusion constructs was done in COS7 cells. Immunoprecipitation with 12CA5 HA antibody was done 48 h post-transfection and verified by Western analysis using HA antibody. *B, in vitro* methyltransferase activity was assessed by incubation of free histones [H3, H4 (F3, F2a1), arginine-rich], purified GST-PRMT1 or HA-tagged proteins/complexes, and [^{3}H]-*S*-adenosyl-L-methyl-methionine. We were unable to detect significant differences between a weak methyltransferase activity associated with MDS1/EVI1-HA immunoprecipitates and EVI1-HA immunoprecipitates. In contrast, GST-PRMT1, a type I protein arginine methyltransferase (46), dramatically increased the methylation of free histone substrates.

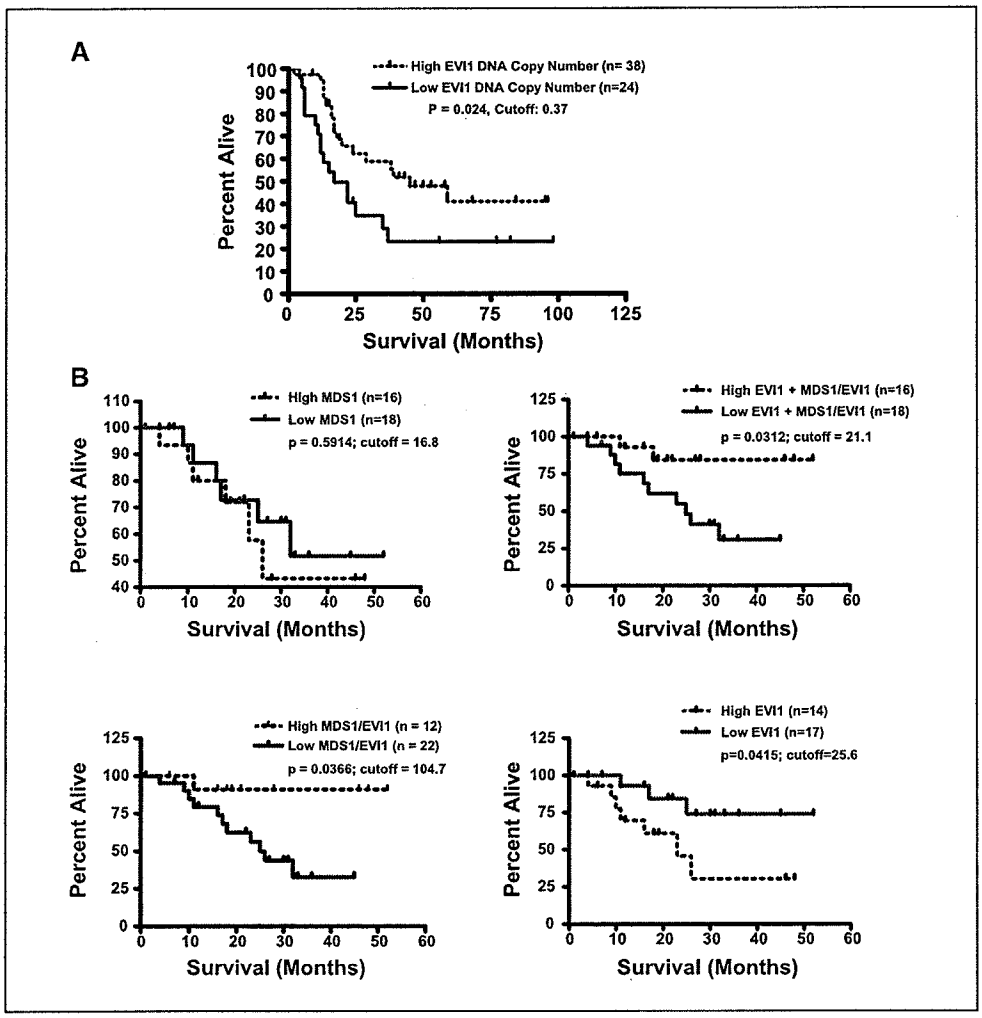

Figure 5. EVI1 and MDS1/EVI1 DNA correlate with good patient prognosis. *A*, increase in EVI1 DNA copy number is an indicator of good prognosis. Overall survival in patients (for patients where survival data were available) with high (>1 copy number increase) EVI1 copy number ($n = 38$) was significantly better ($P < 0.03$) than patients with low EVI1 copy number ($n = 24$). *B*, increase in EVI1 RNA expression is associated with an increased overall survival in ovarian cancer patients. Overall survival in stage III/IV serous epithelial ovarian cancer patients with high total EVI1 and MDS1/EVI1 (exon III primer assessing both EVI1 and MDS1/EVI1) or MDS1/EVI1 RNA levels was significantly better ($P < 0.05$) than patients with low total EVI1 and MDS1/EVI1 or MDS1/EVI1 RNA levels. Overall survival in stage III/IV serous epithelial ovarian cancer patients with high EVI1 (exon I primer assessing only EVI1) was significantly worse ($P < 0.05$) than patients with low EVI1 RNA levels.

to the pattern observed in AML where high EVI1 expression (using EVI1-specific probe against EVI1d) predicts poor patient survival and was associated with the presence of unfavorable cytogenetic abnormalities, whereas MDS1/EVI1 was associated with a favorable karyotype (27). The cutoff value represents the fold-RNA increase at which the *P* value is most significant by iterative analysis of splitting sample sets into high and low. In comparison to ovarian cancers where EVI1 and MDS1/EVI1 transcript levels were dramatically elevated (up to 300-fold), total EVI1 and MDS1/EVI1 transcripts were elevated to a much lesser degree in lung cancer (only up to 20-fold; data not shown). However, despite the modest increase, elevated EVI1 (representing total EVI1 and MDS1/EVI1) levels as assessed by transcriptional profiling (neither MDS1 nor the MDS1/EVI1 intergenic fusion are available in the data set) also indicated good prognosis in lung cancer patients (ref. 36; $n = 86$, $P < 0.05$). Thus, it would seem that MDS1/EVI1 correlates with good prognosis in epithelial cancers not limited to ovary, whereas EVI1 is an indicator of poor patient prognosis in epithelial cancers. However, analysis of additional data sets will be necessary to determine generality across tumor lineages.

Long-term expression of EVI1 and MDS1/EVI1 in immortalized normal ovarian epithelial cells and OVCAR8 cells. To better understand the association of EVI1 and MDS1/EVI1 with patient prognosis, we attempted to generate stable cell lines, including immortalized normal ovarian epithelial cells (T29 and T80) and ovarian cancer cell lines (OVCA420 and OVCAR8). However, using plasmid-based expression systems for both EVI1 and MDS1/EVI1, we were consistently unable to generate stable cell clones. In colony-forming assays with G418 and puromycin selection, the number of stable clones obtained were nonexistent or dramatically reduced compared with vector control. None of the clones expressed the transgenes as analyzed by Western blotting or when expanded survived. Further efforts in generating stable cell lines with EVI1 in OVCAR8 and T29 cells with the retroviral expression vector (pLEGFP-C1) led to the generation of a few EVI1 clones, which were senescent or failed to survive beyond two to three passages. We further attempted to generate stable cell lines using pBABE-puro retroviral expression vectors in OVCAR8 and T29 cells. However, expression of EVI1 in the retroviral pool population was dramatically reduced with passaging even in the presence of antibiotic (puromycin) selection. Thus, it seems that prolonged expression of EVI1 and MDS1/EVI1, in contrast to transient expression, may inhibit cellular proliferation, a process that has been noted with other tumor-promoting genes, such as RAS (37). Thus, these observations suggest that prolonged expression of high levels of EVI1 and MDS1/EVI1 inhibits cellular growth and may contribute to the good prognosis associated with expression of MDS1/EVI1.

Discussion

Regions of chromosomal aberrations frequently harbor novel oncogenes, and thus, the identification of the drivers of these aberrations provides important information for understanding the initiation, progression, and management of cancer. Indeed, our previous studies of genomic amplifications at 3q26 in ovarian cancer identified PIK3CA (11) and PKCι (12, 13) as potential markers of prognosis and therapeutic targets involved in ovarian cancer. The high frequency of activating mutations in PIK3CA in breast and other cancers has confirmed its role as an oncogene (38–41), and parallel studies implicate PKCι as an oncogene in lung cancer (14).

EVI1 has previously been implicated as an oncogene due to the formation of fusion genes with AML1 in AML and MDS (19). However, we have failed to detect evidence for the presence of AML1-MDS1 or AML1-EVI1 fusion genes in ovarian cancer. We now show by high-resolution CGH analysis that EVI1 is located at the center of the minimally aberrant region at 3q26.2, one of the earliest and most frequent genomic amplifications in ovarian cancer. Furthermore, we show that this DNA copy number increase is associated with a marked accumulation of both EVI1 and MDS1/EVI1 (PRDM3) intergenic read-through transcripts in ovarian cancers. The marked increase in RNA levels compared with the modest increase in copy number suggests that mechanisms in addition to genomic amplification contribute to the deregulation of these genes. Acquisition of structural aberrations within the promoters of EVI1 or MDS1 during the rearrangement that accompanies amplification or epigenetic events such as hypomethylation, which has been reported for PRDM16 (MEL1S) in leukemia (42), may contribute to this deregulation. Nevertheless, both RNA and protein levels of MDS1/EVI1 and EVI1 are markedly aberrant in the majority of ovarian cancers.

EVI1 gene copy number and MDS1/EVI1 transcript levels are associated with increased survival duration, whereas EVI1d-specific transcript levels are associated with reduced survival duration in ovarian cancer patients. We have identified a number of splice variants of EVI1,[7] which may account for the poor prognosis associated with the amplification of EVI1 in ovarian cancers. It is currently unclear why the MDS1/EVI1 transcript in ovarian cancers is associated with favorable patient prognosis; however, the difficulty in developing stable MDS1/EVI1-expressing cell lines suggests that long-term expression may limit tumor expansion. EVI1 and MDS1/EVI1 proteins have been reported to exhibit both partially antagonistic and similar biological properties. In our assays, although both EVI1 and MDS1/EVI1 behaved similarly in migration and proliferation studies, and furthermore, that the MDS1/EVI1 PR domain was negative for methyltransferase activity, we did observe that MDS1/EVI1 activated the CAGA promoter in contrast to the repressive effect of EVI1. The altered effects of the constructs may contribute to the differential effects on outcomes. Because TGFβ initially limits tumor formation by inhibiting proliferation and inducing apoptosis but increases the metastatic capacity of advanced tumors (43), blockade of TGFβ signaling by MDS1/EVI1 could increase the likelihood of tumor development but result in a less aggressive tumor, which would be sufficient to explain the increased tumor frequency as well as the improved outcome associated with 3q26 amplification. Furthermore, as indicated by both RNA and protein assays, MDS1/EVI1 seems to be increased in ovarian cancer to a much greater degree than EVI1. Indeed, in a recent study designed to identify genes that may play a role in the resistance of ovarian cancer cells to TGFβ, EVI1 was identified as amplified and overexpressed and to inhibit TGFβ signaling in immortalized ovarian epithelium (18). Importantly, however, these studies did not distinguish between whether EVI1 or MDS1/EVI1 was involved. It remains possible that MDS1/EVI1 or EVI1 is amplified as a prerequisite for the induction of a nearby gene such as SnoN/SkiL as it has been recently reported that SnoN is transcriptionally induced by EVI1 (44). In addition, whereas EVI1 is clearly involved in the prognosis of leukemia, EVI1 transgenic mice failed to develop leukemia, suggesting that cooperating events may be necessary for the full manifestation of the actions of EVI1 or MDS1/EVI1 (45). Indeed, the 3q26.2 amplicon is complex, and cooperating events between genes within this region or with other regions of genomic aberrations may be necessary for the full expression of ovarian tumorigenesis. Taken together, these findings provide a potential explanation for the observation that genomic amplification of MDS1/EVI1 and EVI1 is associated with an improved outcome.

Interfering with EVI1 or MDS1/EVI1 expression or function could have therapeutic utility as >95% of ovarian cancers express elevated mRNA levels. However, the association of the MDS1/EVI1 with an improved outcome suggests that this approach needs to be explored with care. Selective inhibition of EVI1, as it is associated with a worsened outcome, may be beneficial. In addition, the MDS1/EVI1 fusion protein may represent a novel target for immunotherapy or for early diagnosis. The outcomes of the studies described herein may potentially apply broadly to epithelial tumors where the 3q26.2 aberration is present (ovary, breast, head and neck, cervix, and lung) as well as in leukemias.

[7] M. Nanjundan and G.B. Mills, unpublished observations.

Acknowledgments

Received 6/28/2006; revised 11/30/2006; accepted 1/29/2007.

Grant support: National Cancer Institute P50 CA083639 and P30 CA16672 (G.B. Mills), P01 CA64602 (G.B. Mills and J.W. Gray), and in part by the U.S. Department of Energy, Office of Science, Office of Biological and Environmental Research (Contract DE-AC03-76SF00098, J.W. Gray).

The costs of publication of this article were defrayed in part by the payment of page charges. This article must therefore be hereby marked *advertisement* in accordance with 18 U.S.C. Section 1734 solely to indicate this fact.

References

1. Sugita M, Tanaka N, Davidson S, et al. Molecular definition of a small amplification domain within 3q26 in tumors of cervix, ovary, and lung. Cancer Genet Cytogenet 2000;117:9–18.
2. Imoto I, Yuki Y, Sonoda I, et al. Identification of ZASC1 encoding a Kruppel-like zinc finger protein as a novel target for 3q26 amplification in esophageal squamous cell carcinomas. Cancer Res 2003;63:5691–6.
3. Imoto I, Pimkhaokham A, Fukuda Y, et al. SNO is a probable target for gene amplification at 3q26 in squamous-cell carcinomas of the esophagus. Biochem Biophys Res Commun 2001;286:559–65.
4. Riazimand SH, Welkoborsky HJ, Bernauer HS, Jacob R, Mann WJ. Investigations for fine mapping of amplifications in chromosome 3q26.3–28 frequently occurring in squamous cell carcinomas of the head and neck. Oncology 2002;63:385–92.
5. Sattler HP, Rohde V, Bonkhoff H, Zwergel T, Wullich B. Comparative genomic hybridization reveals DNA copy number gains to frequently occur in human prostate cancer. Prostate 1999;39:79–86.
6. Sattler HP, Lensch R, Rohde V, et al. Novel amplification unit at chromosome 3q25–27 in human prostate cancer. Prostate 2000;45:207–15.
7. Weber-Mangal S, Sinn HP, Popp S, et al. Breast cancer in young women (< or = 35 years): genomic aberrations detected by comparative genomic hybridization. Int J Cancer 2003;107:583–92.

8. Wessels LF, van Welsem T, Hart AA, van't Veer LJ, Reinders MJ, Nederlof PM. Molecular classification of breast carcinomas by comparative genomic hybridization: a specific somatic genetic profile for BRCA1 tumors. Cancer Res 2002;62:7110–7.
9. Or YY, Hui AB, Tam KY, Huang DP, Lo KW. Characterization of chromosome 3q and 12q amplicons in nasopharyngeal carcinoma cell lines. Int J Oncol 2005; 26:49–56.
10. Casas S, Aventin A, Fuentes F, et al. Genetic diagnosis by comparative genomic hybridization in adult *de novo* acute myelocytic leukemia. Cancer Genet Cytogenet 2004;153:16–25.
11. Shayesteh L, Lu Y, Kuo WL, et al. PIK3CA is implicated as an oncogene in ovarian cancer. Nat Genet 1999;21:99–102.
12. Eder AM, Sui X, Rosen DG, et al. Atypical PKCι contributes to poor prognosis through loss of apical-basal polarity and cyclin E overexpression in ovarian cancer. Proc Natl Acad Sci U S A 2005;102:12519–24.
13. Zhang L, Huang J, Yang N, et al. Integrative genomic analysis of protein kinase C (PKC) family identifies PKCι as a biomarker and potential oncogene in ovarian carcinoma. Cancer Res 2006;66:4627–35.
14. Regala RP, Weems C, Jamieson L, et al. Atypical protein kinase Cι is an oncogene in human non–small cell lung cancer. Cancer Res 2005;65:8905–11.
15. Guan XY, Fung JM, Ma NF, et al. Oncogenic role of eIF-5A2 in the development of ovarian cancer. Cancer Res 2004;64:4197–200.
16. Estilo CL, O-Charoenrat P, Ngai I, et al. The role of novel oncogenes squamous cell carcinoma-related oncogene and phosphatidylinositol 3-kinase p110α in squamous cell carcinoma of the oral tongue. Clin Cancer Res 2003;9:2300–6.
17. Yokoi S, Yasui K, Iizasa T, Imoto I, Fujisawa T, Inazawa J. TERC identified as a probable target within the 3q26 amplicon that is detected frequently in non–small cell lung cancers. Clin Cancer Res 2003;9:4705–13.
18. Sunde JS, Donninger H, Wu K, et al. Expression profiling identifies altered expression of genes that contribute to the inhibition of transforming growth factor-β signaling in ovarian cancer. Cancer Res 2006;66: 8404–12.
19. Nucifora G, Laricchia-Robbio L, Senyuk V. EVI1 and hematopoietic disorders: history and perspectives. Gene 2006;368:1–11.
20. Liu Y, Chen L, Ko TC, Fields AP, Thompson EA. Evi1 is a survival factor which conveys resistance to both TGFβ- and taxol-mediated cell death via PI3K/AKT. Oncogene 2006;25:3565–75.
21. Snijders AM, Nowak N, Segraves R, et al. Assembly of microarrays for genome-wide measurement of DNA copy number. Nat Genet 2001;29:263–4.
22. Vinatzer U, Taplick J, Seiser C, Fonatsch C, Wieser R. The leukaemia-associated transcription factors EVI-1 and MDS1/EVI1 repress transcription and interact with histone deacetylase. Br J Haematol 2001;114:566–73.
23. Kurokawa M, Mitani K, Irie K, et al. The oncoprotein Evi-1 represses TGF-β signalling by inhibiting Smad3. Nature 1998;394:92–6.
24. Tanaka T, Nishida J, Mitani K, Ogawa S, Yazaki Y, Hirai H. Evi-1 raises AP-1 activity and stimulates c-fos promoter transactivation with dependence on the second zinc finger domain. J Biol Chem 1994;269: 24020–6.
25. Morishita K, Parganas E, Douglass EC, Ihle JN. Unique expression of the human Evi-1 gene in an endometrial carcinoma cell line: sequence of cDNAs and structure of alternatively spliced transcripts. Oncogene 1990;5:963–71.
26. Brooks DJ, Woodward S, Thompson FH, et al. Expression of the zinc finger gene EVI-1 in ovarian and other cancers. Br J Cancer 1996;74:1518–25.
27. Barjesteh van Waalwijk van Doorn-Khosrovani S, Erpelinck C, van Putten WL, et al. High EVI1 expression predicts poor survival in acute myeloid leukemia: a study of 319 *de novo* AML patients. Blood 2003;101:837–45.
28. Whitley BR, Palmieri D, Twerdi CD, Church FC. Expression of active plasminogen activator inhibitor-1 reduces cell migration and invasion in breast and gynecological cancer cells. Exp Cell Res 2004;296:151–62.
29. Sood R, Talwar-Trikha A, Chakrabarti SR, Nucifora G. MDS1/EVI1 enhances TGF-β1 signaling and strengthens its growth-inhibitory effect but the leukemia-associated fusion protein AML1/MDS1/EVI1, product of the t(3;21), abrogates growth-inhibition in response to TGF-β1. Leukemia 1999;13:348–57.
30. Soderholm J, Kobayashi H, Mathieu C, Rowley JD, Nucifora G. The leukemia-associated gene MDS1/EVI1 is a new type of GATA-binding transactivator. Leukemia 1997;11:352–8.
31. Vinatzer U, Mannhalter C, Mitterbauer M, et al. Quantitative comparison of the expression of EVI1 and its presumptive antagonist, MDS1/EVI1, in patients with myeloid leukemia. Genes Chromosomes Cancer 2003;36: 80–9.
32. Steele-Perkins G, Fang W, Yang XH, et al. Tumor formation and inactivation of RIZ1, an Rb-binding member of a nuclear protein-methyltransferase superfamily. Genes Dev 2001;15:2250–62.
33. Chi Y, Senyuk V, Chakraborty S, Nucifora G. EVI1 promotes cell proliferation by interacting with BRG1 and blocking the repression of BRG1 on E2F1 activity. J Biol Chem 2003;278:49806–11.
34. Nitta E, Izutsu K, Yamaguchi Y, et al. Oligomerization of Evi-1 regulated by the PR domain contributes to recruitment of corepressor CtBP. Oncogene 2005;24: 6165–73.
35. Barjesteh van Waalwijk van Doorn-Khosrovani S, Erpelinck C, Lowenberg B, Delwel R. Low expression of MDS1-1–like-1 (MEL1) and EVI1–like-1 (EL1) genes in favorable-risk acute myeloid leukemia. Exp Hematol 2003;31:1066–72.
36. Beer DG, Kardia SL, Huang CC, et al. Gene-expression profiles predict survival of patients with lung adenocarcinoma. Nat Med 2002;8:816–24.
37. Maldonado JL, Timmerman L, Fridlyand J, Bastian BC. Mechanisms of cell-cycle arrest in Spitz nevi with constitutive activation of the MAP-kinase pathway. Am J Pathol 2004;164:1783–7.
38. Campbell IG, Russell SE, Phillips WA. PIK3CA mutations in ovarian cancer. Clin Cancer Res 2005;11: 7042; author reply 42–3.
39. Wang Y, Helland A, Holm R, Kristensen GB, Borresen-Dale AL. PIK3CA mutations in advanced ovarian carcinomas. Hum Mutat 2005;25:322.
40. Campbell IG, Russell SE, Choong DY, et al. Mutation of the PIK3CA gene in ovarian and breast cancer. Cancer Res 2004;64:7678–81.
41. Levine DA, Bogomolniy F, Yee CJ, et al. Frequent mutation of the PIK3CA gene in ovarian and breast cancers. Clin Cancer Res 2005;11:2875–8.
42. Yoshida M, Nosaka K, Yasunaga J, Nishikata I, Morishita K, Matsuoka M. Aberrant expression of the MEL1S gene identified in association with hypomethylation in adult T-cell leukemia cells. Blood 2004;103: 2753–60.
43. Elliott RL, Blobe GC. Role of transforming growth factor β in human cancer. J Clin Oncol 2005;23:2078–93.
44. Yatsula B, Lin S, Read AJ, et al. Identification of binding sites of EVI1 in mammalian cells. J Biol Chem 2005;280:30712–22.
45. Louz D, van den Broek M, Verbakel S, et al. Erythroid defects and increased retrovirally-induced tumor formation in Evi1 transgenic mice. Leukemia 2000;14: 1876–84.
46. Frankel A, Yadav N, Lee J, Branscombe TL, Clarke S, Bedford MT. The novel human protein arginine *N*-methyltransferase PRMT6 is a nuclear enzyme displaying unique substrate specificity. J Biol Chem 2002;277: 3537–43.

Exhibit E

geneSymb	chrLoc	Chr	BAC Coorc	Gene Coor	p value
FLJ22595	Chr:3q26.1	3	6.5E+08	6.51E+08	0.188309
RARRES1	Chr:3q25.32	3	6.5E+08	6.49E+08	0.2295
RARRES1	Chr:3q25.32	3	6.5E+08	6.49E+08	0.285981
RARRES1	Chr:3q25.32	3	6.5E+08	6.49E+08	0.372995
SHOX2	Chr:3q25-q26.1	3	6.5E+08	6.49E+08	0.674756
IL12A	Chr:3p12-q13.2	3	6.5E+08	6.51E+08	0.787672
SHOX2	Chr:3q25-q26.1	3	6.5E+08	6.49E+08	0.827788
SLITRK3	Chr:3q26.1	3	6.55E+08	6.56E+08	0.687166
SI	Chr:3q25.2-q26.:	3	6.55E+08	6.56E+08	0.737786
BCHE	Chr:3q26.1-q26.:	3	6.55E+08	6.57E+08	0.904255
MYNN	Chr:3q26.31	3	6.6E+08	6.61E+08	2.80E-08
TLOC1	Chr:3q26.2-q27	3	6.6E+08	6.61E+08	1.65E-06
PDCD10	Chr:3q26.2	3	6.6E+08	6.58E+08	6.95E-06
SKIL	Chr:3q26	3	6.6E+08	6.61E+08	0.000145
GOLPH4	Chr:3q26.2	3	6.6E+08	6.59E+08	0.000202
PRKCI	Chr:3q26.3	3	6.6E+08	6.61E+08	0.000343
PRKCI	Chr:3q26.3	3	6.6E+08	6.61E+08	0.001585
SKIL	Chr:3q26	3	6.6E+08	6.61E+08	0.002001
FLJ23259	Chr:3q26.31	3	6.6E+08	6.61E+08	0.009757
TLOC1	Chr:3q26.2-q27	3	6.6E+08	6.61E+08	0.012229
EVI1	Chr:3q24-q28	3	6.6E+08	6.6E+08	0.015887
PHC3	Chr:3q26.31	3	6.6E+08	6.61E+08	0.027614
TNIK	Chr:3q26.31	3	6.6E+08	6.62E+08	0.042842
SKIL	Chr:3q26	3	6.6E+08	6.61E+08	0.052169
SLC2A2	Chr:3q26.1-q26.:	3	6.6E+08	6.62E+08	0.056079
GOLPH4	Chr:3q26.2	3	6.6E+08	6.59E+08	0.08586
TNIK	Chr:3q26.31	3	6.6E+08	6.62E+08	0.090801
PRKCI	Chr:3q26.3	3	6.6E+08	6.61E+08	0.110213
CLDN11	Chr:3q26.2-q26.:	3	6.6E+08	6.61E+08	0.132767
SERPINI1	Chr:3q26.2	3	6.6E+08	6.59E+08	0.139543
PHC3	Chr:3q26.31	3	6.6E+08	6.61E+08	0.145223
TNIK	Chr:3q26.31	3	6.6E+08	6.62E+08	0.214128
SERPINI2	Chr:3q26.1-q26.:	3	6.6E+08	6.58E+08	0.277611
FLJ23049	Chr:3q26.2	3	6.6E+08	6.58E+08	0.439807
CLDN11	Chr:3q26.2-q26.:	3	6.6E+08	6.61E+08	0.527569
MDS1	Chr:3q26	3	6.6E+08	6.6E+08	0.531075
EVI1	Chr:3q24-q28	3	6.6E+08	6.6E+08	0.612561
EIF5A2	Chr:3q26.2	3	6.6E+08	6.62E+08	0.875567
PLD1	Chr:3q26	3	6.64E+08	6.62E+08	0.059383
PLD1	Chr:3q26	3	6.64E+08	6.62E+08	0.310018
PLD1	Chr:3q26	3	6.64E+08	6.62E+08	0.494167
PLD1	Chr:3q26	3	6.64E+08	6.62E+08	0.979335
ECT2	Chr:3q26.1-q26.:	3	6.64E+08	6.64E+08	1.46E-06
FAD104	Chr:3q26.31	3	6.64E+08	6.63E+08	0.000208
TNFSF10	Chr:3q26	3	6.64E+08	6.63E+08	0.049043
TNFSF10	Chr:3q26	3	6.64E+08	6.63E+08	0.050247
TNFSF10	Chr:3q26	3	6.64E+08	6.63E+08	0.117767
GHSR	Chr:3q26.31	3	6.64E+08	6.63E+08	0.152847

---	Chr:3q26.31	3	6.64E+08	6.63E+08	0.656003
NLGN1	Chr:3q26.32	3	6.64E+08	6.64E+08	0.795654
IRA1	Chr:3q26.33	3	6.68E+08	6.68E+08	5.27E-05
FXR1	Chr:3q28	3	6.7E+08	6.72E+08	7.18E-08
NDUFB5	Chr:3q27.1	3	6.7E+08	6.7E+08	1.03E-07
FXR1	Chr:3q28	3	6.7E+08	6.72E+08	9.80E-07
MFN1	Chr:3q27.1	3	6.7E+08	6.7E+08	3.30E-06
BAF53A	Chr:3q27.1	3	6.7E+08	6.7E+08	3.47E-06
FXR1	Chr:3q28	3	6.7E+08	6.72E+08	4.45E-06
MFN1	Chr:3q27.1	3	6.7E+08	6.7E+08	4.77E-06
PIK3CA	Chr:3q26.3	3	6.7E+08	6.7E+08	1.20E-05
MFN1	Chr:3q27.1	3	6.7E+08	6.7E+08	8.63E-05
USP13	Chr:3q26.2-q26.	3	6.7E+08	6.7E+08	0.000177
ANC_2H0	Chr:3q27.1	3	6.7E+08	6.7E+08	0.007762
---	---	3	6.7E+08	6.7E+08	0.014268
PEX5R	Chr:3q27.1	3	6.7E+08	6.71E+08	0.037327
KCNMB3	Chr:3q26.3-q27	3	6.7E+08	6.7E+08	0.110647
---	---	3	6.7E+08	6.7E+08	0.195362
KCNMB2	Chr:3q26.2-q27.	3	6.7E+08	6.69E+08	0.19896
WIG1	Chr:3q26.3-q27	3	6.7E+08	6.7E+08	0.860213

Exhibit F

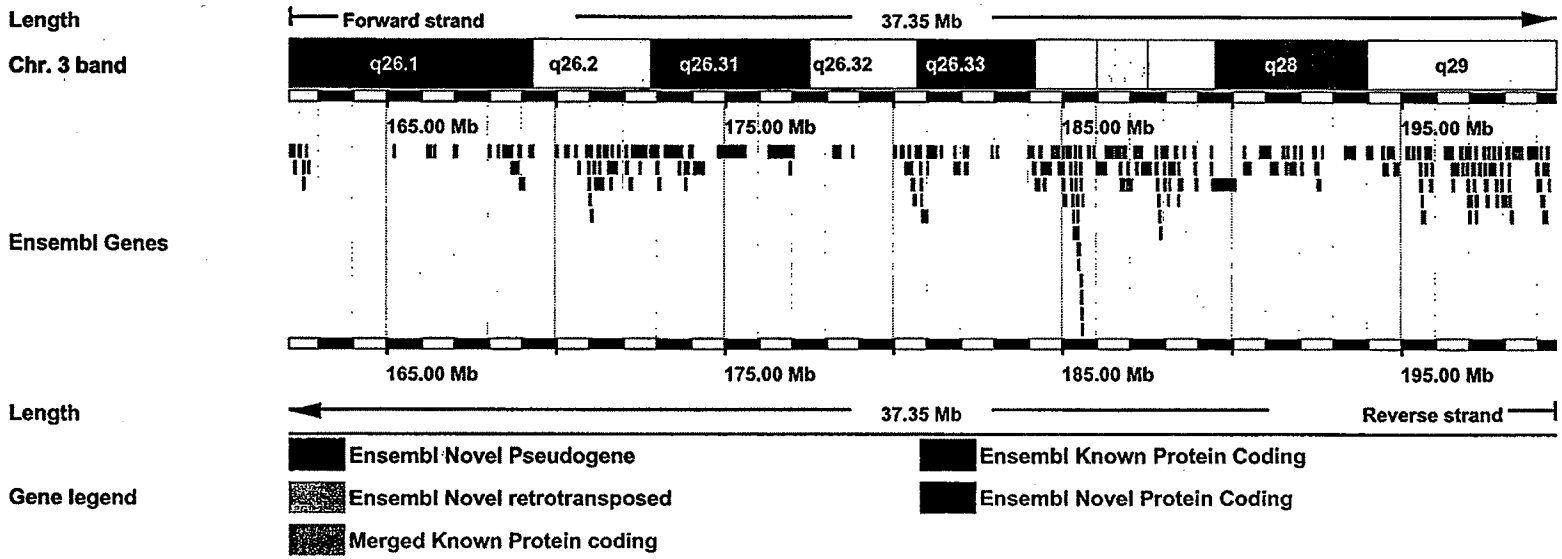
Length
Forward strand
37.35 Mb
Chr. 3 band
q26.1
q26.2
q26.31
q26.32
q26.33
q28
q29
165.00 Mb
175.00 Mb
185.00 Mb
195.00 Mb
Ensembl Genes
165.00 Mb
175.00 Mb
185.00 Mb
195.00 Mb
Length
37.35 Mb
Reverse strand
Gene legend
Ensembl Novel Pseudogene
Ensembl Known Protein Coding
Ensembl Novel retrotransposed
Ensembl Novel Protein Coding
Merged Known Protein coding
There are currently 52 tracks switched off, use the menus above the image to turn them on.

Genes in Chromosome 3 162152104 - 199501827

SeqRegion	Start	End	Ensembl ID	DB	Name
3	161956791	162271511	ENSG00000163590	HGNC	PPM1L
3	162284365	162305854	ENSG00000169255	HGNC	B3GALNT1
3	162421793	162452489	ENSG00000169251	HGNC	NMD3
3	162545274	162572565	ENSG00000196542	HGNC	C3orf57
3	162545283	162573362	ENSG00000179522	Uniprot/SPTREMBL	Q6ZWB5_HUMAN
3	162629609	162630079	ENSG00000129973	-	-novel-
3	162697290	162704424	ENSG00000182447	RefSeq_peptide	NP_001073909.1
3	165202079	165202974	ENSG00000214210	-	-novel-
3	166179381	166278976	ENSG00000090402	HGNC	SI
3	166387227	166397163	ENSG00000121871	HGNC	SLITRK3
3	166973387	167037944	ENSG00000114200	HGNC	BCHE
3	168011639	168012070	ENSG00000185790	-	-novel-
3	168266313	168266807	ENSG00000189245	-	-novel-
3	168440811	168580765	ENSG00000169064	RefSeq_peptide	NP_078963.2
3	168642417	168674515	ENSG00000114204	HGNC	SERPINI2
3	168679169	168853983	ENSG00000174776	HGNC	WDR49
3	168884391	168935345	ENSG00000114209	HGNC	PDCD10
3	168936217	169026048	ENSG00000163536	HGNC	SERPINI1
3	169209925	169296363	ENSG00000173905	HGNC	GOLIM4
3	170012789	170030104	ENSG00000206120	Uniprot/SPTREMBL	Q0D2K5_HUMAN
3	170285244	170347054	ENSG00000085276	HGNC	EVI1
3	170581663	170582016	ENSG00000206115	HGNC	MDS1
3	170684153	170684502	ENSG00000213178	-	-novel-
3	170909777	170910252	ENSG00000184531	-	-novel-
3	170967407	170970377	ENSG00000184378	Uniprot/SWISSPROT	ARPM1_HUMAN
3	170973313	170988027	ENSG00000085274	HGNC	MYNN
3	170993960	171013025	ENSG00000171757	HGNC	LRRC34
3	171022395	171038092	ENSG00000188306	RefSeq_peptide	NP_001073929.1
3	171039736	171070356	ENSG00000114248	HGNC	LRRC31
3	171112054	171139640	ENSG00000187033	HGNC	SAMD7
3	171167274	171198855	ENSG00000008952	HGNC	TLOC1
3	171239397	171285872	ENSG00000173890	HGNC	GPR160
3	171288292	171290072	ENSG00000198511	Uniprot/SPTREMBL	Q8N9A9_HUMAN
3	171295918	171382203	ENSG00000173889	HGNC	PHC3
3	171422906	171506463	ENSG00000163558	HGNC	PRKCI
3	171558208	171593226	ENSG00000136603	HGNC	SKIL
3	171619359	171634577	ENSG00000013297	HGNC	CLDN11
3	171662045	171662440	ENSG00000179656	Uniprot/SPTREMBL	Q8N1Y7_HUMAN
3	171667255	171786552	ENSG00000013293	HGNC	SLC7A14
3	171854329	171854742	ENSG00000213174	-	-novel-
3	172066798	172073165	ENSG00000163584	HGNC	RPL22L1
3	172088898	172109120	ENSG00000163577	HGNC	EIF5A2
3	172196831	172227462	ENSG00000163581	HGNC	SLC2A2
3	172262986	172660812	ENSG00000154310	HGNC	TNIK
3	172483919	172485091	ENSG00000179578	Uniprot/SPTREMBL	Q8N4V4_HUMAN
3	172801314	173010929	ENSG00000075651	HGNC	PLD1
3	172992274	173010408	ENSG00000183657	Uniprot/SPTREMBL	Q8WYW5_HUMAN

3	173043844	173059802	ENSG00000186329	-	-novel-
3	173240112	173601181	ENSG00000075420	HGNC	FNDC3B
3	173645617	173648940	ENSG00000121853	HGNC	GHSR
3	173706159	173723963	ENSG00000121858	HGNC	TNFSF10
3	173831130	173911702	ENSG00000144959	HGNC	AADACL1
3	173844177	173844434	ENSG00000121876	Uniprot/SPTREMBL	Q9P1K3_HUMAN
3	173954992	174021957	ENSG00000114346	HGNC	ECT2
3	174089842	174341700	ENSG00000144962	HGNC	SPATA16
3	174805083	175483810	ENSG00000169760	HGNC	NLGN1
3	175577728	175578489	ENSG00000213169	-	-novel-
3	176297261	177006120	ENSG00000177694	HGNC	NAALADL2
3	176918574	176919150	ENSG00000214192	-	-novel-
3	178212163	178397734	ENSG00000177565	HGNC	TBL1XR1
3	178784487	178784722	ENSG00000203635	-	-novel-
3	180007823	180044899	ENSG00000197584	HGNC	KCNMB2
3	180224221	180272278	ENSG00000172667	HGNC	ZMAT3
3	180349005	180435189	ENSG00000121879	HGNC	PIK3CA
3	180443259	180467532	ENSG00000171121	HGNC	KCNMB3
3	180524245	180536017	ENSG00000121864	HGNC	ZNF639
3	180548174	180593700	ENSG00000171109	HGNC	MFN1
3	180599696	180652065	ENSG00000114450	HGNC	GNB4
3	180664828	180665801	ENSG00000181260	-	-novel-
3	180763402	180788880	ENSG00000136518	HGNC	ACTL6A
3	180788951	180805128	ENSG00000136522	HGNC	MRPL47
3	180805269	180824981	ENSG00000136521	HGNC	NDUFB5
3	180826317	180826851	ENSG00000213165	-	-novel-
3	180853635	180984675	ENSG00000058056	HGNC	USP13
3	181000744	181237211	ENSG00000114757	HGNC	PEX5L
3	181005294	181005703	ENSG00000203634	-	-novel-
3	181413002	181413524	ENSG00000213158	-	-novel-
3	181802625	181818049	ENSG00000163728	HGNC	TTC14
3	181814491	181938356	ENSG00000145075	HGNC	CCDC39
3	182088152	182088557	ENSG00000213157	-	-novel-
3	182113146	182177642	ENSG00000114416	HGNC	FXR1
3	182184200	182190224	ENSG00000205981	HGNC	DNAJC19
3	182912416	182914915	ENSG00000181449	HGNC	SOX2
3	183066827	183067636	ENSG00000213155	-	-novel-
3	183993985	184122113	ENSG00000058063	HGNC	ATP11B
3	184143269	184181020	ENSG00000043093	HGNC	DCUN1D1
3	184215702	184300059	ENSG00000078070	HGNC	MCCC1
3	184322698	184363317	ENSG00000078081	HGNC	LAMP3
3	184378525	184628549	ENSG00000053524	HGNC	MCF2L2
3	184453726	184473872	ENSG00000176597	HGNC	B3GNT5
3	184688013	184756193	ENSG00000172578	HGNC	KLHL6
3	184836105	184884996	ENSG00000114796	HGNC	KLHL24
3	184898300	185013102	ENSG00000163872	HGNC	YEATS2
3	185005880	185006380	ENSG00000212778	Uniprot/SPTREMBL	Q8NBD7_HUMAN
3	185016364	185026059	ENSG00000180834	HGNC	MAP6D1
3	185029870	185085387	ENSG00000175193	HGNC	PARL
3	185120420	185218421	ENSG00000114770	HGNC	ABCC5
3	185232026	185239850	ENSG00000186090	HGNC	HTR3D

3	185253529	185261153	ENSG00000178084	HGNC	HTR3C
3	185300661	185307476	ENSG00000186038	HGNC	HTR3E
3	185316730	185318380	ENSG00000205955	Uniprot/SPTREMBL	Q58FG0_HUMAN
3	185335504	185345793	ENSG00000145191	HGNC	EIF2B5
3	185355978	185374092	ENSG00000161202	HGNC	DVL3
3	185375328	185384572	ENSG00000161203	HGNC	AP2M1
3	185386580	185394487	ENSG00000161204	HGNC	ABCF3
3	185431011	185441034	ENSG00000214162	-	-novel-
3	185435014	185442810	ENSG00000145198	Uniprot/SPTREMBL	Q9BVH8_HUMAN
3	185442811	185449440	ENSG00000214160	HGNC	ALG3
3	185450177	185493512	ENSG00000145194	HGNC	ECE2
3	185459697	185461945	ENSG00000163888	HGNC	CAMK2N2
3	185499189	185509531	ENSG00000175166	HGNC	PSMD2
3	185515050	185535839	ENSG00000114867	HGNC	EIF4G1
3	185538047	185541942	ENSG00000214156	Uniprot/SPTREMBL	Q6ZTF8_HUMAN
3	185538999	185546759	ENSG00000175182	HGNC	FAM131A
3	185546673	185562084	ENSG00000114859	HGNC	CLCN2
3	185563888	185569057	ENSG00000163882	HGNC	POLR2H
3	185572467	185578626	ENSG00000090534	HGNC	THPO
3	185580555	185590311	ENSG00000090539	HGNC	CHRD
3	185762281	185782889	ENSG00000182580	HGNC	EPHB3
3	185911380	185912303	ENSG00000177383	HGNC	MAGEF1
3	186012625	186253096	ENSG00000156931	HGNC	VPS8
3	186278532	186353496	ENSG00000187068	RefSeq_peptide	NP_001020437.1
3	186391108	186454531	ENSG00000113790	HGNC	EHHADH
3	186563664	186683293	ENSG00000073803	HGNC	MAP3K13
3	186691495	186699516	ENSG00000163900	HGNC	TMEM41A
3	186708282	186753063	ENSG00000163898	HGNC	LIPH
3	186786725	186831577	ENSG00000163904	HGNC	SENP2
3	186844228	187025521	ENSG00000073792	HGNC	IGF2BP2
3	186913774	186918649	ENSG00000163915	HGNC	C3orf65
3	187110586	187138495	ENSG00000136527	HGNC	SFRS10
3	187168919	187180320	ENSG00000171658	-	-novel-
3	187246804	187309571	ENSG00000171656	HGNC	ETV5
3	187349706	187562697	ENSG00000058866	HGNC	DGKG
3	187738926	187744861	ENSG00000213139	HGNC	CRYGS
3	187746824	187767823	ENSG00000113838	HGNC	TBCCD1
3	187771161	187786282	ENSG00000090520	HGNC	DNAJB11
3	187813549	187821786	ENSG00000145192	HGNC	AHSG
3	187840843	187853488	ENSG00000090512	HGNC	FETUB
3	187866492	187878716	ENSG00000113905	HGNC	HRG
3	187917814	187944435	ENSG00000113889	HGNC	KNG1
3	187984030	187990377	ENSG00000156976	HGNC	EIF4A2
3	187990378	188006984	ENSG00000163918	HGNC	RFC4
3	188043157	188058944	ENSG00000181092	HGNC	ADIPOQ
3	188100681	188101040	ENSG00000127266	-	-novel-
3	188131210	188279035	ENSG00000073849	HGNC	ST6GAL1
3	188133031	188134876	ENSG00000203632	-	-novel-
3	188321435	188339957	ENSG00000163923	HGNC	RPL39L
3	188397572	188408111	ENSG00000198491	Uniprot/SPTREMBL	Q6ZSS5_HUMAN
3	188397968	188401943	ENSG00000175077	HGNC	RTP1

3	188418632	188492446	ENSG00000127241	HGNC	MASP1
3	188568862	188572061	ENSG00000136514	HGNC	RTP4
3	188869399	188870895	ENSG00000157005	HGNC	SST
3	188898741	188903039	ENSG00000198471	HGNC	RTP2
3	188921859	188936942	ENSG00000113916	HGNC	BCL6
3	189379025	189381292	ENSG00000197088	Uniprot/SPTREMBL	Q6UXS4_HUMAN
3	189379637	189380683	ENSG00000213132	RefSeq_dna	NM_207488
3	189413415	190080135	ENSG00000145012	HGNC	LPP
3	190351296	190351457	ENSG00000181238	Uniprot/SPTREMBL	Q9BZK4_HUMAN
3	190372457	190523964	ENSG00000188001	HGNC	FAM79B
3	190831910	191107935	ENSG00000073282	HGNC	TP63
3	191157213	191321407	ENSG00000090530	HGNC	LEPREL1
3	191506197	191522909	ENSG00000163347	HGNC	CLDN1
3	191588535	191611027	ENSG00000113946	HGNC	CLDN16
3	191629142	191650359	ENSG00000198398	RefSeq_peptide	NP_997199.1
3	191714585	191851995	ENSG00000196083	HGNC	IL1RAP
3	191846266	191858537	ENSG00000214148	Uniprot/SPTREMBL	Q8N9C1_HUMAN
3	192031798	192032656	ENSG00000214147	-	-novel-
3	192053362	192061350	ENSG00000205835	-	-novel-
3	192413016	192450604	ENSG00000188729	HGNC	OSTN
3	192467652	192531019	ENSG00000188958	HGNC	UTS2D
3	192529568	192592658	ENSG00000152492	HGNC	CCDC50
3	192661646	192661939	ENSG00000205833	RefSeq_peptide	NP_001076777.1
3	193342424	193609532	ENSG00000114279	HGNC	FGF12
3	193997301	194118644	ENSG00000180611	HGNC	C3orf59
3	194441608	194471337	ENSG00000127252	HGNC	HRASLS
3	194475525	194579208	ENSG00000187527	HGNC	ATP13A5
3	194602563	194755470	ENSG00000127249	HGNC	ATP13A4
3	194793707	194898294	ENSG00000198836	HGNC	OPA1
3	195157857	195204142	ENSG00000214146	Uniprot/SPTREMBL	Q8N375_HUMAN
3	195336628	195339066	ENSG00000114315	HGNC	HES1
3	195488267	195513284	ENSG00000214145	Uniprot/SPTREMBL	Q0VG78_HUMAN
3	195542190	195553306	ENSG00000178772	HGNC	CPN2
3	195557274	195571761	ENSG00000172061	HGNC	LRRC15
3	195596839	195601284	ENSG00000178732	HGNC	GP5
3	195604692	195664208	ENSG00000133657	HGNC	ATP13A3
3	195700704	195703392	ENSG00000198579	Uniprot/SPTREMBL	Q8N266_HUMAN
3	195704821	195717408	ENSG00000205823	-	-novel-
3	195789692	195835707	ENSG00000145014	HGNC	TMEM44
3	195842814	195874209	ENSG00000041802	HGNC	LSG1
3	195887911	195891051	ENSG00000185112	HGNC	FAM43A
3	196270306	196473166	ENSG00000173950	HGNC	C3orf21
3	196476768	196645041	ENSG00000114331	HGNC	CENTB2
3	196502065	196502363	ENSG00000203631	-	-novel-
3	196722514	196751362	ENSG00000184203	HGNC	PPP1R2
3	196776867	196792278	ENSG00000189058	HGNC	APOD
3	196870145	196900884	ENSG00000214135	HGNC	SDHALP2
3	196912000	196924416	ENSG00000205814	Uniprot/SPTREMBL	Q6ZRC0_HUMAN
3	196933520	196946094	ENSG00000176945	HGNC	MUC20
3	196959307	197023545	ENSG00000145113	HGNC	MUC4
3	196991089	196992630	ENSG00000214119	-	-novel-

3	196995841	196997718	ENSG00000205811	-	-novel-
3	197074633	197120277	ENSG00000061938	HGNC	TNK2
3	197122682	197124532	ENSG00000198174	Uniprot/SPTREMBL	Q8N9P1_HUMAN
3	197171055	197173943	ENSG00000214116	Uniprot/SPTREMBL	Q6ZUY0_HUMAN
3	197174603	197201530	ENSG00000185485	-	-novel-
3	197184123	197184381	ENSG00000203630	-	-novel-
3	197260553	197293343	ENSG00000072274	HGNC	TFRC
3	197408721	197422697	ENSG00000163958	HGNC	ZDHHC19
3	197427780	197444696	ENSG00000163959	RefSeq_peptide	NP_689885.3
3	197449652	197498981	ENSG00000161217	HGNC	PCYT1A
3	197502496	197529542	ENSG00000213123	RefSeq_peptide	NP_689986.1
3	197534818	197549655	ENSG00000145107	HGNC	TM4SF19
3	197564768	197643670	ENSG00000163960	HGNC	UBXD7
3	197683026	197714979	ENSG00000163961	HGNC	RNF168
3	197718147	197726634	ENSG00000214097	HGNC	C3orf43
3	197765475	197779810	ENSG00000185798	HGNC	WDR53
3	197780238	197798553	ENSG00000174013	Uniprot/SWISSPROT	FBSP1_HUMAN
3	197851046	197873269	ENSG00000174004	HGNC	LRRC33
3	197918318	197923491	ENSG00000174007	HGNC	C3orf34
3	197923682	197946161	ENSG00000163964	HGNC	PIGX
3	197951312	198043749	ENSG00000180370	HGNC	PAK2
3	198079174	198142480	ENSG00000119231	HGNC	SENP5
3	198146670	198153861	ENSG00000114503	HGNC	NCBP2
3	198153980	198154810	ENSG00000179823	Uniprot/SPTREMBL	Q6P6A7_HUMAN
3	198157612	198180101	ENSG00000119227	HGNC	PIGZ
3	198214640	198241043	ENSG00000163975	HGNC	MFI2
3	198255819	198509844	ENSG00000075711	HGNC	DLG1
3	198721051	198784591	ENSG00000161267	HGNC	BDH1
3	198883253	198960656	ENSG00000145016	HGNC	KIAA0226
3	198961018	198995581	ENSG00000122068	HGNC	FYTTD1
3	199002542	199082851	ENSG00000186001	HGNC	LRCH3
3	199088071	199088874	ENSG00000212777	Uniprot/SPTREMBL	Q6ZQT1_HUMAN
3	199100346	199171271	ENSG00000114473	HGNC	IQCG
3	199161449	199167844	ENSG00000182899	HGNC	RPL35A
3	199171468	199254988	ENSG00000185621	HGNC	LMLN
3	199268805	199291939	ENSG00000214090	RefSeq_dna	NR_003291.1
3	199268805	199291939	ENSG00000213114	RefSeq_dna	NM_182631
3	199330983	199332046	ENSG00000213113	-	-novel-

Exhibit G

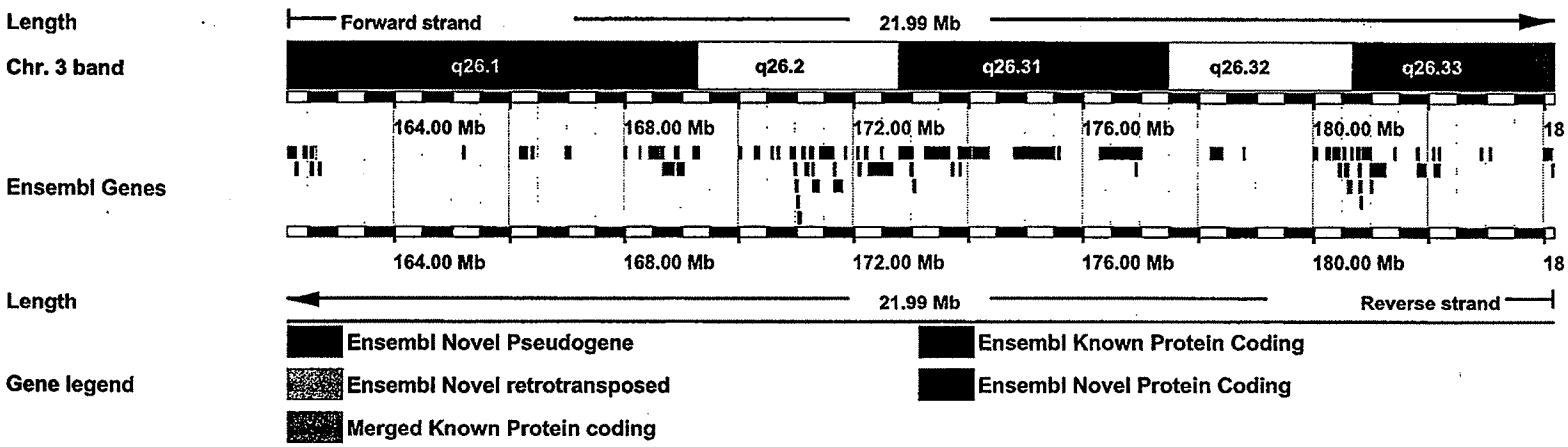
Length
Forward strand
21.99 Mb
Chr. 3 band
q26.1
q26.2
q26.31
q26.32
q26.33
164.00 Mb
168.00 Mb
172.00 Mb
176.00 Mb
180.00 Mb
18
Ensembl Genes
164.00 Mb
168.00 Mb
172.00 Mb
176.00 Mb
180.00 Mb
18
Length
21.99 Mb
Reverse strand
Gene legend
Ensembl Novel Pseudogene
Ensembl Known Protein Coding
Ensembl Novel retrotransposed
Ensembl Novel Protein Coding
Merged Known Protein coding
There are currently 52 tracks switched off, use the menus above the image to turn them on.

Genes in Chromosome 3 162152104 - 184145606

SeqRegion	Start	End	Ensembl ID	DB	Name
3	161956791	162271511	ENSG00000163590	HGNC	PPM1L
3	162284365	162305854	ENSG00000169255	HGNC	B3GALNT1
3	162421793	162452489	ENSG00000169251	HGNC	NMD3
3	162545274	162572565	ENSG00000196542	HGNC	C3orf57
3	162545283	162573362	ENSG00000179522	Uniprot/SPTREMBL	Q6ZWB5_HUMAN
3	162629609	162630079	ENSG00000129973	-	-novel-
3	162697290	162704424	ENSG00000182447	RefSeq_peptide	NP_001073909.1
3	165202079	165202974	ENSG00000214210	-	-novel-
3	166179381	166278976	ENSG00000090402	HGNC	SI
3	166387227	166397163	ENSG00000121871	HGNC	SLITRK3
3	166973387	167037944	ENSG00000114200	HGNC	BCHE
3	168011639	168012070	ENSG00000185790	-	-novel-
3	168266313	168266807	ENSG00000189245	-	-novel-
3	168440811	168580765	ENSG00000169064	RefSeq_peptide	NP_078963.2
3	168642417	168674515	ENSG00000114204	HGNC	SERPINI2
3	168679169	168853983	ENSG00000174776	HGNC	WDR49
3	168884391	168935345	ENSG00000114209	HGNC	PDCD10
3	168936217	169026048	ENSG00000163536	HGNC	SERPINI1
3	169209925	169296363	ENSG00000173905	HGNC	GOLIM4
3	170012789	170030104	ENSG00000206120	Uniprot/SPTREMBL	Q0D2K5_HUMAN
3	170285244	170347054	ENSG00000085276	HGNC	EVI1
3	170581663	170582016	ENSG00000206115	HGNC	MDS1
3	170684153	170684502	ENSG00000213178	-	-novel-
3	170909777	170910252	ENSG00000184531	-	-novel-
3	170967407	170970377	ENSG00000184378	Uniprot/SWISSPROT	ARPM1_HUMAN
3	170973313	170988027	ENSG00000085274	HGNC	MYNN
3	170993960	171013025	ENSG00000171757	HGNC	LRRC34
3	171022395	171038092	ENSG00000188306	RefSeq_peptide	NP_001073929.1
3	171039736	171070356	ENSG00000114248	HGNC	LRRC31
3	171112054	171139640	ENSG00000187033	HGNC	SAMD7
3	171167274	171198855	ENSG00000008952	HGNC	TLOC1
3	171239397	171285872	ENSG00000173890	HGNC	GPR160
3	171288292	171290072	ENSG00000198511	Uniprot/SPTREMBL	Q8N9A9_HUMAN
3	171295918	171382203	ENSG00000173889	HGNC	PHC3
3	171422906	171506463	ENSG00000163558	HGNC	PRKCI

3	171558208	171593226	ENSG00000136603	HGNC	SKIL
3	171619359	171634577	ENSG00000013297	HGNC	CLDN11
3	171662045	171662440	ENSG00000179656	Uniprot/SPTREMBL	Q8N1Y7_HUMAN
3	171667255	171786552	ENSG00000013293	HGNC	SLC7A14
3	171854329	171854742	ENSG00000213174	-	-novel-
3	172066798	172073165	ENSG00000163584	HGNC	RPL22L1
3	172088898	172109120	ENSG00000163577	HGNC	EIF5A2
3	172196831	172227462	ENSG00000163581	HGNC	SLC2A2
3	172262986	172660812	ENSG00000154310	HGNC	TNIK
3	172483919	172485091	ENSG00000179578	Uniprot/SPTREMBL	Q8N4V4_HUMAN
3	172801314	173010929	ENSG00000075651	HGNC	PLD1
3	172992274	173010408	ENSG00000183657	Uniprot/SPTREMBL	Q8WYW5_HUMAN
3	173043844	173059802	ENSG00000186329	-	-novel-
3	173240112	173601181	ENSG00000075420	HGNC	FNDC3B
3	173645617	173648940	ENSG00000121853	HGNC	GHSR
3	173706159	173723963	ENSG00000121858	HGNC	TNFSF10
3	173831130	173911702	ENSG00000144959	HGNC	AADACL1
3	173844177	173844434	ENSG00000121876	Uniprot/SPTREMBL	Q9P1K3_HUMAN
3	173954992	174021957	ENSG00000114346	HGNC	ECT2
3	174089842	174341700	ENSG00000144962	HGNC	SPATA16
3	174805083	175483810	ENSG00000169760	HGNC	NLGN1
3	175577728	175578489	ENSG00000213169	-	-novel-
3	176297261	177006120	ENSG00000177694	HGNC	NAALADL2
3	176918574	176919150	ENSG00000214192	-	-novel-
3	178212163	178397734	ENSG00000177565	HGNC	TBL1XR1
3	178784487	178784722	ENSG00000203635	-	-novel-
3	180007823	180044899	ENSG00000197584	HGNC	KCNMB2
3	180224221	180272278	ENSG00000172667	HGNC	ZMAT3
3	180349005	180435189	ENSG00000121879	HGNC	PIK3CA
3	180443259	180467532	ENSG00000171121	HGNC	KCNMB3
3	180524245	180536017	ENSG00000121864	HGNC	ZNF639
3	180548174	180593700	ENSG00000171109	HGNC	MFN1
3	180599696	180652065	ENSG00000114450	HGNC	GNB4
3	180664828	180665801	ENSG00000181260	-	-novel-
3	180763402	180788880	ENSG00000136518	HGNC	ACTL6A
3	180788951	180805128	ENSG00000136522	HGNC	MRPL47
3	180805269	180824981	ENSG00000136521	HGNC	NDUFB5
3	180826317	180826851	ENSG00000213165	-	-novel-
3	180853635	180984675	ENSG00000058056	HGNC	USP13
3	181000744	181237211	ENSG00000114757	HGNC	PEX5L
3	181005294	181005703	ENSG00000203634	-	-novel-
3	181413002	181413524	ENSG00000213158	-	-novel-
3	181802625	181818049	ENSG00000163728	HGNC	TTC14
3	181814491	181938356	ENSG00000145075	HGNC	CCDC39
3	182088152	182088557	ENSG00000213157	-	-novel-
3	182113146	182177642	ENSG00000114416	HGNC	FXR1
3	182184200	182190224	ENSG00000205981	HGNC	DNAJC19
3	182912416	182914915	ENSG00000181449	HGNC	SOX2
3	183066827	183067636	ENSG00000213155	-	-novel-
3	183993985	184122113	ENSG00000058063	HGNC	ATP11B
3	184143269	184181020	ENSG00000043093	HGNC	DCUN1D1

11. RELATED PROCEEDINGS APPENDIX

none